The effects of selected health supplements on drug intestinal epithelial permeation

S. du Plessis

orcid.org/0000-0002-5196-768X

Dissertation submitted in fulfilment of the requirements for the degree Master of Science in Pharmaceutics at the North West University

Supervisor: Dr. JD Steyn

Co-supervisor: Prof. JH Hamman

Graduation ceremony: May 2019

Student number: 24162949

ACKNOWLEDGEMENTS

"Your first step towards perfection is acknowledging your imperfections." – Wahab H. Butt

I am not perfect, nor do I think any person in life is perfect, but you have people in your life that make you feel more perfect than you think you are. These are the people that supported me throughout my studies during my first 4 years of obtaining my pharmacy degree and now during the last 2 years of my master's degree. I certainly have imperfections as all people, but I have learned by great support how to deal with them.

All honour goes to God for giving me the talents, abilities and opportunities to write this acknowledgement and being able to complete my master's degree.

I would like to show my greatest appreciation to my mother, Susan, and my father, Jan. You supported and motivated me in times that I felt like giving up. To my dearest and best friend, Elwray, I would like to give special thanks for helping me through difficult times. When I wanted to give up you made me see the bigger picture, what we are working for and the life we want for ourselves. I can never thank God enough for sending you on my path.

Lastly, I would like to express my gratitude to the NWU and NRF for the funding of my studies the last 2 years. Without this I would not have been able to complete, or even start my master's degree. The NWU and NRF make a big difference in the lives of students of all ages.

I also want to give a big thanks to Dr. Steyn and Prof. Sias for assisting me when I needed advice, suggestions and warm encouragement. I appreciate all the feedback and comments you gave me in order for me to have completed my dissertation. Without your guidance and persistent help my dissertation would not have been possible.

Handing in my dissertation is one of the happiest moments in my life and I am an extremely blessed young woman with these amazing people in my life. I would not have been able to do this without you guys.

ABSTRACT

With the growing popularity of health supplement usage to support and maintain a healthy body there is an increasing concern for possible drug-drug and drug-supplement interactions because health supplements are not subjected to the demanding pre-market clinical testing as registered prescription drugs. During this study emphasis was placed on 5 selected commercially available health supplements (acetyl-L-carnitine, berberine, chondroitin sulfate, D-glucosamine and silymarin) and their modulating effects on the intestinal permeation of a model compound. Rhodamine-123 (RH-123), which is a known substrate of the active efflux transporter P-glycoprotein (P-gp), was used to assess the membrane permeation modulating effects of the selected commercially available health supplements.

The bi-directional transport studies were conducted with RH-123 in the presence and absence of the selected health supplements across excised pig intestinal tissue using a Sweetana-Grass diffusion chamber apparatus. Over a period of 2 hours samples of 180µl were withdrawn at 20 min intervals. The RH-123 concentration in each sample was determined by using a validated fluorescence spectroscopic method on the Spectramax Paradigm® plate reader. Lucifer yellow was used to conduct a transport study to prove that the mounting technique of the excised pig intestinal tissue did not affect the viability and integrity of the tissue. All the transport experiments were conducted in triplicate at two different concentrations (a low and high concentration) of each of the selected health supplements. The bi-directional transport studies were conducted, and the resultant data was used to calculate the percentage transport and apparent permeability coefficient (P_{app}) values. The P_{app} values were then used to calculate efflux ratio (ER) values. Trans-epithelial electrical resistance (TEER) was also measured at the beginning (T_0) and end (T_{120}) of each transport experiment using a Warner Instruments® EC-825A epithelial voltage clamp. If the TEER values decreased it may be considered indicative of permeation altering effects based on changes in the membrane integrity due to the presence of the selected health supplements which may have mediated changes in the tight junction integrity.

The study conducted with RH-123 in the presence of acetyl-L-carnitine (ALC) rendered a statistically significant increase in transport of RH-123 in the absorptive (apical to basolateral) direction when compared to the negative control (RH-123 alone). Berberine showed a statistically significant decrease between the secretory (basolateral to apical) direction and the negative control and RH-123 in the presence of the low concentration (0.000566% w/v) berberine. The ER values of RH-123 in the presence of either berberine or chondroitin sulfate (CS) indicated that the possible transport mechanism of RH-123 transport could be via paracellular transport or passive diffusion while the ER value of RH-123 in the

presence of D-glucosamine indicated a possible inhibition of P-gp related efflux. The transport of RH-123 in the secretory direction (BL-AP) in the presence of silymarin showed an increase in RH-123 transport when compared to the negative control (RH-123 alone). The ER values for the transport of RH-123 in the presence of a high silymarin concentration (0.272% w/v) showed possible inhibitory effects on P-gp related efflux.

The *ex vivo* pharmacokinetic interactions obtained during this study proved that the selected health supplements may indeed induce membrane permeation altering effects when administered in conjunction with prescription drugs. Further *in vivo* studies should be conducted to investigate the clinical significance of these results.

Key words: Rhodamine 123, P-glycoprotein, Lucifer yellow, *ex vivo,* pharmacokinetic interactions, acetyl-L-carnitine, berberine, chondroitin sulfate, D-glucosamine, silymarin

Table of Contents

LIST OF TABLES

LIST OF FIGURES

LIST OF ABBREVIATIONS

%RSD	Percentage relative standard deviation
3 R	Replacement, reduction, refinement
ABC	ATP-binding cassette
ADME	Absorption, distribution, metabolism & elimination
ADME-Tox	Absorption, distribution, metabolism, elimination & toxicology
AhR	Aryl hydrocarbon receptors
ALC	Acetyl-L-carnitine
AMPK	5’ adenosine monophosphate activated protein kinase
AP-BL	Apical to basolateral
ATP	Adenosine triphosphate
AUC	Area under the concentration-time curve
BCRP	Breast cancer resistant protein
BL-AP	Basolateral to apical
C_{max}	Peak plasma concentration
Caco-2	Human colorectal carcinoma cells
CAR (NR113)	Constitutive androstane receptors
cm	Centimetre
COX-2	Cyclooxygenase-2
CO_2	Carbon dioxide
CRP	C-reactive protein
CS	Chondroitin sulfate
CYP450	Cytochrome P450
Da	Dalton
DPP-IV	Dipeptidyl Peptidase IV

e.g.	*Exempli gratia* (for example)
ER	Efflux ratio
g	Gram
GIT	Gastrointestinal tract
GR	Glucocorticoid receptor
h	Hour
HCP	Health care provider
hOAT1	Human organic anion transporter 1
HPLC	High performance liquid chromatography
IC_{50}	Inhibitory concentration at 50%
i.e.	*Id est* (In other words)
IL-6	Interleukin-6
IPIL	Vascularly perfused intestine-liver
kDa	Kilodalton
KRBB	Krebs-Ringer bicarbonate buffer
L	Litre
LC/MC/MC	Liquid chromatography and tandem mass spectrometry
LOD	Limit of detection
LOQ	Limit of quantification
LY	Lucifer yellow
m	meter
MCP-1	Monocyte chemoattractant protein-1
MDCK	Madin-Darby canine kidney cells
MDR	Multidrug resistance
mg	Milligram
min	Minute

ml	Millilitre
MRP1	Multi-drug resistance-associated protein-1
MRP2	Multi-drug resistance-associated protein-2
MRP3	Multi-drug resistance-associated protein-3
ng	Nanogram
nm	Nanometre
OAT	Organic anion transporters
OATP	Organic anion transporting polypeptides
OCT	Organic cation transporters
O_2	Oxygen
P_{app}	Apparent permeability coefficient
P-gp	P-glycoprotein
PXR (NR112)	Pregnane X receptor
RH-123	Rhodamine 123
r^2	Correlation coefficient
S	Slope
SD	Standard deviation
sec	Second
SLC	Solute carriers
SYSADOAS	Symptomatic Slow Acting Drugs for Osteoarthritis
$T_{1/2}$	Half-life
T_{max}	Time to C_{max}
TEER	Trans-epithelial electrical resistance
US	United States
USP-NF	The United States Pharmacopeia and the National Formulary
VDR	Vitamin D receptor

µg	Micro gram
µl	Micro litre
µM	Micro molar

CHAPTER 1: INTRODUCTION

1.1 Background and justification

1.1.1 The use of health supplements

Health supplements are defined as products that are used to supplement a diet with benefits beyond those of normal nutrients and/or to support and maintain the healthy functions of the body (Yong *et al*., 2014). Consumers of commercially available health supplements usually neglect to inform their health care providers about using these supplements concomitantly with their prescription medication. The risk for health supplement-drug interactions may be greater in patients using multiple chronic medication regimes (Yamada *et al*., 2014). Health supplements are not subjected to the same demanding pre-market quality tests and registration processes as with registered prescription drugs and consequently there is not enough systematic evaluation of possible interactions with pharmaceutical drugs (Gardiner *et al*., 2011).

Several studies have shown that users of dietary health supplements are generally known to maintain healthier lifestyles and tend to consume more nutrient dense diets (Yong *et al*., 2014). In 2012, an estimated 40.6 million adults in the US used supplements while 53.6 million adults indicated that they have used supplements at some point (Wu *et al*., 2014).

1.1.2 Pharmacokinetic interactions

Pharmacokinetics can be defined as the study and characterization of the kinetics of drug absorption, distribution, metabolism and elimination (ADME) (Ashford*,* 2013). The most important part of drug discovery is evaluating the ADME properties of the possible new drug and when the ADME of the new drug is not desirable it may lead to sub-therapeutic or toxic levels in the body. The ADME and toxicology properties of a new drug are typically studied together and termed ADMET or ADME-Tox (Xu *et al.,* 2017). Drug absorption, and subsequently bioavailability, refers to the total amount of unchanged drug which enters the body from the administration site and is distributed via the blood to the sampling site and/or the site of pharmacological action. When drugs are administered orally, the drug molecules move from the intestinal lumen through the gastrointestinal wall into the portal vein to the circulatory system. The term bioavailability describes the rate and extent of absorption of the active ingredient and the amount that becomes available, in its unchanged form, at the site of action. Drug disposition is described as both drug distribution and elimination (Shargel *et al*., 2012). Distribution can be described as the concurrent transport of drug to organs and tissues by arterial blood, while elimination is the permanent removal of the drug

from the body. Elimination occurs either by means of metabolism or excretion or a combination of the two processes (Kang *et al*., 2004).

Two main transport mechanisms are available for drug absorption across gastrointestinal epithelial cells namely transcellular and paracellular transport. Paracellular transport is the movement of drug molecules through openings (tight junctions) between adjoining cells, while transcellular transport is the movement of drug molecules across the epithelial cells. Transcellular transport of drugs may be further divided into passive diffusion and carrier mediated transport (facilitated diffusion and active transport). The transport of drug molecules from an area of a high concentration (lumen) to a lower concentration (blood) is termed passive diffusion. Active drug transport occurs when the drug forms a complex with a carrier/transporter, which transports it across the intestinal membrane. In cases where this transport takes place against the concentration gradient (from a low to a high drug concentration) it is termed active transport and if transport takes place with the concentration gradient it is known as facilitated diffusion. The small intestine contains numerous carrier-mediated transport systems which are located on either the basolateral or on the apical side of the membrane. P-glycoprotein (P-gp) is a prime example of these transport proteins and its effects on drug bioavailability are often studied and described in the literature (Ashford, 2013).

Intestinal P-gp is a member of the ATP-binding cassette (ABC) superfamily of active transporters. P-gp is primarily situated on the apical membranes of epithelial cells including the surface of the small intestinal lumen, colon, brain capillaries and the proximal tubules of the kidney. By actively transporting toxins against the concentration gradient, P-gp can protect the cells against accumulation of these toxins. P-gp may also limit the absorption of orally administered drugs and may consequently have a negative effect on the bioavailability of certain drugs (Wempe *et al*., 2009). P-gp is not the only contributing factor to poor bioavailability of certain drugs, because pre-systemic drug metabolism by cytochrome P450 (CYP450) enzymes may also decrease the bioavailability of substrate molecules. Intestinal CYP450 mediated metabolism can reduce the bioavailability of orally administered drugs to a large extent before reaching the systemic circulation. CYP3A4 is found in all individuals and is the most abundant form of CYP450 in the intestinal epithelium and liver and it is also responsible for more than 50% of all drug metabolism (Xie *et al*., 2016).

Health supplements are becoming more popular as a preventative measure against certain diseases. Multi-drug combination therapy (i.e. health supplements in combination with modern pharmaceuticals) for multiple chronic health issues is a standard treatment approach in the modern society aiming to achieve synergistic therapeutic effects. According to Yong

et al. (2014), health supplements are the second most commonly used complementary and alternative medicine in the general population. Currently, there is a lack of information concerning health supplement-drug interactions and there is a pressing need to investigate and report pharmacokinetic interactions between supplements and drugs. The inhibition or induction of CYP450 enzymes and P-gp efflux transporters, due to co-administration of health supplements, lies at the core of these pharmacokinetic interactions (Bahadur *et al*., 2017).

1.1.3 Health supplements

For this study, five commonly used health supplement ingredients (acetyl-L-carnitine, berberine, chondroitin sulafte, D-glucosamine and silymarin) were selected for identifying potential pharmacokinetic interactions with a model compound. The selection was based on commercial availability, cost and lack of information on pharmacokinetic interactions with drugs. The selected compounds are available in many different commercial health supplement products. Each of the selected compounds are discussed in further detail below.

1.1.3.1 Acetyl-L-carnitine

Acetyl-L-carnitine (ALC), a commonly used health supplement, which is commercially available in health stores is the short-chain ester of carnitine. It is reported to improve muscle strength and energy levels and it also has numerous effects on brain metabolism, it also protects against neurotoxic insults with the addition of possible helpful effects on depression. It was previously reported that chronic ALC supplementation may decrease the extent/rate of glucose to lactate metabolism, which may result in altered monoamine neurotransmitter levels with a subsequent increase in energy metabolites. Known metabolites of carnitine are adenosine nucleotides, *myo*-inositol and phosphocreatine (Smeland *et al*., 2012). ALC has also been reported to be useful for the treatment of Parkinson's disease by improving motor performance (Zaitone *et al*., 2012). According to a study done by Pettegrew *et al*. (1995) a dose of 3000 mg acetyl-L-carnitine per day may have positive effects on Alzheimer's disease.

1.1.3.2 Berberine

Berberine is an isoquinoline plant alkaloid, which may be obtained from a variety of plants such as *Berberineeris* species, *Hydrastis canadensis* L. and *Arcungelisia flaw* (Mistry *et al*., 2017). Berberine has been reported to have multiple biological properties, which include anti-hypertensive, anti-hyperglycaemic, anti-tumour, and anti-inflammatory effects (Lin *et al*.,

2017). A study done by de Oliveira *et al*. (2016) investigated the possible effect of berberine on Alzheimer's-like dementia involving acetylcholinesterase. The study concluded that berberine may act as a potential neuroprotective agent and may help prevent memory loss by increasing acetylcholinesterase activity which may prevent cell death and subsequently impede the progression of diseases like Alzheimer's disease (a neurodegenerative disease). Studies have shown that berberine exhibits anti-diabetic properties and that it may also promote body weight reduction and improve insulin action with a subsequent reduction in blood glucose levels (Ye *et al*., 2016). In a study done by Zhang *et al.* (2013), berberine experienced a significant increase in absorption rate and permeability in the presence of verapamil (a known P-gp inhibitor). This result indicated that berberine is a substrate of intestinal P-gp and may therefore compete with other substrates of P-gp. The recommended dose of berberine is 300 mg taken three times daily. This dosage regime has been reported to provide the best results and least possible adverse effects (Yin *et al*., 2008).

1.1.3.3 Chondroitin sulfate

According to Rani *et al*. (2017) chondroitin sulfate (CS) forms part of the connective tissues in the body and play a major role in a variety of biological processes such as the promotion of cartilage integrity and resilience and the maintenance of synovial fluid in the joints. CS is categorised as a sulfated glycosaminoglycan. CS is implicated in central nervous system development and it is also widely used as a health supplement for the treatment of osteoarthritis. CS is not well absorbed following oral administration and its bioavailability usually ranges between 0–13% (Shang *et al*., 2016). CS with a molecular mass of 4.1 kDa is considered to be a low molecular mass chondroitin and can be used as an oral health supplement to reduce joint pains, swelling and stiffness associated with osteoarthritis (Rani *et al*., 2017; Xiao *et al*., 2016). A dose of 400 mg three times a day of CS is usually the recommended dose for most ailments (Bourgeois *et al*., 1998).

1.1.3.4 D-glucosamine

D-glucosamine is a natural component in glycosaminoglycan, which can be found in the cartilage matrix and synovial fluid. When D-glucosamine is administered exogenously, it elicits pharmacological effects on chondrocytes and osteoarthritic cartilage. *In vitro* D-glucosamine reduces prostaglandin E2 production and inhibits the activation of the kappa β pathway (a nuclear factor), therefore inhibiting the cytokine intracellular signalling cascade in synovial cells and chondrocytes. D-glucosamine is usually administered at a dose of 1500 mg once a day (Bruyère *et al.*, 2016).

1.1.3.5 Silymarin

Silymarin is extracted from Milk thistle (*Silybum marianum*). It is a health supplement, which is claimed to help improve liver function and to treat liver diseases (Wu *et al*., 2009; Chang *et al*., 2015). Reports state that silymarin protects the liver against different medications, which are known to cause hepatotoxicity, for instance acetaminophen, amanitin and thioacetamide. Current studies are also investigating silymarin for the possible treatment of prostate cancer and liver diseases, such as alcoholic liver disease, acute and/or chronic hepatitis and toxin or drug induced hepatitis. This health supplement's concentration peaks in plasma at 2–3 h following oral administration and has an elimination half-life of 2–4 h. Silybinin is the main component in Milk thistle and recent studies have shown possible interactions of silybinin with CYPs and therefore the opportunity exists for herb-drug interactions. In the liver microsomes, silybin is a non-competitive inhibitor of CYP3A4 (IC_{50} = 29 µM) and CYP2C9 (IC_{50}=44 µM) activity (Komoroski, 2000). A dose of up to 1440 mg daily is considered to be safe when taking silymarin orally (Wu *et al.*, 2009).

1.2 Intestinal absorption models

The different models, which may be used for evaluation and prediction of drug absorption are commonly divided into five categories namely *in situ*, *in silico*, *in vivo*, *in vitro* and *ex vivo* models.

- *In situ* models consist of an organ(s) as part of a living organism on which studies are performed. An example of this type of model is the single pass perfusion or closed-loop perfusion technique that utilises an isolated part of the intestinal tract of an animal/human subject (Holmstock *et al.,* 2012).
- *In silico* models make use of high-performance computer aided modelling or simulations to determine significant pharmacokinetic parameters (Yang, 2009).
- *In vivo* studies are executed in living organisms (animal or human subjects). When the compound is administered, usually extravascular, the permeation (through intestinal wall into the blood) and distribution (into the tissue compartments) is measured using tissue biopsies and blood sampling (Hidalgo, 2001).
- During the initial stages of drug development, it is not feasible to perform studies on living animal models due to time constraints, cost implications and ethical considerations. These aspects have led to the development of various *in vitro* models (Deferme *et al.,* 2008). *In vitro* models have been developed to investigate the transport of compounds across intestinal tissues in glass containers or in diffusion chambers (Tarirai, 2011). Other *in vitro* models include transport across artificial membranes, shake flask methods,

transport across cell culture monolayers and surface plasma resonance biosensor analysis (Ashford, 2013).

- *Ex vivo* models are *in vitro* models that specifically entail the use of whole organs or excised tissues, which are removed from living organisms for experimental purposes. Examples include the use of excised tissues for everted sacs and excised tissue pieces for use in a diffusion chamber apparatus (Ussing chambers) (Alqahtani *et al.,* 2013).

1.3 Research problem

Evidence exists that despite the high prevalence of health supplement use, patients rarely disclose the use of these supplements to their health care providers. This may be because most patients are not aware of the possibility of potentially dangerous health supplement-drug interactions that may occur. Studies have shown that one in every four patients whom use Western medication are also taking additional health supplements without their health care provider's knowledge (Yong *et al*., 2014). Furthermore, the risk for potentially adverse supplement-drug interactions may be higher in patients using several medications for treatment of a number of chronic medical conditions (Yamada *et al*., 2014). Alteration of drug pharmacokinetics often leads to unwanted effects by drugs, especially those with narrow therapeutic ranges (Wu *et al*., 2016). Screening of health supplements to identify pharmacokinetic interactions with drug molecules is essential to inform patients accordingly in order to prevent potential drug failure or adverse events.

1.4 Aim and objectives

1.4.1 General aim

The aim of this study is to investigate potential pharmacokinetic interactions between selected commercially available health supplement compounds, namely acetyl-L-carnitine, berberine, chondroitin sulfate, D-glucosamine and silymarin, and a model compound, Rhodamine 123, which is a known P-gp substrate, by using an *ex vivo* permeation model.

1.4.2 Specific objectives

- To conduct a systematic literature review on commercially available health supplements to identify suitable candidate supplements to evaluate their effects on drug membrane permeability across excised pig intestinal tissue.
- To validate a fluorometric method for the analysis of Rhodamine 123 in terms of linearity, precision, repeatability, limit of detection (LOD) and limit of quantification (LOQ).

- To conduct bi-directional transport studies of Rhodamine 123 (basolateral to apical and apical to basolateral), in the presence and absence of the selected health supplements, across excised pig intestinal tissue mounted in a Sweetana-Grass diffusion chamber apparatus and at 2 different experimental concentrations for each of the health supplements.
- To measure and record changes in TEER (trans-epithelial electrical resistance) in the presence and absence of the selected commercially available health supplements across excised pig intestinal tissue.
- To process and interpret the transport data in terms of percentage TEER reduction, apparent permeability coefficient (P_{app}) and efflux ratio (ER) values of Rhodamine 123 in the presence and absence of the selected health supplements.
- To statistically evaluate the processed transport data and to make unbiased conclusions in terms of the potential permeation altering effects that the selected health supplements may have on P-gp substrates.

1.5 Ethics

The pig intestinal tissue that was used in this study were collected from Potchefstroom abattoir. Here the pigs are only slaughtered for meat production and not for the purpose of research. Therefore, obtaining pig intestinal tissue in this matter complies with the 3R principle (Replacement, Reduction and Refinement) because the pigs are slaughtered for meat production purposes (Kobayashi *et al*., 2012). Ethics approval are still required for the site of collection of the pig intestinal tissue (Potchefstroom abattoir) and the correct procedures needs to be followed regarding disposal of the pig intestinal tissue after the transport experiments are completed.

An ethics application which address the above stated ethical concerns for the use of pig intestinal tissue was submitted and has been approved by the Ethics Committee (AnimCare) of the North-West University (NWU00025-15-A5 – from 2015 to 2020) (Addendum A).

1.6 Dissertation layout

In chapter 1, the rationale of the study is discussed in conjunction with the specific aims, objectives and relevant experimental models. Chapter 2 entails an in-depth literature review of relevant literature pertaining to this study. Chapter 3 covers the experimental materials and methods that were used to conduct this study. In chapter 4, the experimental results, statistical analysis and interpretation of the results are discussed. Chapter 4 also includes the calculated P_{app} and ER values and reports on changes in the %TEER values that were

recorded during the permeation studies. Final conclusions and future recommendations based on the results of this study are presented in chapter 5.

CHAPTER 2: PHARMACOKINETIC EFFECTS OF SELECTED HEALTH SUPPLEMENTS ON DRUG INTESTINAL EPITHELIAL PERMEATION

2.1 Introduction

Health supplements are described in the literature as products that are used to maintain or support the healthy functioning of the body and are used to supplement a diet with benefits beyond that of normal nutrients. In general health, supplements usually contain one or more of the following constituents; amino acids, vitamins, botanicals or herbs and/or minerals and from these constituents the most frequently consumed and popular health supplements are multi-vitamins, mineral supplements, calcium, vitamin C, animal and botanical products (Yong *et al*., 2014). Supplementation of nutrients that are not abundantly found in diets such as vitamin D 6 and 7 are also popular (Gahche *et al.,* 2017).

Patients that use commercially available health supplements generally neglect to inform their health care providers (HCP) about using supplements concurrently with their prescribed medications. Even though the risk for supplement-drug interactions is more pronounced in patients on multiple chronic drug therapy, these patients usually still fail to inform the HCP of their use of supplements (Yamada *et al*., 2014). It was reported that patients usually fail to disclose this information to their HCP because they believed that this information was not significant/relevant to their HCP and it was also noted that HCP rarely asked about a patient's health supplement usage (Young *et al*., 2008). Health supplements are not subjected to the same pre-market quality assurance tests and the registration processes as in the case with prescription medicines and consequently, there is not sufficient evaluation and reporting of possible interactions with other substances (Gardiner *et al*., 2011).

Studies have shown that users of dietary and health supplements are generally known to maintain healthier lifestyles and tend to consume more nutrient dense diets. People mostly took health supplements for the prevention or treatment of a disease or for their overall well-being (Yong *et al*., 2014). According to the study conducted by Yong *et al*. (2014) patients that were reported to consume health supplements more regularly were typically non-smokers with a higher level of education and/or level of income.

In 2012, an estimated 40.6 million adults in the US were taking supplements while 53.6 million adults indicated that they had taken supplements at some point in their lives. Even though the effectiveness of health supplements is debated frequently, patients still feel inclined to use these supplements and believe that these products have less side effects due

to their natural origin (Wu *et al*., 2014). Wu *et al*. (2014) reported that some of the most common dietary health supplements that patients used were glucosamine, chondroitin, coenzyme Q-10 and fish oils. The study concluded that the growing demand for these supplements may be due to the continuously growing elderly population, since ageing causes an ever-increasing demand for prevention and treatment of joint problems (chondroitin and glucosamine) and cardiovascular diseases (Coenzyme Q-10 and fish oils).

Orally consumed products may interact with other substances during absorption from the gastrointestinal tract. It is therefore necessary to describe the physiology and functions of the gastrointestinal tract in order to understand the implication of these interactions.

2.2 The gastrointestinal tract

2.2.1 Anatomy of the human gastrointestinal tract

The human gastrointestinal tract (GIT) is comprised of the oral cavity, pharynx, oesophagus, stomach and the small and large intestines, which ends in the anus. The small intestine consists of the duodenum (approximately 0.25 m in length), the jejunum (approximately 2.50 m in length) and the ileum (approximately 3.50 m long). The junction between the duodenum and the jejunum can be identified by the sudden turn/bend in the intestine. The jejunum is the primary site where absorption of medications and nutrients occur due to the high expression of villi and micro-villi, which significantly increases the absorption area in this segment of the small intestine. The large intestine is approximately 1.50 m in length and the circumference is 0.24 m and can be sub-divided into the cecum, colon and the rectum (Kararli, 1995; Martini *et al.,* 2012).

2.2.2 Comparison between the anatomy of the human and pig gastrointestinal tract

Pig intestinal tissue is often used to assess drug absorption from medicinal formulations and it is imperative that researchers are familiar with the differences and similarities (e.g; biochemical, physiological and anatomical attributes) between the GIT of humans and pigs (Kararli, 1995). A comprehensive comparison between the human and pig GIT is presented in Table 1.

Table 2.1: Comparison between the human and pig gastrointestinal tract anatomy

	Human GIT	**Pig GIT**
Length of small intestine	Approximately 6.25 m (Martini *et al.,* 2012)	Approximately 18.29 m (Kararli, 1995)
Diameter of the small intestine	5 cm (Kararli, 1995)	2.5-3.5 cm (Kararli, 1995)
GIT pH fasted	1.7 (Kararli, 1995)	1.6-1.8 (Kararli, 1995)
GIT pH fed	5.0 (Kararli, 1995)	<2.0 (Kararli, 1995)
Capacity of the stomach	Approximately 1-1.6 L (Kararli, 1995)	Approximately 8.0 L (Kararli, 1995)

2.3 Drug absorption mechanisms from the gastrointestinal tract

The most commonly used route for the administration of drugs or health supplements is the oral route because of the convenience, especially with chronic drug use (Xiao *et al*., 2016). The oral route of administration is very user-friendly since there is no need for medical personnel to administer drugs (compared to the intravenous and/or intramuscular injection route where trained health care workers are needed to do the injections), there is no risk of infection and no pain is associated with this route of administration (Lennernäs, 2007; Sarmento *et al.,* 2012).

Most drugs are absorbed via passive diffusion where molecules are transported from an area with a high concentration to a low concentration and no external energy is required to aid the transport of molecules across biological membranes. The high drug concentration on the one side of the biological membrane (mucosal side/GIT) and the low concentration on the other side (the blood) is the driving force behind passive diffusion (Shargel *et al.,* 2012).

Active transport is the opposite of passive diffusion and describes the transport of drug molecules from a low concentration to a high concentration, thus against the concentration gradient and this process is energy dependant. Active transport requires carrier molecules to transport the drug molecules across biological membranes and once the drug-transporter complex has crossed the membrane the drug is detached from the carrier and released into the blood (Shargel *et al.,* 2012).

2.3.1 Passive paracellular transport

Passive diffusion through the intercellular spaces via tight junctions (aqueous pores) between adjoining cells rather than across cells is known as paracellular transport. These tight junctions are holding epithelial cells together, which are located in many different sites throughout the body and the “tightness” of these tight junctions may vary significantly due to differences in cellular composition (Ashford, 2013). The cut-off weight for molecules which are absorbed via this mechanism is considered to be approximately 200 Da and favours hydrophilic molecules, ions and amino acids (Ashford, 2013; Sarmento *et al.,* 2012).

2.3.2 Passive transcellular transport

Molecules that are most likely to diffuse across biological membranes via the transcellular pathway are lipophilic drug molecules such as medium chain triglycerides, surfactants and fatty acids (Sarmento *et al.,* 2012). The term sink conditions are used to describe an extra volume amount of a medium that allows a solid drug (such as tablets) to continuously dissolve in the GIT. For sink conditions to apply the concentration of drug on the acceptor side (the blood) needs to be lower than on the donor side (the GIT) for the concentration gradient to exist and this happens due to the blood flow lessening the drug and allowing more drug to be transported across the membrane (Flaten *et al.,* 2006; Shargel *et al.,* 2012).

2.3.3 Carrier-mediated transport

Carrier-mediated transport describes the process where a drug molecule or compound is transported across a biological membrane by forming a complex (carrier-drug complex) with a transporter molecule located on the apical surface of the membrane and the complex is then transported across the membrane, which is followed by a subsequent dissociation of the carrier-drug complex on the basolateral side of the membrane. The transporter will then resume its original position on the apical side of the membrane in its re-activated form ready to form another carrier-drug complex (Ashford, 2013; Shargel *et al.,* 2012).

Carrier-mediated transport can be sub-divided into two distinct processes namely, facilitated diffusion/transport and active transport. Secondary active transporters are indirectly coupled to the ATP energy possibly through the generated gradients with diverse energy mechanisms like Na^+/K^+ ATPase and proton gradient, while primary active transport straight uses ATP throughout the transport cycle (Sarmento *et al.,* 2012). Facilitated diffusion is a transport mechanism where a drug molecule is transported by forming a carrier-drug complex, while the direction of transport occurs from a region with a high drug concentration to a region with a low drug concentration (along the concentration gradient). This form of

carrier-mediated transport does not require energy, but the carriers may become saturated at high substrate concentrations and the carriers are selective for the compounds which it binds and transports (Shargel *et al.,* 2012)

2.3.4 Efflux transport

Efflux transporters or proteins play an important role in drug bioavailability and these transporters are responsible for reducing the uptake of xenobiotics from the lumen to the blood (Ashford, 2013; Shargel *et al.,* 2012). Efflux transport is discussed in more detail in section 2.4.2.2 (P-glycoprotein) of this dissertation.

2.3.5 Vesicular transport

Vesicular transport is described as engulfing of dissolved materials or particles by the cell and is divided into phagocytosis and pinocytosis. Pinocytosis is the process of engulfment of small solutes and fluids for transport (Shargel *et al.,* 2012).

2.4 Health supplement-drug pharmacokinetic interactions

The term “Pharmacokinetics” is defined as the classification and study of drug absorption, distribution, metabolism and elimination (ADME) of a drug over a specific time course (Ashford, 2013). The various drug transport mechanisms and metabolizing enzymes are key factors that influence/mediate pharmacokinetic interactions between different drugs, supplements and herbs and are in most cases responsible for mediating changes in drug distribution and/or excretion (Wu *et al*., 2016).

2.4.1 Effects of health supplements on drug metabolism

Environmental factors, endogenous host factors and several genetic factors are known to affect the activity of cytochrome P450 (CYP450) enzymes (Pelkonen *et al.,* 2008). Drugs and supplements that undergo a high degree of intestinal metabolism not only have low bioavailability but are more prone to drug-drug or supplement-drug interactions with CYP450 inducers or substrates. Their pharmacokinetic profiles usually also present with large variations due to the extensive degree of intestinal metabolism. The degree of intestinal metabolism or biotransformation may chiefly be attributed to the various CYP450 enzyme isoforms, which are present in the specific tissue and great effort has been made to elucidate the various CYP450 enzyme isoforms that occur in human and animal models (Xie *et al.,* 2016).

The superfamily of CYP450 consists of 57 CYP450 genes as encoded by the human genome. In the human body, CYP450, is sub-divided into 18 families, which are collectively responsible for the metabolism/biotransformation of xenobiotic substrates, endogenous hormone synthesis (including retinoids, steroids and eicosanoids). A significant number of CYP450 splice/joint variations from subfamilies 1A, 1B, 2C, 2D, 3A, 4F, 19A and 24A have been identified and some have been directly linked to disease pathology (Table 2) because of their catalytic function or alternative subcellular distribution (Annalora *et al.,* 2017; Go *et al.,* 2015). In the human body, the CYP3 family is the most abundant CYP450 subfamily responsible for drug biotransformation and represents approximately 30% of the total hepatic CYP450. The CYP3 family consists of CYP3A34 (pseudoprotein) and three proteins (CYP3A4, CYP3A5 and CYP3A7). The CYP3 family metabolizes a wide range of compounds which include; midazolam, testosterone, simvastatin, erythromycin and sildenafil (Lin & Lu, 1998; Pelkonen *et al.,* 2008).

Table 2.2: CYP450 splice/joint variations and linked pathologies (adapted from Annalora *et al.,* 2017)

CYP450 Isoform	Linked pathology
CYP1A1	Ovarian cancer
CYP1B1	Glaucoma
CYP2A6	Lung cancer
CYP2B6	Liver/colon cancer
CYP19A1	Aromatase deficiency
CYP24A1	Colon, prostate/breast cancer Atherosclerosis

CYP1 family, a CYP450 isoform, forms part of the CYP450 super family and consists of three proteins, including CYP1A1, CYP1A2 and CYP1B1. CYP1 family plays an important role in the metabolism of xenobiotics and endogenous hormones. CYP1A1 is mainly found in the human body at the following sites: extrahepatic tissues that include the thymus, uterus, pancreas and small intestine and contributes to the metabolism of a diverse range of xenobiotics. CYP1B1 is recurrently over-expressed in tumour and cancer tissues but is also found in extrahepatic tissues such as the uterus, breasts and prostate (Annalora *et al.,* 2017; Go *et al.*, 2015).

The most relevant CYP450 enzymes that are usually present at the areas where absorption and/or metabolism of health supplements and drugs occur are listed in Table 3.

Table 2.3: Cytochrome P450 enzymes that are commonly found in the small intestine and/or liver (adapted from Pavek & Dvorak, 2008)

CYP450 enzyme	Small intestine	Liver
CYP1A1	+	++
CYP1A2	-	+++
CYP1B1	+	+
CYP2A6	-	+++
CYP2D6	++/+	+++
CYP3A4	+++	+++
CYP3A5	+++/++	+++/++

+++ High expression
++ Moderate expression
+ Low expression
- Unnoticeable expression
+/- Debatable expression

2.4.1.1 Induction of cytochrome P450 enzymes

Some exogenous compounds are known to induce CYP450 enzymes by ligand-activated transcription factors and the induction process may include intracellular receptors such as nuclear receptors (pregnane X receptor or PXR, NR112), constitutive androstane receptors (CAR, NR113) and aryl hydrocarbon receptors (AhR). These receptors act in a symbiotic manner to regulate the activity of phase 1 and 2 metabolizing enzymes and various transporters. The glucocorticoid receptor and oestrogen receptors have also been implicated in the induction process of CYP450. Induction of enzymes may decrease pharmalogical effect and increase elimination of a drug that is active in its parent form (Pelkonen *et al*., 2008).

A range of drugs, herbs and supplements that are often associated with the induction of CYP3A4 and CYP3A5 are listed in Table 4.

Table 2.4: Cytochrome 3A4 and 3A5 inducers and the associated receptors (adapted from Pavek & Dvorak, 2008; Pelkonen *et al.,* 2008; Xie *et al.,* 2016)

Enzyme	Inducer	Receptor involved
CYP3A4	Rifampicin	PXR
	Ritonavir	PXR
	St. John's wort	PXR
	Carbamazepine	CAR
	Efavarenz	CAR
	Nevirapine	CAR
	Phenytion	CAR/PXR
	Dexametazone	PXR/GR
	Prednisolone	PXR/GR
	Black pepper (piperine)	PXR
	Vitamin D3 (1α,25-dihydroxyvitamin D3)	VDR, NR111
	3.3'-diindolylmethane (a herbal nutritional supplement)	PXR
CYP3A5	Rifampicin	PXR
	Topical Clobetasol 17-propionate	GR

2.4.1.2 Inhibition of cytochrome P450

The most common cause for drug-drug or supplement-drug interactions is the inhibition of CYP450 enzymes and this can lead to increased bioavailability or decreased first-pass metabolism. The steady state concentration can increase if the metabolism via single-pathway is inhibited. Cytochrome P450 inhibition reactions can be divided into two main categories namely reversible and irreversible reactions (also known as mechanism-based inhibition). Reversible inhibition takes place without metabolism and as a result it occurs due to competition at the enzymes active site, while irreversible inhibition or mechanism-based inhibition occurs after inhibitor biotransformation. The latter occurs via strong covalent binding of intermediates to the heme or protein of CYP450 enzyme or the forming of complexes with the metabolite intermediate. The most common type of enzymatic inhibition is reversible inhibition (binding of substrate with the enzyme is typically with weak bonds such as Van der Waals forces and hydrogen bonds) and can be divided into uncompetitive, non-competitive, competitive and mixed type inhibition. During uncompetitive inhibition, the inhibitor does not bind to the free enzyme unit but to the enzyme-substrate complex, in non-competitive inhibition the active site for binding of the inhibitor and substrate are different, for competitive inhibition the substrate and inhibitor compete for the same position on the enzyme (the active site) and mixed type inhibition displays a combination of elements from the mentioned inhibition mechanisms (Lin & Lu, 1998; Pelkonen *et al.*, 2008).

2.4.2 Effects of health supplements on efflux transporters

2.4.2.1 ATP-binding cassette (ABC) superfamily

The two major transporter superfamilies that are involved in drug-drug, herb-drug and supplement-drug interactions include solute carrier (SLC) and ABC transporters. SLC transporters are comprised of organic cation and anion transporters (OCTs & OATs) and organic anion-transporting polypeptides (OATPs). ABC transporters are P-gp, breast cancer resistance protein (BCRP/ ABCG2) and multi-drug resistance protein (MRPs). There are currently six recognized MRPs and the most generally known is MRP1 (ABCC1), MRP2 (ABCC2) and MRP3 (ABCC3) and they interrupt drug disposition. The ABC transporters primarily facilitates the efflux of drug and supplement molecules. The main efflux pumps of ABC transporters (P-gp, MRPs and ABCG2) are largely expressed in the proximal tubules of the kidney, hepatocytes canaliculi and luminal membrane (Shargel *et al.,* 2012; Wu *et al.,* 2016).

2.4.2.2 P-glycoprotein (P-gp)

P-glycoprotein belongs to the collection of transporters known as adenosine triphosphate binding cassette (ATP-binding cassette or ABC) and is a 170 kDa plasma membrane glycoprotein molecule. P-gp is present on the superficial columnar intestinal epithelial cells and is highly articulated on the enterocyte apical side of the GIT membrane the P-gp present on the apical surface of the intestinal epithelia cells may affect drug and supplements elimination, distribution and absorption (Sarmento *et al.,* 2012; Zhao *et al.,* 2016).

P-gp a product of the MDR1 gene (multi-drug resistance) is also termed ABCB1 and can bind to a wide range of substrates. P-gp is found in several epithelial cells, including; the proximal tubules in the kidney, the colon, the endothelial cells in the brain capillaries, the testis, the placenta, adrenal glands and the luminal surface of the small intestine. Expressively higher levels of P-gp is found in the small intestine compared to the colon in the large intestine. P-gp is also expressed extensively in tumour cells. The cells in the human body are protected against toxins by P-gp because P-gp removes toxins by actively transporting the toxins out of the cells. Drug absorption is also limited by P-gp related efflux and is responsible for the limited oral bioavailability of many drugs, which are known P-gp substrates (Ashford, 2013; Shargel *et al.,* 2012; Wempe *et al.,* 2009; Wu *et al.,* 2016; Zhao *et al.,* 2016).

Efflux transporters, for example P-gp (on the apical side of enterocytes), serve as a first-mark barrier for different orally administered drug and supplement compounds to be absorbed into systemic circulation (Wu *et al.,* 2016).

Rhodamine-123 is a selective marker and model substrate for P-gp and may be used to study P-gp's functional action and probable drug interactions (Al-Mohizea *et al.*, 2015). Grapefruit juice can increase the plasma level of many drugs that are CYP450 substrates because it contains naringin that inhibits certain CYP450 enzymes. The increase in drug plasma levels is due to a decrease in pre-systemic elimination in the liver or GIT. Grapefruit juice is one of the food groups that contains substrates for P-gp and inhibits the efflux and affects the transport of drugs and supplements in the intestinal wall (Shargel *et al.,* 2012). In *in vivo* interactions, berberine and verapamil inhibited P-gp and indomethacin inhibited MRP1. Silymarin inhibited hOAT1 (uptake transporter found in proximal tubule and hepatocytes basolateral side) in *in vitro* interaction studies (Shargel *et al*., 2012; Wu *et al.,* 2016).

Table 2.5: *In vitro* and *in vivo* interactions of supplements and drugs with transporters (adapted from Shargel *et al.,* 2012; Wu *et al.*, 2016)

	***In vitro* interactions**	***In vivo* interactions**
Supplement or drug		
Berberine	Induction of P-gp Inhibition of P-gp ABCG2 down-regulation	Inhibition of P-gp
Silybinin (Silymarin/ Milk thistle)	Inhibition of hOAT1	
Verapamil		Inhibition of P-gp
Indomethacin		Inhibition of MRP1

2.5 Models for the evaluation of drug permeation

2.5.1 *In situ* models

In situ models refer to the use of an organ(s) as part of a living organism on which studies are performed, thus the experiment is performed on parts of the body that has not been completely removed from the host. These models offer many advantages such as intact blood flow, nerve systems, intestinal mucosal layers and the presence of drug transporters and metabolising enzymes (Holmstock *et al.,* 2012). These methods require highly sophisticated surgical procedures and instrumentation and thus not every laboratory can perform these complex procedures. *In situ* studies entail direct and indirect *in situ* measurements; direct *in situ* measurements refer to the absorption of the drug and subsequent measurement of the drug fraction that was removed from the gastrointestinal tract during a specific time interval. Indirect *in situ* measurements entails the use of secondary indicators such as elapsed time before pharmacological action, urinary excretion versus time values or lag time/onset time values (Luo *et al*., 2013). According to Luo *et al*. (2013) there are 7 types of *in situ* perfusion techniques that are commonly used namely the closed-loop method, Thiry-Vella fistula, intestinal single-pass perfusion, intestinal recirculating perfusion, intestinal perfusion with venous sampling, vascularly perfused intestine-liver (IPIL) and Loc-I-Gut.

2.5.2 *In silico* models

In silico models make use of high-performance computer aided modelling or simulations to determine significant pharmacokinetic parameters (Yang, 2009). According to Grime *et al*. (2013) the use of *in silico* models to assist in the design of therapeutically active compounds that have the main aim to direct drug metabolism and pharmacokinetic property studies and not just predict human pharmacokinetics by itself are very helpful for directing drug designs.

In silico methods include three-dimensional quantitative structure-activity relationship analysis, structure-activity relationship investigations, pharmacophore identification and also simple rule-based modelling such as the use of Lipinski's "rule of five" for candidate drugs that made it to clinical trials (phase II) with adequate absorption properties (Grime *et al*., 2013; Yang, 2009).

2.5.3 *In vivo* models

In vivo studies are performed in living organisms (animal or human subjects) and are of paramount clinical importance to help determine drug specific pharmacokinetic parameters such as absorption, distribution, metabolism and elimination (ADME) following either intravenous or extravascular drug administration (Yang, 2009). Drugs may be administered via various routes followed by blood sampling and/or tissue biopsies at specific time points and the resultant drug concentrations in the samples are then determined by analytical methods such as HPLC or LC/MS/MS analysis (Hidalgo, 2001).

2.5.4 *In vitro* models

During the initial stages of drug discovery and development, it is not feasible to perform studies on living animal models due to ethical considerations, cost implications, and time constraints. These considerations have led to the development of various *in vitro* models that may be used during the initial stages of drug discovery and development to help identify possible lead compounds which may then be subjected to further testing (Deferme *et al.,* 2008; Sarmento *et al*., 2012). *In vitro* models have been developed to investigate the transport of compounds across intestinal tissues in glass containers, in diffusion chambers, across artificial membranes, shake flask methods, transport across cell culture monolayers and surface plasma resonance biosensor analysis (Ashford, 2013; Tarirai, 2011).

Table 2.6: Comparison of various *in vitro* models and techniques to highlight their associated advantages and limitations

***In vitro* models / techniques**	**Technique**	**Advantages**	**Limitations**
Cell culture models			
Caco-2 cell monolayer	• Isolated human colorectal carcinoma cells. • These cells grow in a monolayer, differentiate structurally and functionally. • They form several different pathways for transport. • They contain membrane transporters, tight junctions and P-gp (Sarmento *et al*., 2012).	• Used in the early stages of drug discovery to assess drug permeability (Rozehnal *et al.,* 2012) • Caco-2 cell monolayer is the most used model for simulating intestinal epithelial monolayer and to predict the transport of drugs across the human intestinal wall. • The apical and basolateral compartments can be separated from each other (like in human intestinal tissue) (Sarmento *et al*., 2012).	• This technique lacks the physiological and morphological features of the intestines (Rozehnal *et al.,* 2012). • This model does not show a high enzyme content for CYP450 activity (Wempe *et al.,* 2009). • It also contains lower P-gp levels than other cell culture models (Sarmento *et al*., 2012). •
MDCK (Madin-Darby canine kidney) cells	• Isolated dog kidney epithelial cells. • Cells grow in a monolayer	• The MDCK cells are widely used for drugs that are passively absorbed (Sarmento	• The MDCK cells of non-human origin can be seen as a disadvantage because it has a

	(Sarmento *et al*., 2012). • The MDCK cells are used to study transport mechanisms, cell growth and drug metabolism in the distal renal epithelium (Irvine *et al*., 1999).	*et al*., 2012).	lower expression of metabolic activity and transport proteins in comparison to Caco-2 cells (Sarmento *et al*., 2012).
Excised tissue techniques			
Everted intestinal rings and closed everted sac technique	• This technique is used to predict the intestinal metabolism and transfer of drugs. • The carefully chosen intestinal piece is everted on a glass rod after the excision and is then filled with a solution of the drug that is being tested. • The absorption is determined by the intestinal weight difference before and after the fluid is drained (Luo *et al*., 2013).	• It is a very easy technique to use. • It helps to predict the possible intestinal metabolism and transfer of a drug (Luo *et al*., 2013).	• The everted sac can regularly lose its structural integrity (Luo *et al*., 2013).
Ussing Chambers	• Selection of appropriate tissue, cut/ dissected into strips of appropriate size. • Then mounted on the selected	• This technique is useful to investigate transport and metabolism *in vitro.* • Animal tissue is used to	• When the intestinal tissue is to thick the diffusion chambers can leak, and this can lead to problems with samples that is

	device (e.g. Sweetana-Grass diffusion chamber) • Transport of the drug is measured across the membrane (Legen *et al*., 2005).	investigate the intestinal transport of supplements/drugs and recognize reginal variations in transport (Lennernäs, 2007). • This technique can be used to study the processes of drug transport, different and possible drug-drug interactions, different absorption mechanisms and poorly absorbed drug permeability studies (Luo *et al.*, 2013).	withdrawn (Luo *et al*., 2013).

2.5.5 *Ex vivo* models

Ex vivo models are *in vitro* models that specifically entail the use of whole organs or excised tissues, which are removed from living organisms for experimental purposes. Examples include the use of excised tissues for everted sacs, excised tissue pieces for use in a diffusion chamber apparatus (Ussing chambers) and intestinal perfusion methods (Alqahtani *et al.,* 2013; Luo *et al*., 2013). Advantages of the *ex vivo* methods/technique include the presence of a viable mucosal layer and transporter proteins present in the intestine and the epithelium of the small intestine can be used to study paracellular permeability and metabolism of drugs (Luo *et al.,* 2013).

Ex vivo methods offer a quick and easy technique to study transport and metabolism of drugs in the intestine and may be used to study drug-drug interactions (Luo *et al.,* 2013). According to Luo *et al*. (2013) several disadvantages/limitations are also associated with the use of intestinal tissue in *ex vivo* models such as the presence of a serosa layer, which needs to be removed prior to the start of experimental procedures. If the serosa is not removed properly, the underlying tissue may be damaged which may have a detrimental effect on the drug permeation results and inconsistent/inaccurate data will be generated. These studies also require that large numbers of experiments are conducted to ensure that statistically justifiable conclusions can be made based on the generated data.

2.6 Commercially available health supplements selected for use in this study

2.6.1 Acetyl-L-carnitine

2.6.1.1 Uses and health related applications of acetyl-L-carnitine

Acetyl-L-carnitine (ALC) is a commonly used health supplement and it is commercially available in health stores. ALC can be acquired as an isolated health supplement and it is the short-chain ester of carnitine. It is reported to improve muscle strength and energy levels and it also has numerous effects on muscle and brain metabolism, defends against neurotoxic insults and in the future may be used as an effective treatment for specific types of depressions and neurological diseases such as diabetic neuropathies, helping in Alzheimer's dementia and Parkinson's disease (Malaguarnera *et al.,* 2008; Smeland *et al*., 2012; Zaitone *et al.,* 2012).

In developed countries there is a higher than normal prevalence of elderly people due to the availability of excellent health care facilities which increases life expectancy. Fatigue is certainly one of the conditions that the elderly complain about the most and ALC can help to

remove the excess short and medium fatty acids from the mitochondria that collect during metabolism to help with energy production (Malaguarnera *et al.,* 2008).

2.6.1.2 Mechanism of action of acetyl-L-Carnitine

When acetylcholine production is enhanced, phospholipid and protein syntheses occur due to the absorption of acetyl-coenzyme-A into the mitochondria for fuel and all of this happens during oxidation of long chain fatty acids. When the accumulated fatty acids produced during metabolism needs to be removed from the mitochondria, the removal process is facilitated by ALC. ALC also facilitates the transport of the long chain fatty acids required by the mitochondria (Malaguarnera *et al.,* 2008). In tissue that solely rely on fatty acid oxidation for high tissue-to-plasma concentration ratios of acetyl-L-carnitine and tissues of the body (e.g. muscle tissue), carrier-mediated transport is very important for the absorption of ALC. ALC is dependent on passive diffusion and carrier mediated transport for effective absorption from the GIT (Evans & Fornasini, 2003).

2.6.1.3 Pharmacokinetics of acetyl-L-carnitine

According to Evans & Fornasini (2003), the absolute bioavailability of an oral dose of ALC (1-6 g) is 5-18% and it is primarily eliminated via urinary excretion. The renal clearance for ALC is 1-3 ml/min. ALC can be found in three separate compartments throughout the human body namely the slow equilibrating tissues (likely to include the cardiac and skeletal muscle), fast equilibrating tissue (kidneys and liver) and in the extracellular fluid (initial distribution volume). Excretion of a 2 g dose is mainly from the kidneys and 70-90% of unchanged drug is found in the urine after 24 h (Evans & Fornasini, 2003). According to the study done by Evans & Fornasini (2003), when a 2 g oral dose of ALC was given to healthy patients (average values are given) the AUC (area under the concentration-time curve) was 779.9 µmol/h/L, the C_{max} (peak plasma concentration) was 80.3 µmol/L and the T_{max} (time to C_{max}) was 3.3 h.

2.6.2 Berberine

2.6.2.1 Uses and health related applications of berberine

Berberine is an isoquinoline plant alkaloid, which may be obtained from a variety of plants such as *Berberineeris* species, *Hydrastis canadensis* L., *Arcungelisia flaw* and *Coptidis rhizome* (Mistry *et al*., 2017; Tsang *et al.,* 2009). Because berberine is considered to be a traditional medicine or health supplement (and therefore not registered as a medicine) it does not have to go through all the strict preclinical and clinical testing that is mandatory by

regulatory agencies (Qiu *et al.,* 2009). Berberine has been reported to have multiple biological properties, which include anti-hypertensive, anti-hyperglycaemic, anti-tumour (in hepatoma and nasopharyngeal carcinoma), and anti-inflammatory effects (Lin *et al*., 2017; Tsang *et al.,* 2009). According to Tsang *et al.* (2009), berberine exhibits dose dependant effects, at high dosages (300 µM) berberine was found localized in the cell nucleus and at lower dosages (50 µM) it was found localized in the mitochondria of the cell. During a study performed by de Oliveira *et al*. (2016), which investigated the possible effect of berberine on Alzheimer's-like dementia involving acetylcholinesterase, it was reported that berberine may be employed as a potential neuroprotective agent and may help prevent memory loss by increasing acetylcholinesterase activity. Increased acetylcholinesterase activity may in turn prevent cell death and subsequently impede the progression of diseases like Alzheimer's disease (a neurodegenerative disease). Studies have also shown that berberine exhibits anti-diabetic properties and that it may promote body weight reduction and improve insulin action with a subsequent reduction in blood glucose levels and advantageous effects on lipid metabolism (Ye *et al*., 2016; Yin *et al.,* 2008).

2.6.2.2 Mechanism of action of berberine

Berberine's anti-diabetic action occurs via various mechanisms such as; glycolysis induction, mimicking insulin, increasing the action of insulin by activating 5' adenosine monophosphate activated protein kinase (AMPK), inhibiting DPP-IV activity, and the decrease of insulin resistance by the up-regulation of kinase C-dependant protein expression of the insulin receptor (Bahadur *et al.,* 2017). Berberine's anticancer activity may be attributed to a range of mechanisms which include apoptosis (natural cell death), induction of cell cycle arrest and the inhibition of NF-$_K$B paths (Tsang *et al.,* 2009).

2.6.2.3 Pharmacokinetics of berberine

In general, berberine has been reported to exhibit poor bioavailability due to its low aqueous solubility characteristics and also due to the influence of P-gp related efflux (Bahadur *et al.,* 2017). In a study done by Zhang *et al.* (2013), the absorption of berberine was significantly increased in the presence of verapamil (a known P-gp inhibitor), which suggested that berberine is a substrate of intestinal P-gp and may therefore compete with other P-gp substrates at the drug-binding site of P-gp. Berberine exhibited a K_i (inhibition constant) of 0.54 µM in a study conducted by Mak *et al.* (2014), which investigated the inhibition of acetylcholinesterase. The following pharmacokinetic parameters of berberine have been documented by Alolga *et al.,* (2016) after 600 mg berberine was taken orally; $T_{1/2}$ = 2.57 h,

T_{max} = 4.00 h, C_{max} = 0.16 ng/ml, AUC = 0.96 ng/h/ml and the apparent volume of distribution was documented as 1926.46 ml.

2.6.3 Chondroitin sulfate

2.6.3.1 Uses and health related applications of chondroitin sulfate

According to Rani *et al*. (2017), chondroitin sulfate (CS) forms part of the connective tissues in the body and plays a major role in a variety of biological processes such as the promotion of cartilage integrity and resilience and the maintenance of synovial fluid in the joints. CS is categorised as a sulfated glycosaminoglycan and can largely be found in nerve tissues, ligaments, tendons and cartilage (in the extracellular matrix) (Xiao *et al.,* 2016). CS has been widely used as a health supplement for the treatment of osteoarthritis and associated joint pain and stiffness (Rani *et al*., 2017; Shang *et al*., 2016). CS administered at high dosages, also exhibited anti-inflammatory effects during a study conducted by Roman-Blas and colleagues 2017.

2.6.3.2 Mechanism of action of chondroitin sulfate

CS forms part of the group glycosaminoglycans, which are comprised of sulfate esters and repeating disaccharides of uronic acid and hexosamine (Doege *et al.,* 1997). According to a study done by Xiao *et al.* 2016 CS inhibited the expression of interleukin-6 (IL-6), cyclooxygenase-2 (COX-2), monocyte chemoattractant protein-1 (MCP-1) and C-reactive protein (CRP), in the peripheral blood mononuclear cells CS helps to reduce the nuclear translocation of nuclear factor-κB (NF-κB).

2.6.3.3 Pharmacokinetics of chondroitin sulfate

CS is known for its poor bioavailability, which usually ranges between 0–13% following oral administration (Shang *et al*., 2016). The C_{max} of CS was reported to be approximately 200 ng/ml in the plasma after a single orally administered dose of 1200 mg and the AUC was 3.60 µg/h/ml (Jackson *et al.,* 2010; Onishi *et al.,* 2013).

2.6.4 D-glucosamine

2.6.4.1 Uses and health related applications of D-glucosamine

D-glucosamine is a natural component in glycosaminoglycan, which can be found in the cartilage matrix and synovial fluid (Bruyère *et al.*, 2016). D-glucosamine is regularly used in

the treatment of osteoarthritis and exhibits anti-inflammatory effects, it is seen as Symptomatic Slow Acting Drugs for Osteoarthritis (SYSADOAS) (Roman-Blas *et al.,* 2017).

2.6.4.2 Mechanism of action of D-glucosamine

When D-glucosamine is administered exogenously, it elicits pharmacological effects on chondrocytes and osteoarthritic cartilage. *In vitro* D-glucosamine reduces prostaglandin E2 production, inhibits the activation of the kappa β pathway (a nuclear factor) and reduces nitric oxide, therefore inhibiting the cytokine intracellular signalling cascade in synovial cells and chondrocytes (Bruyère *et al.*, 2016; Roman-Blas *et al.,* 2017).

2.6.4.3 Pharmacokinetics of D-glucosamine

D-glucosamine has a low bioavailability and it was believed to be due to first-pass metabolism in the liver, but according to Ibrahim *et al.* (2012), low D-glucosamine bioavailability in the rat model was due to gastrointestinal metabolism and not metabolism in the liver. The bioavailability of D-glucosamine is dose independent and varies from 0.05-0.06%. According to Jackson *et al.* (2010), the following values for glucosamine were noted: AUC was 2380 ng/h/ml, C_{max} was 492 ng/ml and T_{max} was noted as 2.31 h.

2.6.5 Silymarin

2.6.5.1 Uses and health related applications of silymarin

Silymarin is extracted from Milk thistle (*Silybum marianum*) and is used as a bioactive for the potential treatment of a wide variety of liver diseases. It is a health supplement, which is advertised to offer possible therapeutic benefits for liver function and to treat liver diseases like chronic hepatitis (Chang *et al*., 2015; Wu *et al*., 2009). Silymarin has hepatoprotective effects, and some reports state that silymarin may protect the liver against different medications, which are known to cause hepatotoxicity, for instance acetaminophen, amanitin and thioacetamide (Komoroski, 2000; Wu *et al*., 2009). According to Komoroski (2000), patients only reported that the use of milk thistle gave them a mild laxative effect at high dosages.

2.6.5.2 Pharmacokinetics of silymarin

This health supplement's concentration peaks in plasma (T_{max}) at 2–3 h following oral administration, it has an elimination half-life ($t_{1/2}$) of 2–4 h and the C_{max} value of 1.1-1.3 µg/ml. Silibinin is the main component in Milk thistle and recent studies have shown possible interactions of silybin with CYPs and therefore the opportunity exists for herb-drug

interactions. In the liver microsomes, silymarin is a non-competitive inhibitor of CYP3A4 (IC_{50} = 29 µM) and CYP2C9 (IC_{50}=44 µM) activity. Silymarin is largely excreted into urine and bile because of the numerous conjugation reactions it experiences from the phase I & II metabolism (Komoroski, 2000; Wu *et al*., 2009). According to Wu *et al*. (2009) the *in vivo* effect of silymarin on drug pharmacokinetics are limited in spite of the inhibiting effect on P-gp related transport and the inhibition of CYP450 enzymes.

2.7 Summary

From the literature it is clear that consumers of commercially available health supplements usually neglect to inform their HCP about using health supplements/bioactive supplements in conjunction with their prescription medication and that HCP also neglect to ask their patients about their health supplement usage. This may be because most patients are not aware of the possibility of potentially dangerous health supplement-drug interactions that may occur. Studies have shown that one in every four patients whom use Western medication are also taking additional health supplements without their HCP's knowledge. The risk for health supplement-drug interactions may be greater in patients using multiple chronic drug regimens for several chronic medical conditions (Yamada *et al*., 2014; Yong *et al*., 2014).

Alteration of drug pharmacokinetics often leads to unwanted effects by drugs, especially those with narrow therapeutic ranges (Wu *et al*., 2016). Screening of health supplements to identify pharmacokinetic interactions with drug molecules is essential to inform patients accordingly to prevent potential drug failure or adverse events.

A wide variety of experimental models are available to researchers, which may be employed to investigate potential supplement-drug interactions. These models include *in situ* (performed on organs that is still part of the living organism), *in sillico* (computer simulations), *ex vivo* (excised tissue), *in vitro* (cell culture studies) and *in vivo* (experiments executed on living organisms).

The use of pig intestinal tissue is relevant due to many similarities between human and pig intestinal tissue. The presence of CYP450 enzymes, tight junctions and P-gp in the viable intestinal tissue will make it possible to investigate various interactions such as P-gp related efflux inhibition/induction, TEER reduction and a range of other possible interactions.

In conclusion, based on the literature study, it is evident that health supplements form an important part of many treatment approaches related to various health issues, but the current literature regarding these health supplements pharmacokinetic interactions (interactions with drugs and different supplements) is still not sufficient to understand all the possible drug-supplement interactions. It is of great importance to investigate the possibility

of potential interactions that may occur between these health supplements and co-administered medication and these investigations should be conducted in the form of properly planned scientific studies. The results gained from this study will contribute to the health related knowledge of the broader community, scientific community and health care practitioners.

CHAPTER 3: MATERIALS AND METHODS

3.1 Introduction

In this study, the effect of selected commercially available health supplements on membrane permeation was investigated using rhodamine-123 (RH-123), which is a well-known P-gp substrate, as a marker molecule. The membrane permeation altering effects of the selected health supplements were studied using excised pig intestinal tissue mounted between the half-cells of a Sweetana-Grass diffusion apparatus as an *ex vivo* model (Al-Mohizea *et al*., 2015). The selection of pig intestinal tissue as an *ex vivo* model was based on the many similarities, which are shared between pig and human intestinal tissue and also to comply with the 3R's principle (Kararli, 1995). Bi-directional membrane permeation studies of RH-123 were conducted in Krebs-Ringer bicarbonate buffer (KRBB) in the absence and presence of the selected commercially available health supplements where absorption is represented by the apical-basolateral (AP-BL) transport of RH-123 and secretion by the basolateral-apical (BL-AP) transport of RH-123. The experimental samples were collected at predetermined time intervals and analysed for their RH-123 content using a validated fluorescence spectrometry method. The validation of the fluorescence spectrometry method was done in terms of linearity, accuracy, precision, limit of detection, limit of quantification and specificity and the results confirmed compliance of the analytical method (USP-NF, 2018).

3.2 Materials

Sodium bicarbonate, Krebs-Ringer bicarbonate buffer (KRBB), RH-123 and Lucifer Yellow (LY) CH dilithium salt were bought from Sigma-Aldrich (Johannesburg, Gauteng, South Africa) and the selected health supplements and the relevant suppliers are listed in Table 3.1. Verapamil was donated (Novartis) and the Costar® 96-well plates was purchased from The Scientific Group (Randburg, Gauteng, South Africa). Excised pig intestinal tissue was collected on the day of each experiment from the local abattoir in Potchefstroom, North-West.

Table 3.1: List of the selected health supplements and their suppliers

Health supplement	Supplier
Acetyl-L-Carnitine HCl	Warren Chem Specialities, Johannesburg
Berberine chloride	Alfa Aesar, Johannesburg
Chondroitin sulfate	Warren Chem Specialities, Johannesburg
D-Glucosamine hydrochloride	Alfa Aesar, Johannesburg
Silymarin	Sigma-Aldrich, Johannesburg

3.3 Fluorescence spectrometry method validation for Rhodamine 123 and Lucifer yellow

The RH-123 and LY content of all the transport samples were analysed by means of fluorescence spectrometry (Spectramax® Paradigm plate reader). The fluorescence of the transport samples (180 µl) was measured at excitation and emission wavelengths of 480 nm and 520 nm for RH-123 and excitation and emission wavelengths of 485 nm and 530 nm for LY, respectively (Irvine *et al.,* 1999; Kaprelyants & Kell, 1992).

3.3.1 Linearity

Linearity of an analytical method describes the ability of the method to obtain detection values (peak areas) in direct correlation to the concentration of analyte in the sample. Determining the useful concentration range where the instrument response can be considered accurate, in relation to the analyte concentration in the sample, forms an essential part of the process. Three to six samples of each concentration in the specified range should be analysed and a correlation coefficient value of at least $r^2 > 0.998$ should be obtained before it can be considered an acceptable fit of data to the regression line (Shabir, 2003; Singh, 2013; USP-NF, 2018).

To determine linearity of the fluorometric analytical method, two RH-123 stock solutions were prepared (5 µM and 2.5 µM), respectively. The stock solutions were then diluted by a factor of ten, four and three, respectively. The final concentrations of the dilution range (i.e. 5 µM, 2.5 µM, 0.5 µM, 0.25 µM, 0.05 µM, 0.025 µM, 0.005 µM, 0.0025 µM and 0.0005 µM) were analysed in triplicate and the respective average concentration values were used to construct a calibration curve and to calculate a corresponding r^2- value.

A stock solution of LY (50 µg/ml) was used to prepare serial dilutions of 50 µg/ml, 25 µg/ml, 12.5 µg/ml, 6.25 µg/ml, 3.125 µg/ml, 1.5625 µg/ml, 0.78125 µg/ml, 0.390625 µg/ml and

0.195313 µg/ml. The concentrations of the dilution range were analysed in triplicate and the respective average concentration values were used to construct a calibration curve and to calculate a corresponding r^2- value.

3.3.2 Accuracy

A sample containing a known concentration of an analyte may be used to determine the accuracy of an analytical method. The procedure entails analysis of at least nine samples of the test solution in order to determine how close the measured concentration values are in relation to the known concentration value of the prepared sample. The analytical method may be considered accurate if the percentage recovery of the samples is 100 ± 2% from the known concentration value (Shabir, 2003; USP-NF, 2018).

For the purposes of this study, ten samples containing either RH-123 (5 µM, 2.5 µM and 0.125 µM) or LY (50 µg/ml, 25 µg/ml and 12.5 µg/ml) were analysed and the respective concentration values were used to calculate the percentage recovery and the accuracy of the analytical method.

The accuracy was calculated for RH-123 and LY and it was concluded that the analytical method did comply with the stated criteria.

3.3.3 Precision

The term precision describes the degree of scatter that occurs between a series of measurements acquired from the same homogeneous sample under controlled environmental conditions. It is generally recommended that a series of at least nine sample measurements (three concentrations and three samples from each) should be acquired and that the sample concentrations should fall within the expected concentration range of the experimental samples (Singh, 2013). The precision of the analytical method was determined in terms of intra-day and inter-day repeatability according to the procedures discussed in the following paragraphs.

3.3.3.1 Intra-day repeatability

Intra-day repeatability entails a series of sample collections from the same sample solutions and analysis of the collected samples over a short time interval (i.e. on the same day). A percentage relative standard deviation (%RSD) value of ≤ 2% is considered acceptable between the consecutive measurements (Shabir, 2003).

Three test solutions containing different concentrations of RH-123 (5 µM and 2.5 µM and 0.125 µM) were analysed in triplicate three times during a one-day (24 h) period. The %RSD was calculated for each of the three concentrations.

For LY three different concentrations (50 µg/ml, 25 µg/ml and 12.5 µg/ml) was used and analysed three times at three different time intervals during a one-day (24 h) period. The %RSD was calculated for each of the three concentrations.

3.3.3.2 Inter-day repeatability

Solutions that contain RH-123 at three different concentrations (5 µM and 2.5 µM and 0.125 µM) were analysed on three consecutive days in triplicate (every day for three days on the exact same time). A %RSD of ≤ 2% between the average concentration values that were calculated during the three-day period is considered acceptable (Shabir, 2003). The analytical method did comply with the stated criteria.

To determine the inter-day precision of LY the same three concentrations were used (50 µg/ml, 25 µg/ml and 12.5 µg/ml). The LY concentrations in the three solutions were analysed on three consecutive days (every day for three days on the exact same time). The %RSD was calculated for each of the three concentrations.

3.3.4 Limit of detection (LOD) and limit of quantification (LOQ)

3.3.4.1 Limit of detection

The LOD of an analytical method is defined as the lowest concentration of an analyte in a sample that can be detected but not necessarily quantitated as an exact value (Singh, 2013). The LOD was calculated using Equation 1 (Shabir, 2013).

$$LOD = 3.3 \times \left(\frac{SD}{S}\right) \qquad \textit{(Equation 1)}$$

Where 3.3 represent the signal-to-noise ratio, SD is the standard deviation of the plate blanks and S represents the slope of the calibration curve.

3.3.4.2 Limit of quantification

LOQ describes the least amount of an analyte in a sample that can be quantitatively determined with appropriate accuracy and precision (Singh, 2013). LOQ was calculated using Equation 2 (Shabir, 2003).

$$LOQ = 10 \times \left(\frac{SD}{S}\right) \qquad \textit{(Equation 2)}$$

Where 10 represent the signal-to-noise ratio, SD represents the standard deviation of the plate blanks and S represents the slope of the calibration curve.

3.3.5 Specificity

Specificity is described as the ability of the combination of both the equipment and the analytical method/technique to accurately detect the analyte in the presence of other compounds in solution that may influence the detection of the specific analyte. An analytical method is considered to be adequately specific if the recovery of the analyte in the presence of other compounds that could be present is 100 ± 2% (USP-NF, 2018).

Solutions containing RH-123 alone and in combination with selected commercially available health supplements (acetyl-L-carnitine, chondroitin sulfate and D-glucosamine) were prepared and transferred to Costar® 96-well plates for analysis. Three test solutions were prepared, each containing 5 µM RH-123 in combination with one of the selected health supplements per test solution. A control sample was also prepared which contained 5 µM RH-123 only. The recorded fluorescence values (control and test solutions) were compared to each other to determine if the health supplements had interfered with the detection of RH-123. The analytical method did comply with the stated specificity criteria.

A different method was used to determine the concentration of RH-123 in the presence of berberine and silymarin because these supplements interfered with the specificity. The r^2 values of RH-123 in the presence of the highest concentration of these two supplements were calculated by using the method as described in section 3.3.1 (Linearity) of this dissertation.

3.4 Preparation of the buffer for transport studies

One container KRBB powder mixture (Sigma-Aldrich) was used and 1.26 mg sodium bicarbonate was added to the powder and the combination was made up to one (1) litre with distilled water to obtain a solution with a pH of 7.4. The KRBB was then mixed with the aid of a magnetic stirrer to ensure that all the powder was dissolved to obtain a homogenous solution. The prepared KRBB was stored in the fridge until it was required for experimental purposes (on the same day of preparation).

3.5 *Ex vivo* transport studies

3.5.1 Preparation of experimental solutions

The selected commercially available health supplements were used to prepare test solutions at two different concentrations. The specific experimental supplement concentrations were

chosen based on previously published literature where the first concentration represents the concentration in the extra-cellular fluid and plasma (i.e. a daily dose dissolved in 53 l) while the second concentration represents the anticipated extreme concentration that may be present in the small intestine directly after transition from the stomach (i.e. daily dose dissolved in 0.53 l) (Hellum *et al*., 2007).

Table 3.2: Selected health supplement concentration (% w/v) used in the bi-directional transport study (Hellum *et al.,* 2007)

Selected commercially available health supplement	**Recommended daily dose**	**Concentration of the health supplement in the experimental solution (% w/v)**	
		Daily dose in 53 l (low)	**Daily dose in 0.53 l (high)**
Acetyl-L-carnitine	3000 mg	0.005660	0.5660
Berberine	300 mg	0.000566	0.0566
Chondroitin sulfate	400 mg	0.000755	0.0755
D-glucosamine	1500 mg	0.002830	0.2830
Silymarin	1440 mg	0.002720	0.2720

The bi-directional transport of RH-123 across pig intestinal tissue was evaluated in the presence and absence of all the selected health supplements at the above-mentioned concentrations. RH-123 was added to the experimental solutions at a concentration of 5 µM to serve as a marker molecule to evaluate alterations in the extent of bi-directional membrane transport due to the presence of the selected health supplements (Forster *et al.,* 2012). RH-123 was chosen as a marker molecule and added to the experimental solutions because it is a known P-gp substrate, is relatively inexpensive, easy to detect with spectrophotometric methods and it shows negligible interference with metabolic processes (Al-Mohizea *et al.,* 2015).

The experimental test solutions (50 ml total volume) were prepared by adding RH-123 to KRBB to obtain a final RH-123 concentration of 5 µM. During the apical to basolateral transport (absorptive direction) experiments, the health supplement was mixed with RH-123 test solution (5 µM final concentration) and 7 ml were added to each chamber on the donor

side (apical) of the Sweetana-Grass diffusion chambers while the acceptor (basolateral) side of the diffusion chambers only received 7 ml KRBB.

During the BL-AP transport (secretory direction) experiments two separate test solutions were prepared. For the apical (acceptor) side, KRBB was mixed with the health supplement and 7 ml of this mixture were added to the Sweetana-Grass diffusion chambers while for the basolateral (donor) side a 5 µM RH-123 solution was prepared in KRBB and 7 ml was the added to the donor side of the chambers. The experimental health supplement solutions were prepared by weighing specific amounts of each supplement and then adding KRBB to achieve a final volume of 50 ml. The specific amounts of each supplement that were used to prepare the supplement experimental solutions are listed in Table 3.3.

Table 3.3: The amount (in grams) of each health supplement that was used to prepare the supplement solutions for the transport studies

Selected commercially available health supplement	**Quantity in g added to 50 ml total volume**	
	53 l	**0.53 l**
Acetyl-L-carnitine	0.002830	0.2830
Berberine	0.000283	0.0283
Chondroitin sulfate	0.000377	0.0377
D-glucosamine	0.001420	0.1420
Silymarin	0.001360	0.1360

3.5.2 Collection and preparation of pig intestinal tissue for *ex vivo* transport studies

Pig intestinal tissue was excised from the gastrointestinal tract of pigs (on each day of experimentation), which were slaughtered at the local abattoir (Potchefstroom abattoir, North-West) for meat production purposes. Directly after the pigs were slaughtered, a 30 cm segment of jejunum tissue was excised, flushed and rinsed with ice cold KRBB solution, with a pH adjusted to 7.4. After being rinsed, the excised tissue was immersed in ice cold KRBB solution and put on ice in a cooler box and transported to the laboratory (Zhao *et al*., 2016). Upon arrival at the laboratory, the excised pig jejunum was pulled over a dampened glass rod (Figure 3.1 A), and the serosa was removed using blunt dissection (Figure 3.1 B).

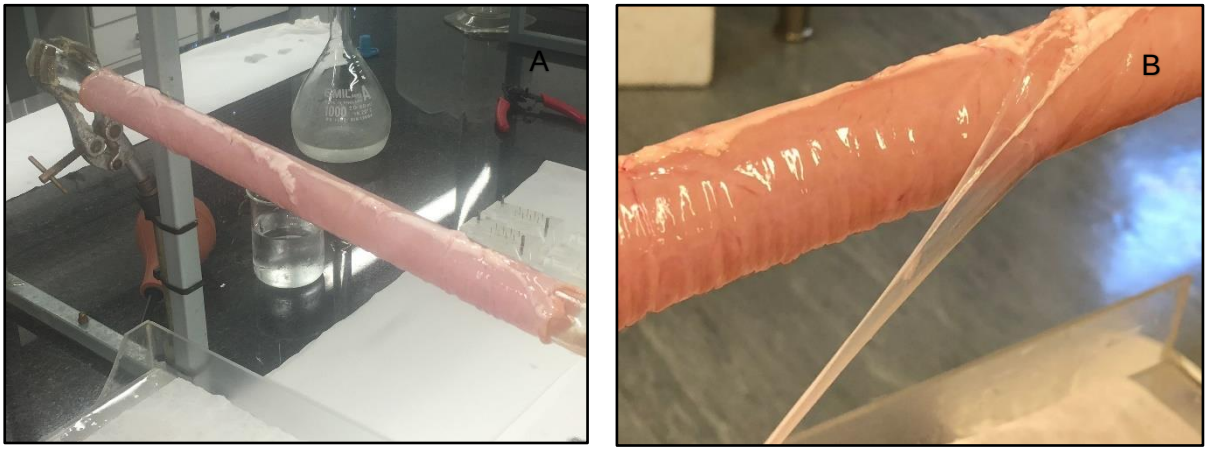

Figure 3.1: Photographs showing **A)** The pig intestinal tissue (with the mesenteric border visible on top) mounted on a glass tube, **B)** The serosal layer being carefully removed

After removal of the serosa, the intestinal tissue was inspected for Peyer's Patches (Figure 3.2) this tissue was not used for the transport studies.

Figure 3.2: Photograph showing a Peyer's patch on the excised pig intestinal tissue

After removal of the serosa the jejunum was cut along the mesenteric border (Figure 3.3 A) and placed onto a piece of heavy duty filter paper, on a glass plate, moistened and the excess GIT remains was cleaned with KRBB solution (Figure 3.3 B). Placing the tissue on the filter paper ensured that the tissue maintained a smooth surface texture (Figure 3.3 C).

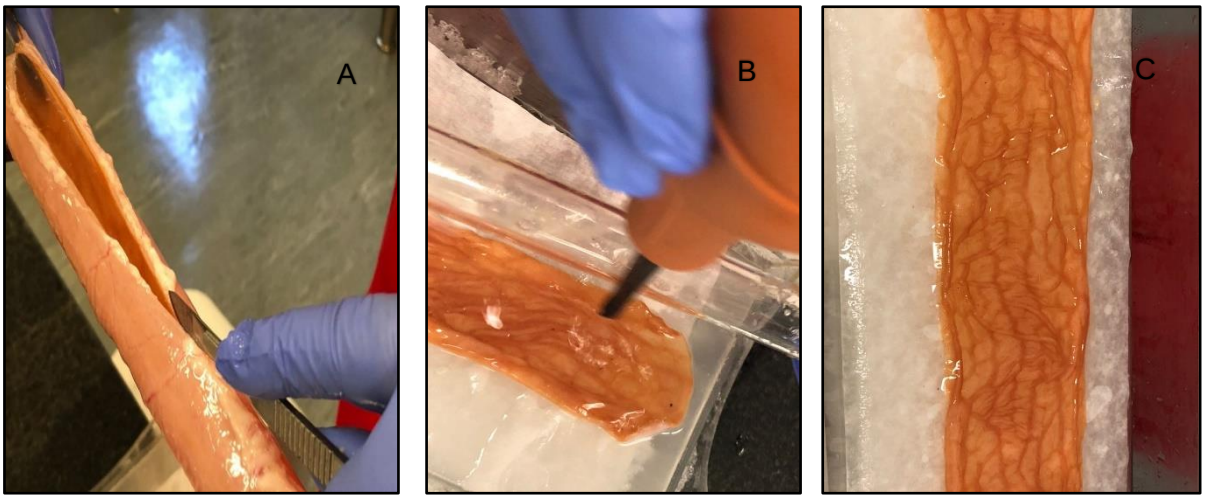

Figure 3.3: Photographs showing **A)** cutting the jejunum along the mesenteric border, **B)** transferring the jejunum from the glass tube and **C)** transferred to the filter paper ready to be cut into the correct size pieces

The pig jejunum was then cut into smaller segments of approximately 3 cm in length and 2 cm in width (Figure 3.4 A & B). The tissue segments were then mounted between the half cells of a Sweetana-Grass diffusion chamber apparatus (Figure 3.4 C-F). Six chambers were prepared for each of the transport experiments and the completed chambers were connected to the Sweetana-Grass diffusion chamber heating block (37°C) system and the system was then saturated with carbogen (95 % O_2-5 % CO_2) (Dahan & Hoffman, 2007; Legen *et al*., 2005; Pietzonka *et al.,* 2002).

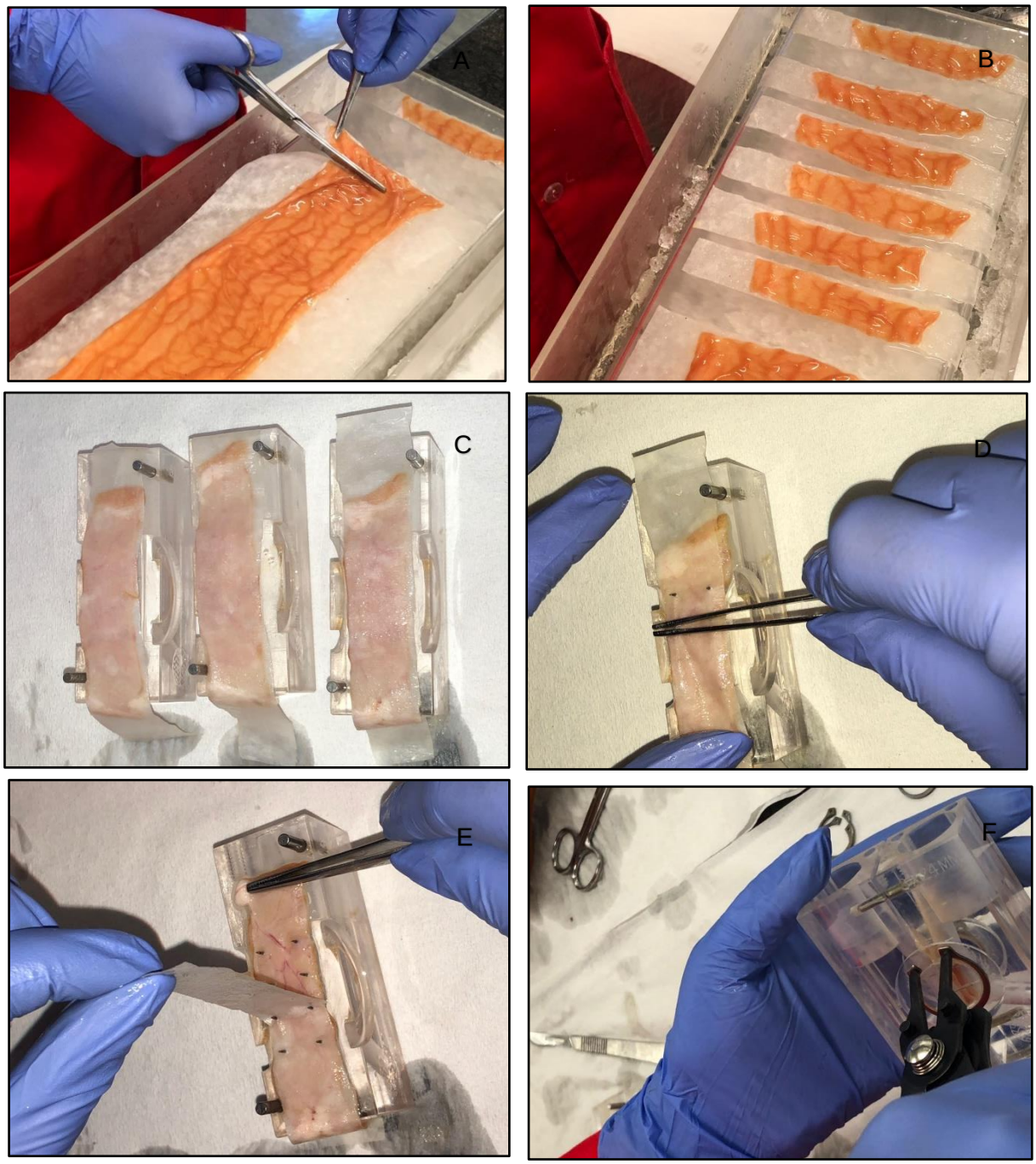

Figure 3.4: Photographs showing: **A)** and **B)** the process of cutting the jejunum into smaller pieces, **C)** and **D)** The process of the jejunum tissue being mounted on the half cells, **E)** the filter paper being removed and **F)** assembling the half cells into one single diffusion chamber ready for use

Figure 3.5: Photographs showing a completed Sweetana-Grass diffusion apparatus with mounted pig intestinal tissue between the half cells

3.5.3 Bi-directional transport studies using the Sweetana-Grass diffusion apparatus technique

The transport study experiments were performed in both the AP-BL and BL-AP directions for each of the selected health supplements. The tissue was allowed to equilibrate with the surrounding environment by adding 7 ml preheated KRBB to both sides of the membrane (apical and basolateral) and a 15 min incubation period was allowed. After 15 min, the KRBB was removed from both sides of the membrane and replaced with RH-123 and health supplement solution (AP-BL) on the donor side and for BL-AP, it was replaced with KRBB and health supplement (acceptor side) and RH-123 (donor side).

The membrane integrity and viability were monitored at the start and end of each experiment by taking TEER measurements (Addendum D). The TEER was measured using a dual epithelial voltage clamp (using Warner Instruments® EC-825A) (Pietzonka *et al*., 2002). Samples (180 µl) were withdrawn at the following time intervals; 20, 40, 60, 80, 100, 120 minutes from the acceptor side. After each withdrawal the volume was replaced with 180 µl of KRBB (apical to basolateral) and 180 µl of KRBB and health supplement solution (basolateral to apical). The solution and KRBB that was used to replace the withdrawn amount was preheated to 37°C.

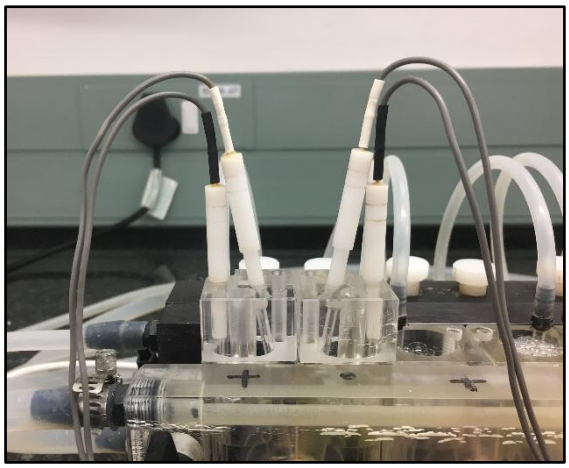

Figure 3.6: Photograph showing the measurement of TEER (with a dual epithelial voltage clamp) during the bi-directional transport studies using the Sweetana-Grass diffusion chamber apparatus

3.5.4 Analysis of transport samples

The concentration of RH-123 in the transport samples was determined by using the Spectramax Paradigm® multi-mode detection platform reader.

3.6 Assessment of intestinal tissue integrity with Lucifer yellow

Transport studies, with a marker molecule (i.e. Lucifer Yellow), was also conducted to monitor the tissue integrity over the duration of the transport study. Lucifer Yellow (LY) is a well-known fluorescent marker which is transported via the paracellular pathway and it can be used to verify the integrity of the tight junctions and to determine if any mechanical damage had occurred during the removal of the serosal layer. A 50 ml solution of LY (2.5 mg) and KRBB was prepared and used to perform apical to basolateral transport studies. LY was quantified with a validated fluorometric method and the excitation wavelength was set at 485 nm and the emission wavelength at 530 nm. The fluorescence values were used to calculate corresponding transport and P_{app} values to determine if membrane integrity was maintained for the duration over which the transport experiments were conducted (Irvine *et al*., 1999; Rozehnal *et al*., 2012).

3.7 Positive and negative control for Rhodamine 123 experiments

During the transport experiments two control groups were included. The control groups were included in this study to ensure that the effect/s observed was not a result of external factors or interference but a result of the modulator's ability to modulate. The control groups included a negative control (RH-123 alone) and a positive control group (RH-123 and 100 µM Verapamil). Verapamil, which is a well-known P-gp inhibitor, was used as a

control/reference against which P-gp related efflux effects of the selected commercially available health supplements on RH-123 could be compared (Zhang *et al.,* 2013).

3.8 Data processing and statistical analysis

3.8.1 Percentage transport (% Transport)

The average % transport was calculated at each sampling interval using equation 3 and relevant correction factors to compensate for dilution and the resultant values are expressed as a percentage of the initial dose. The use of a correction factor is important due to the removal of sampling solution at each sampling interval and then the subsequent addition of an equal volume of the relevant solution to maintain a chamber volume of 7 ml at all times to compensate for any possible loss during the sample withdrawals. The correction factor used in this study was: 180 µl (sample volume) divided by 7 ml (chamber size), which equals 0.0257. The obtained values were then plotted on a graph to acquire a % transport versus time curve for each of the bi-directional transport studies.

$$\% \text{ Transport} = \frac{\text{Mean fluorescence value at specific time}}{\text{Mean value fluorescence of donor solution}} \text{ x } 100 \qquad \textit{Equation 3}$$

3.8.2 Apparent permeability coefficient (P_{app})

The apparent permeability coefficient (P_{app}) for RH-123, was calculated using equation 4:

$$P_{app} = \frac{dC}{dt}\left(\frac{1}{A.60.C_0}\right) \qquad \textit{Equation 4}$$

Where P_{app} represents the apparent permeability coefficient ($cm.s^{-1}$), $\frac{dC}{dt}$ represents the permeability rate (the amount of RH-123 permeated per min), A represents the membrane surface area (cm^2) available for diffusion and C_0 represents the initial concentration of the marker molecule (mg/ml) (Zhao *et al*., 2016). All P_{app} values are represented in addendum B.

3.8.3 Efflux ratio

The efflux ratio was calculated from the data collected during the experimental procedures by using equation 5:

$$ER = \frac{P_{app}(B\text{-}A)}{P_{app}\ (A\text{-}B)} \qquad \textit{Equation 5}$$

Where P_{app} (B-A) is the apparent permeability coefficient for the permeation of the model compound (RH-123) in the basolateral to apical direction and the P_{app} (A-B) value is the

same variable in the apical to basolateral direction. Thus P_{app} (B-A) and P_{app} (A-B) represents the average of the permeability coefficients from the secretory and absorptive directions respectively (Zhao *et al*., 2016). All ER values are represented in addendum C.

3.8.4 Statistical analysis of experimental results

A statistical analysis was performed on the apparent permeability coefficient (P_{app}) that were obtained from all the transport experiments by using the non-parametric Kruskal-Wallis test to determine if statistically significant differences were evident between selected data groups. Differences between the P_{app} values of the control and experimental groups were considered statistically significant if the p-values were less than or equal to 0.05 (therefore $p \leq 0.05$) (Addendum E).

CHAPTER 4: RESULTS AND DISCUSSION

4.1 Introduction

During this study, supplement-drug pharmacokinetic interactions were investigated when the supplement was co-applied with a P-glycoprotein (P-gp) substrate to excised pig intestinal tissues. Bi-directional *ex vivo* transport studies across excised pig intestinal tissue were conducted to determine if the presence of each of the selected health supplements (Acetyl-L-carnitine, berberine, chondroitin sulfate, D-glucosamine and silymarin) had any altering effects on the membrane permeation of rhodamine-123 (RH-123). RH-123 is a known P-gp substrate and was selected as a marker molecule for inclusion in the bi-directional transport studies to investigate if the selected health supplements had any altering effects on the extent of P-gp mediated efflux of RH-123. All the bi-directional transport studies were done in triplicate by mounting pig intestinal tissues between the Sweetana-Grass diffusion apparatus half cells.

To ensure that the concentration measurements were accurate, the fluorometric analytical method was validated. The validation of the analytical method was done prior to conducting the experiments.

The percentage transport was used to determine the apparent permeability coefficient (P_{app}) values of RH-123 in the absence and presence of the selected herbal supplements. The values were expressed as an average P_{app} value and an average standard deviation for the three experiments. The P_{app} values for apical to basolateral (AP-BL) and basolateral to apical (BL-AP) was used to calculate the efflux ratio (ER) values.

A transport study with Lucifer yellow (LY), an exclusion marker molecule commonly used in membrane integrity tests, was done prior to the transport experiments to confirm the method of mounting the excised pig intestinal tissue between the half cells was suitable and that the tissue remained viable over the entire period of conducting the transport experiments. This method of membrane integrity testing can indicate that the *ex vivo* diffusion method is acceptable in terms of tissue viability and is suitable to be used in the RH-123 transport studies.

As discussed in Chapter 3, there were also two control groups included in this study, a negative control (RH-123 alone) and a positive control (RH-123 with Verapamil). These control groups serve as a reference against which all the transport results were compared and to possibly indicate if the changes in transport was due to interactions caused by the health supplements.

The TEER (trans-epithelial resistance) was measured during all the transport experiments at pre-determined times. All the P_{app} values were statistically analysed and were compared to that of the control groups If there were reductions in the TEER it might be due to the opening of tight junctions and this may be the mechanism for increased transport via the paracellular pathway.

4.2 Fluorescence spectrometry method validation for Rhodamine 123 and Lucifer yellow

A fluorescence spectrometry method (performed on a Spectramax® Paradigm plate reader) was used to determine the RH-123 and LY content of all experimental samples. The excitation and emission wavelengths were set at 480 nm and 520 nm for RH-123 and at 485 nm and 530 nm for LY, respectively (Irvine *et al*., 1999; Kaprelyants & Kell, 1992). The analytical method was validated in terms of linearity, accuracy, precision, inter- and intra-day precision, limit of detection, limit of quantification and specificity.

4.2.1. Method validation results for Rhodamine 123

4.2.1.1. Linearity

Linearity was determined from a standard curve which was constructed from data generated from analysis of a series of RH-123 solutions with varying concentrations with the obtained results (Table 4.1). The regression curve was constructed by plotting fluorescence values as a function of RH-123 concentrations (Figure 4.1).

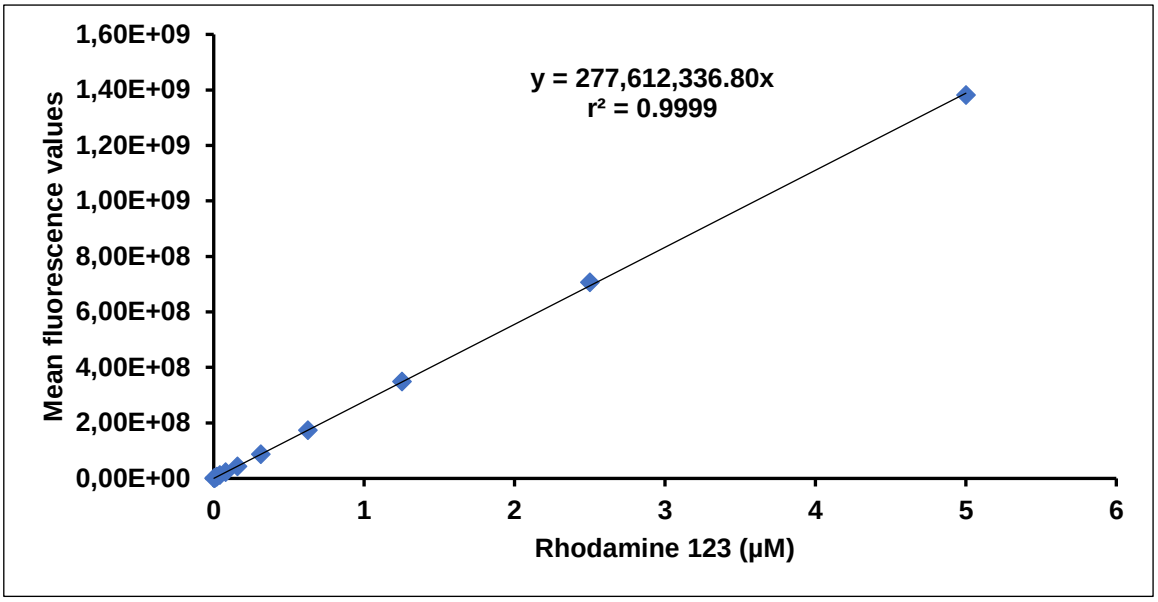

Figure 4.1: Regression curve for Rhodamine 123 and straight line equation with correlation coefficient (r^2) value

Table 4.1: Mean fluorescence values of Rhodamine 123 recorded over a specific concentration range

RH-123 concentration (µM)	Mean fluorescence value
5	1381551509.00
2.5	706358101.40
1.25	348503061.40
0.625	173687557.40
0.313	86144677.40
0.156	43131337.40
0.078	21696871.40
0.039	11219209.40
0.020	5651871.40
0.010	2883441.40
0.005	1475181.40
0.002	660174.40
Slope	**277612336.80**
r^2	**0.9999**

According to Singh (2013) it is required from an analytical method to render a correlation coefficient value (r^2) of 0.998 or better to conform to linearity requirements. The analytical method for RH-123 met the specified linearity requirements (r^2 = 0.9999) as can be seen from the collected data, which are presented in Figure 4.1 and Table 4.1.

4.2.1.2 Limit of detection and limit of quantification

The LOD and LOQ were calculated by using the slope of the regression curve and the standard deviation of KRBB sample measurement (blank values). The slope of the regression curve is shown in Figure 4.1, while the standard deviation values of the KRBB blank samples are presented in Table 4.2.

Table 4.2: Background noise (blank fluorescence values) with the standard deviation, limit of detection and limit of quantification values

Blank fluorescence values	Average	Standard deviation	LOD (µM)	LOQ (µM)
35579	35656.60	974.32	1.11×10^{-5}	3.35×10^{-5}
35735				
36630				
36297				
36911				
34884				
34885				
34813				
36921				
33911				

The RH-123 content in the experimental samples was considerably higher than the calculated LOD and LOQ values and confirms that the analytical method was able to accurately quantify the RH-123 concentrations that were present in the test samples.

4.2.1.3 Accuracy

In Table 4.3 the information regarding the accuracy (% recovery) of the analytical method is provided. Three RH-123 samples with varying concentrations were analysed and the test results showed that the accuracy was acceptable for the three concentrations used and that it met the recovery requirements of 100 ± 2% (Shabir, 2003).

Table 4.3: Results of Rhodamine-123 sample analysis across a specified concentration range to determine the accuracy potential of the analytical method

Theoretical concentration (µM)	**5**	**2.5**	**0.125**
Fluorescence values	1413897472	815178496	40815532
	1381045120	810532352	40367324
	1385916672	825840000	40250316
	1407709824	805127872	41932784
	1410791424	825467968	40342464
	1562932480	826158592	41937036
	1409393152	808697408	42031720
	1427188992	809072128	41232124
	1421632640	831579648	40565328
	1403218688	804754112	39778132
Average of fluorescence values	1422372646	816240858	41382786
Actual concentration (µM)	5.07	2.55	0.125
Accuracy (% recovery)	101.36	101.80	100.29

4.2.1.4 Precision

4.2.1.4.1 Intra-day precision

Solutions containing three different concentrations of RH-123 (5 µM, 2.5 µM and 0.125 µM) were analysed in triplicate at three pre-selected time points during a one-day (24 h) period. The results were then used to calculate the corresponding standard deviation (SD) and percentage relative standard deviation (%RSD) values to determine the intra-day precision of the analytical method. The test results that were used to determine the intra-day precision is presented in Table 4.4.

Table 4.4: Data used to determine the intra-day precision of the analytical method

Rhodamine-123 concentration (µM)	Repeat	Mean fluorescence value	Standard deviation	%RSD
5	**1**	1413643904	87320088.40	1.86
	2	1406516736		
	3	1552839424		
2.5	**1**	810343872	11906505.00	1.06
	2	804255424		
	3	815178496		
0.125	**1**	42184116	731253.08	1.77
	2	40815532		
	3	41666968		

A %RSD of ≤ 2% is considered acceptable and the analytical method did comply with the stated requirement for intra-day precision (Shabir, 2003).

4.2.1.4.2 Inter-day precision

Solutions that contain RH-123 at three different concentrations (5 µM, 2.5 µM and 0.125 µM) were analysed in triplicate on three consecutive days on the exact same time. The results were then used to calculate the corresponding standard deviation (SD) and percentage relative standard deviation (%RSD) values to determine the inter-day precision of the analytical method. The test results that were used to determine the inter-day precision is presented in Table 4.5.).

Table 4.5: Data used to calculate the inter-day precision of the analytical method

Rhodamine-123 concentration (µM)	Repeat	Mean fluorescence value	Standard deviation	% RSD
5	**1**	1413643904	98668997.71	1.79
	2	1540658048		
	3	1413643904		
2.5	**1**	810343872	13540210.00	1.38
	2	811181376		
	3	809157632		
0.125	**1**	42268912	747964.50	1.78
	2	41666968		
	3	41388044		

A %RSD of ≤ 2% is considered acceptable and the analytical method did comply with the stated requirement for inter-day precision (Shabir, 2003).

4.2.1.5 Specificity

The analytical method was able to accurately quantify the RH-123 concentration in test samples with an accuracy of 100 ± 2% (USP-NF, 2018) in the presence of three of the selected health supplements. Acetyl-L-carnitine, chondroitin sulfate and D-glucosamine did not show any interference or discrepancies with regards to accuracy and therefore complied with the criteria for specificity as shown in Table 4.6.

Table 4.6: Summary of specificity validation data in the presence of three of the selected health supplements

Supplement and RH-123 mixture	Theoretical concentration (µM)	Mean fluorescence value	Actual concentration (µM)	Accuracy (%)
Acetyl-L-carnitine	5.00	1294188810	5.18	101.95
Chondroitin sulfate	5.00	1183995685	5.00	100.27
D-glucosamine	5.00	1186990533	5.03	100.70

The analytical method did show interferences during the analysis of RH-123 in the presence of berberine and silymarin and it was therefore necessary to construct standard curves of

RH-123 in the presence of these supplements to eliminate these interferences. The constructed standard curves were then subjected to linear regression that could be used to determine RH-123 concentrations in solutions where berberine and silymarin were present. An r^2 value of at least 0.998 (Singh, 2013) was required for the standard curves of RH-123 in the presence of berberine and silymarin and the results showed that the analytical method did meet the specified criterium (Table 4.7).

Table 4.7: Summary of the linearity data of Rhodamine-123 in the presence of berberine and silymarin

Health supplement	r^2
Berberine	0.9999
Silymarin	0.9983

4.2.2 Method validation results of Lucifer yellow

4.2.2.1 Linearity

A series of LY solutions with varying concentrations (Table 4.8) was prepared and analysed to determine linearity. The generated fluorescence values were then used to construct a regression curve of fluorescence versus the concentration of LY in the samples. The resultant regression curve is presented in Figure 4.2.

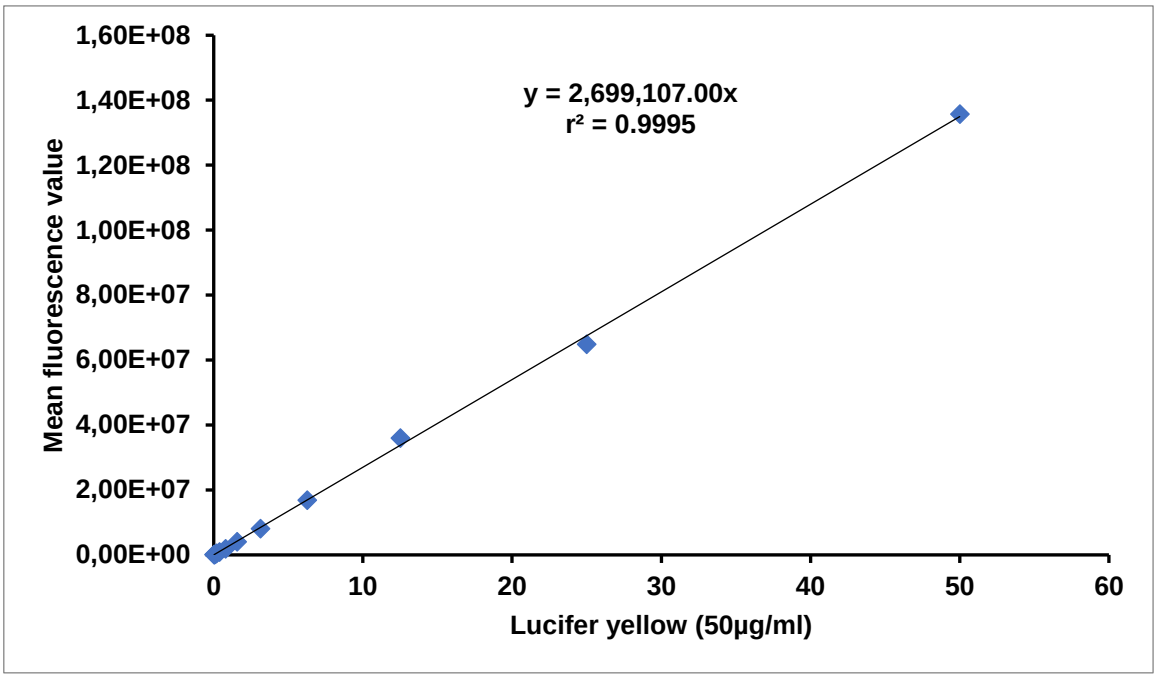

Figure 4.2: Linear regression curve for Lucifer yellow and straight line equation with the representative correlation coefficient (r^2) value

Table 4.8: Mean fluorescence values of Lucifer yellow recorded across a specific concentration range

Lucifer yellow concentration (µg/ml)	Mean fluorescence value
50	135735904.00
25	64872712.00
12.5	35971352.00
6.25	16847768.00
3.125	8084926.00
1.563	4050083.00
0.781	1834305.00
0.391	860445.00
0.195	431599.00
0.098	168511.00
0.049	113177.00
0.024	84711.00
Slope	**2699107.00**
r^2	**0.9995**

According to Singh (2013) it is required from an analytical method to render a correlation coefficient value (r^2) of 0.998 or better to conform to linearity requirements. The analytical

method for LY did meet the specified linearity requirement (r^2 = 0.9995) as can be seen from the collected data which are presented in Figure 4.2 and Table 4.8.

4.2.2.2 Limit of detection and limit of quantification

The LOD and LOQ were calculated by using the slope of the regression curve and the standard deviation of KRBB sample measurement (blank values). The slope of the regression curve and the standard deviation values of the KRBB blank samples are presented in Figure 4.2 and Table 4.9, respectively.

Table 4.9: Background noise (blank fluorescence values) with the standard deviation, limit of detection and limit of quantification values

Blank fluorescence values	Average	Standard deviation	LOD (µg/ml)	LOQ (µg/ml)
67366	68904.70	9972.82	12.19×10^{-3}	36.95×10^{-3}
67582				
86786				
55427				
70877				
74736				
48826				
71143				
71291				
75013				

The LY content in the experimental samples was considerably higher than the calculated LOD and LOQ values and confirms that the analytical method was able to accurately quantify the LY concentrations that were present in the test samples.

4.2.2.3 Accuracy

In Table 4.10 the information regarding the accuracy (% recovery) of the analytical method is provided. Three LY samples with varying concentrations were analysed and the test results showed that the accuracy was acceptable for the three concentrations used and that it met the recovery requirements of 100 ± 2% (Shabir, 2003).

Table 4.10: Results of Lucifer yellow sample analysis across a specified concentration range to determine the accuracy potential of the analytical method

Theoretical concentration (µg/ml)	**50**	**25**	**12.5**
Fluorescence values	135201056	67790256	34267064
	134119568	69382504	33934212
	133482160	71635904	34861580
	134803760	69744160	34913004
	137103312	69382504	33718416
	134119568	68021296	34982528
	133482160	69954608	34637052
	132338200	69385208	33518310
	134803760	69744160	33103364
	132421320	69385208	33312278
Average of fluorescence values	134187486	69442581	34124781
Actual concentration (µM)	50.01	25.16	12.53
Accuracy (% recovery)	100.02	100.62	100.27

4.2.2.4 Precision

4.2.2.4.1 Intra-day precision

Solutions containing three different concentrations of LY (50 µg/ml, 25 µg/ml and 12.5 µg/ml) were analysed in triplicate at three pre-selected time points during a one-day (24 h) period. The results were then used to calculate the corresponding standard deviation (SD) and percentage relative standard deviation (%RSD) values to determine the intra-day precision of the analytical method. The test results that were used to determine the intra-day precision is presented in Table 4.11.

Table 4.11: Data used to determine the intra-day precision of the analytical method

Concentration (µg/ml)	Repeat	Mean fluorescence value	Standard deviation	% RSD
50	**1**	137103312	1627416.30	1.04
	2	137892256		
	3	135447040		
25	**1**	69954608	998624.30	1.44
	2	70413784		
	3	70790872		
12.5	**1**	34140704	505868.20	1.49
	2	34162848		
	3	34267064		

A %RSD of ≤ 2% is considered acceptable and the analytical method did comply with the stated requirement for intra-day precision (Shabir, 2003).

4.2.2.4.2 Inter-day precision

Solutions that contain LY at three different concentrations (50 µg/ml, 25 µg/ml and 12.5 µg/ml) were analysed in triplicate on three consecutive days on the exact same time. The results were then used to calculate the corresponding standard deviation (SD) and percentage relative standard deviation (%RSD) values to determine the inter-day precision of the analytical method. The test results that were used to determine the inter-day precision is presented in Table 4.12.).

Table 4.12: Data used to calculate the inter-day precision of the analytical method

Concentration (µg/ml)	Repeat	Mean fluorescence value	Standard deviation	% RSD
50	**1**	135201056	1878886.10	1.16
	2	135828784		
	3	135413168		
25	**1**	71635904	899212.60	1.30
	2	70891448		
	3	70059640		
12.5	**1**	34289508	594058.80	1.75
	2	34209468		
	3	34684888		

A %RSD of ≤ 2% is considered acceptable and the analytical method did comply with the stated requirement for inter-day precision (Shabir, 2003).

4.3 Summary of validation results

The data obtained during the analytical method validation assessment for the analysis of RH-123 and LY samples across specified concentration ranges proved that the analytical methods that were used on the Spectramax Paradigm® plate reader did comply with the necessary validation criteria.

4.4 Bi-directional transport studies

The *in vitro* transport study experiments were performed in both the apical to basolateral (AP-BL) and basolateral to apical (BL-AP) directions (bi-directional transport) across pig intestinal tissue mounted between the half cells of a Sweetana-Grass diffusion apparatus to investigate if the selected health supplements had any permeation altering effects on the transport of RH-123. As stated in Chapter 3, two control groups were also included in the study namely a negative control (RH-123 alone) and a positive control group (RH-123 with 100 µM verapamil, which is a known P-gp inhibitor) (Zhang *et al.,* 2013).

4.4.1 Acetyl-L-carnitine (ALC)

Figure 4.3 represents the average percentage transport of RH-123 in the AP-BL direction, while Figure 4.4 shows the average percentage transport of RH-123 in the BL-AP direction in the presence of different concentrations of ALC.

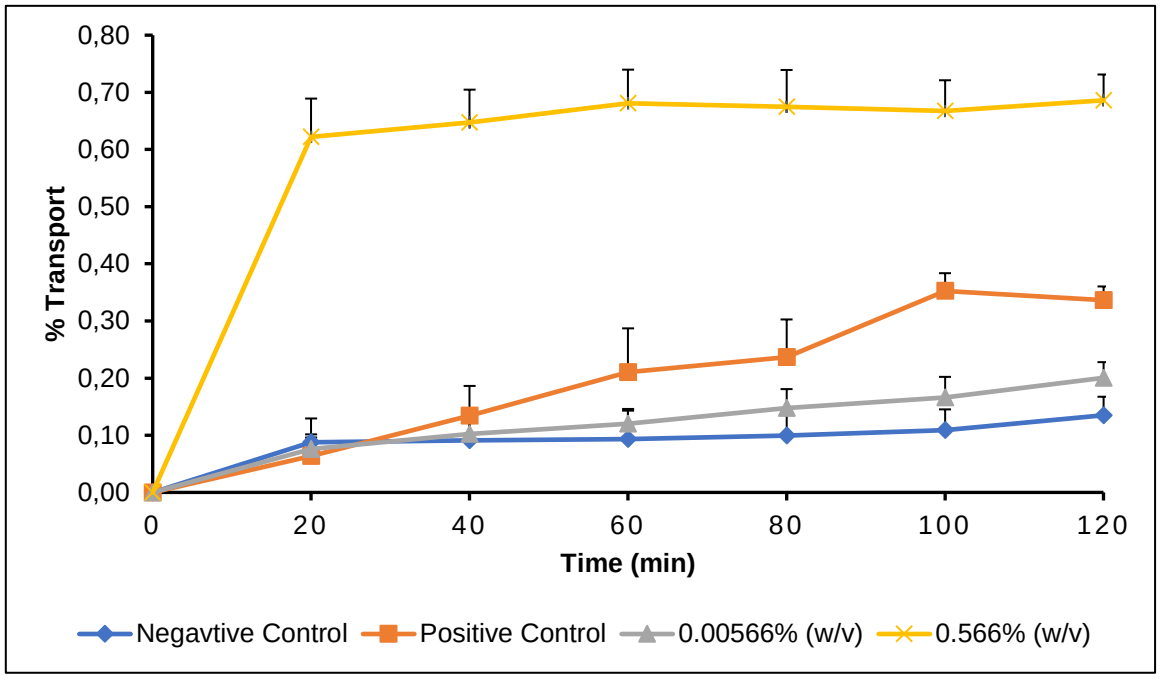

Figure 4.3: Apical-basolateral transport of Rhodamine-123 in the presence of two concentrations of acetyl-L-carnitine across excised pig intestinal tissue plotted as a function of time

The results showed that the addition of verapamil (positive control) did mediate an increase in RH-123 transport in the AP-BL direction, possibly due to inhibition of efflux of RH-123. It is further evident from the results that the low ALC concentration (0.00566% w/v) has mediated only a slight increase in RH-123 transport when compared to the negative control (RH-123 alone), while a high concentration of ALC (0.566% w/v) has mediated a statistically significant ($p < 0.05$) increase in RH-123 transport in the AP-BL direction when compared to the negative control. TEER values after application of the ALC high concentration yielded a reduction in the percentage TEER of 5.60% and this indicates that the tight junctions might have been opened. The % transport of RH-123 in the presence of a high concentration ALC was 0.69%, which is approximately 5 times higher than the transport of RH-123 in the negative control group (% transport of 0.13%).

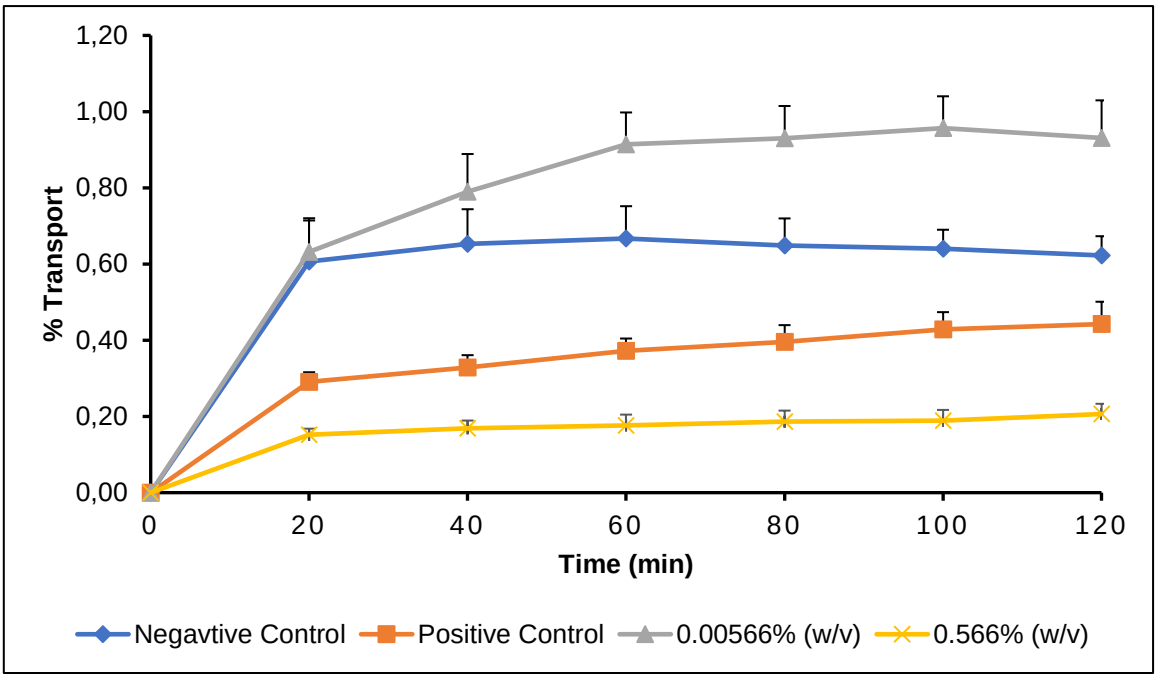

Figure 4.4: Basolateral-apical transport of Rhodamine-123 in the presence of two concentrations of acetyl-L-carnitine across excised pig intestinal tissue plotted as a function of time

For BL-AP transport of RH-123 in the presence of the low concentration (0.00566% w/v) ALC, the biggest increase in RH-123 transport was observed with a reduction in the percentage TEER of 7.09%. The low concentration (0.00566% w/v) of ALC increased RH-123 transport by 1.5-fold in comparison to the negative control group and increased transport of RH-123 by 2-fold when compared to the positive control group. At the high ALC concentration (0.566% w/v), there was no significant increase in the transport of RH-123 when compared to the control groups and there was only a slight decrease in the percentage TEER of 3.04% and this can indicate that the tight junctions did not open sufficiently to allow for RH-123 transport. There was a statistically significant difference between the transport of RH-123 in the presence of the low and high concentrations of ALC when compared to the negative control groups.

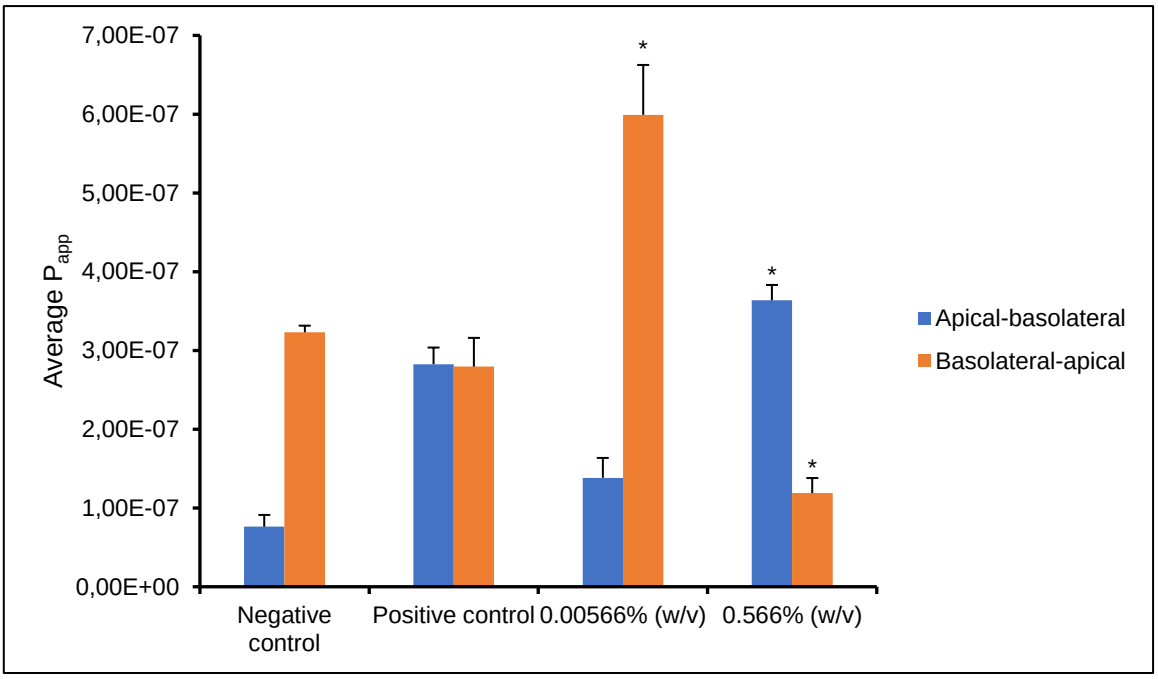

Figure 4.5: Average P_{app} values for bi-directional transport of Rhodamine-123 across excised pig intestinal tissue in the presence of acetyl-L-carnitine (* shows statistically significant differences where $p \leq 0.05$)

In Figure 4.5, the summary of calculated P_{app} values in both the AP-BL and BL-AP directions can be seen. From this figure, it can be seen that ALC low concentration (0.00566% w/v) had a pronounced increasing effect on RH-123 transport in the secretory (BL-AP) direction that caused a reduction of the RH-123 transport in the AP-BL direction. There was a statistically significant difference ($p \leq 0.05$) between the high concentration (0.566% w/v) of acetyl-L-carnitine and the negative control for AP-BL transport and there was also a statistically significant difference between the high (0.566% w/v) and low (0.00566% w/v) concentrations of BL-AP transport. The efflux ratio (ER) value for the low concentration (0.00566% w/v) of ALC was 4.33. The ER value for ALC high concentration (0.566% w/v) was 0.33 and according to Bock *et al.* (2003) if an ER << 1 it is indicative of absorptive uptake possibly due to decreased efflux. The ER value for the high concentration (0.566% w/v) ALC calculated from the experimental results suggests that transport of RH-123 was increased. Evans & Fornasini (2003) concluded in their study of ALC that if the dosage of ALC increases the more likely it is that passive diffusion becomes the dominant absorption pathway.

4.4.2 Berberine

In Figure 4.6, the AP-BL transport of RH-123 can be seen and in Figure 4.7, the BL-AP transport of RH-123 in the presence of two different concentrations of berberine can be seen.

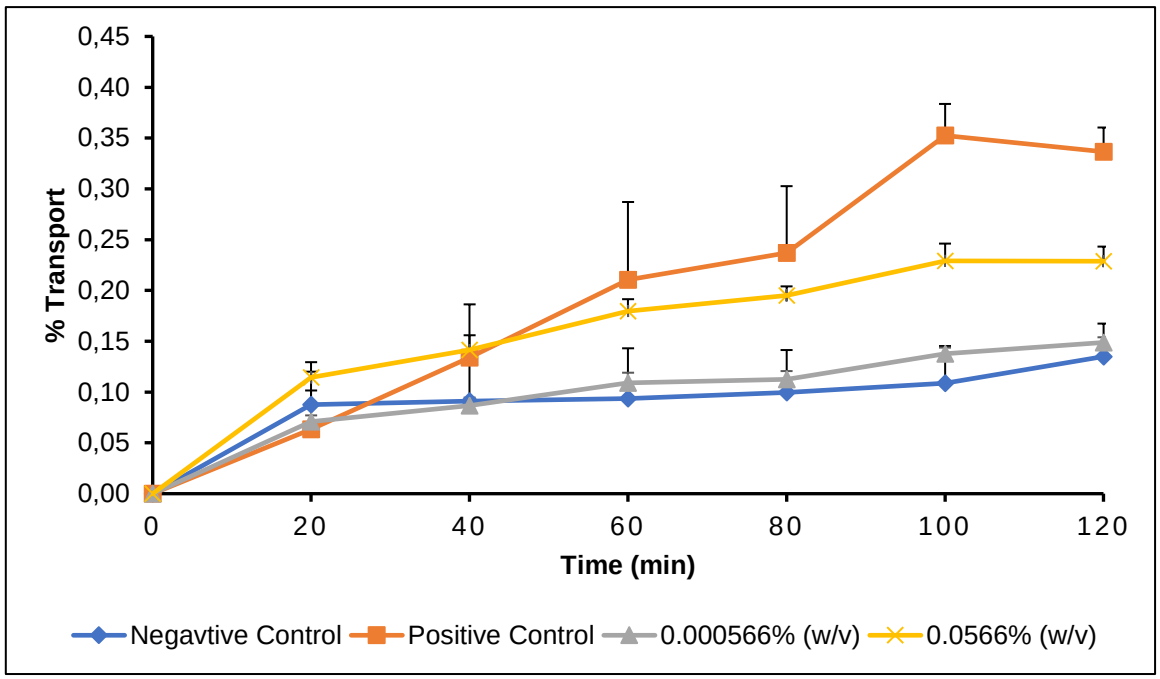

Figure 4.6: Apical-basolateral transport of Rhodamine-123 in the presence of two concentrations of berberine across excised pig intestinal tissue plotted as a function of time

In Figure 4.6, it can be seen that the positive control (the addition of verapamil, a known P-gp inhibitor) increased the uptake of RH-123 in the AP-BL direction. The high concentration of berberine (0.0566% w/v) mediated a 1.8-fold increase in RH-123 AP-BL transport when compared to the negative control. This was also the effect noted by Lin *et al.* (2017) that RH-123 efflux decreased when the concentration of berberine was increased. The low concentration of berberine (0.000566% w/v) showed a very slight increase, from 0.135% to 0.149%, in RH-123 AP-BL transport when compared to the negative control. The TEER (seen in table 4.14) values showed a decrease in TEER (by 4.2% for the high concentration and by 2.86% for the low concentration), which indicated that the tight junction integrity was compromised that contributed to an increase in RH-123 transport, via the paracellular pathway, when compared to the negative control group. The ER value for the low concentration (0.000566% w/v) berberine was 0.53 and for the high concentration (0.566% w/v) berberine it was 0.92 and according to Bock *et al.* (2003) if an ER << 1 it could be indicative of absorptive uptake possibly due to decreased efflux.

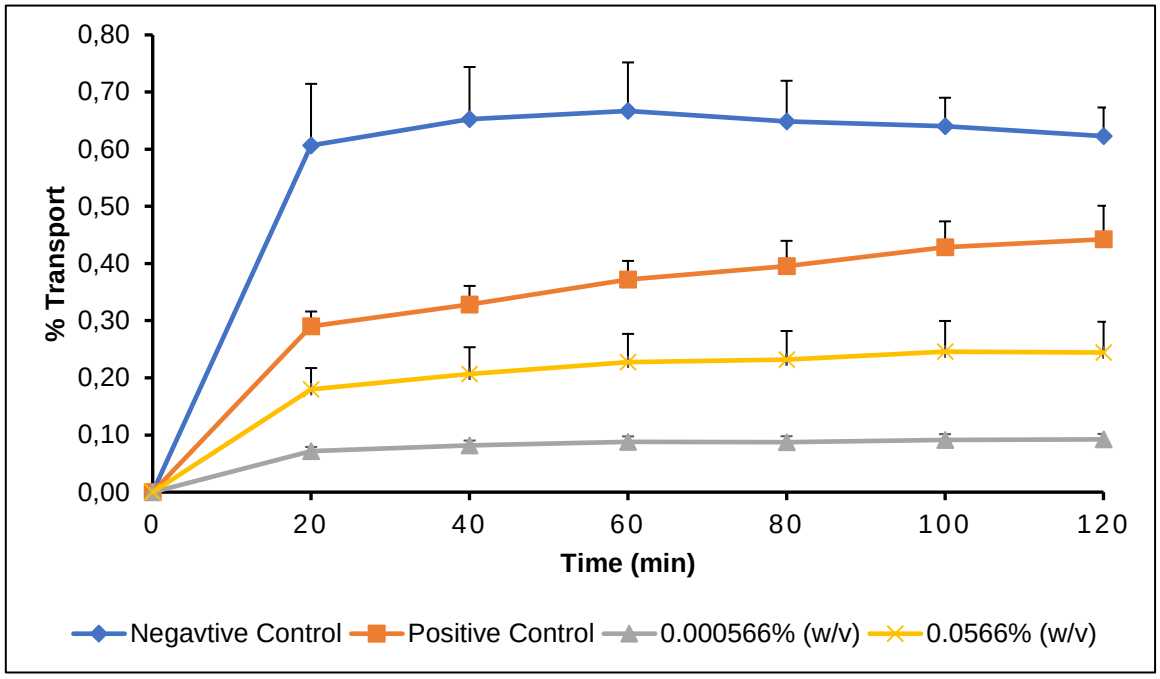

Figure 4.7: Basolateral-apical transport of Rhodamine-123 in the presence of two concentrations of berberine across excised pig intestinal tissue plotted as a function of time

In Figure 4.7, it can be seen that berberine had a decreasing effect on the transport of RH-123 in the BL-AP direction. When comparing the RH-123 transport in the experimental groups to the negative control group, the low concentration (0.000566% w/v) of berberine decreased RH-123 transport the most by 6.8-fold. There was a statistically significant ($p \leq 0.05$) difference between the RH-123 BL-AP transport in the presence of the low concentration (0.000566% w/v) of berberine when compared to the negative control. At the two different concentrations of berberine there was a decrease in RH-123 transport with only slight change in percentage TEER (Table 4.14) and this can indicate that the tight junctions did not open sufficiently to allow for RH-123 transport.

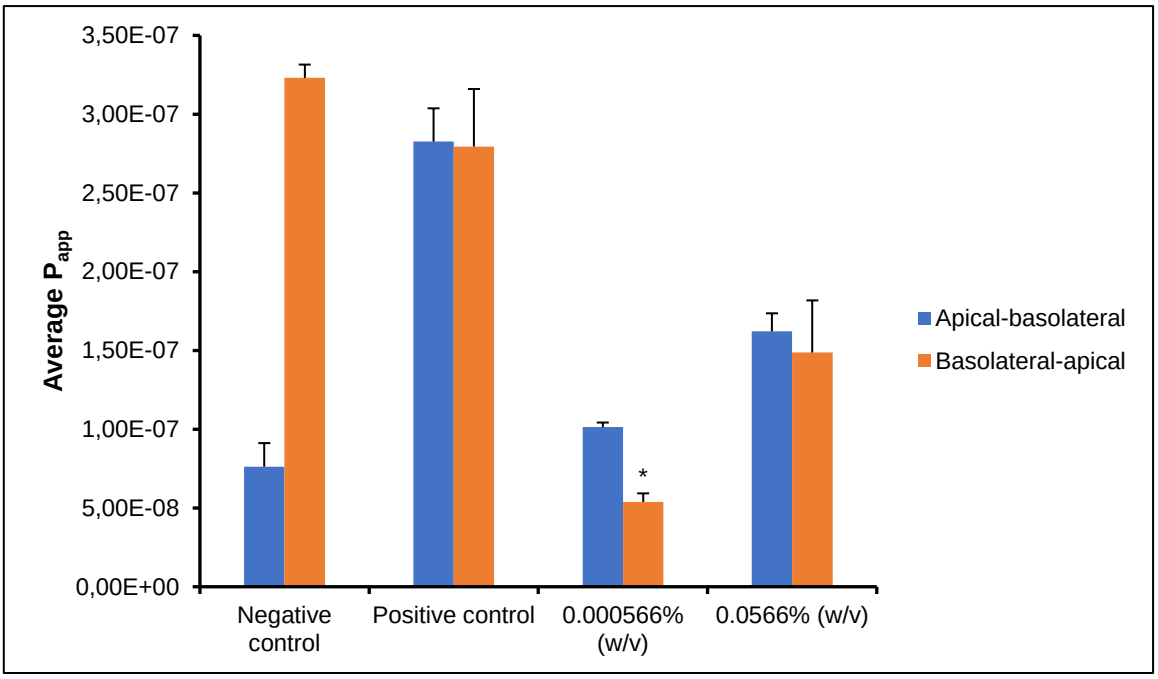

Figure 4.8: Average P_{app} values for bi-directional transport of Rhodamine-123 across excised pig intestinal tissue in the presence of berberine (* shows statistically significant differences with the control group where $p \leq 0.05$)

Figure 4.8 shows a concentration dependent increase in RH-123 transport in the AP-BL direction. The RH-123 transport in the presence of the low concentration (0.000566% w/v) of berberine was lower than in the presence of the high concentration (0.0566% w/v). From the results it is clear that berberine increased the absorptive transport (AP-BL) of RH-123 by means of inhibiting efflux or secretory transport (BL-AP) and also by opening tight junctions (as indicated by TEER reduction).

4.4.3 Chondroitin sulfate

The AP-BL transport of RH-123 in the presence of different concentrations of chondroitin sulfate (CS) are presented in Figure 4.9, while the BL-AP transport of RH-123 in the presence of different concentrations of CS are presented in Figure 4.10.

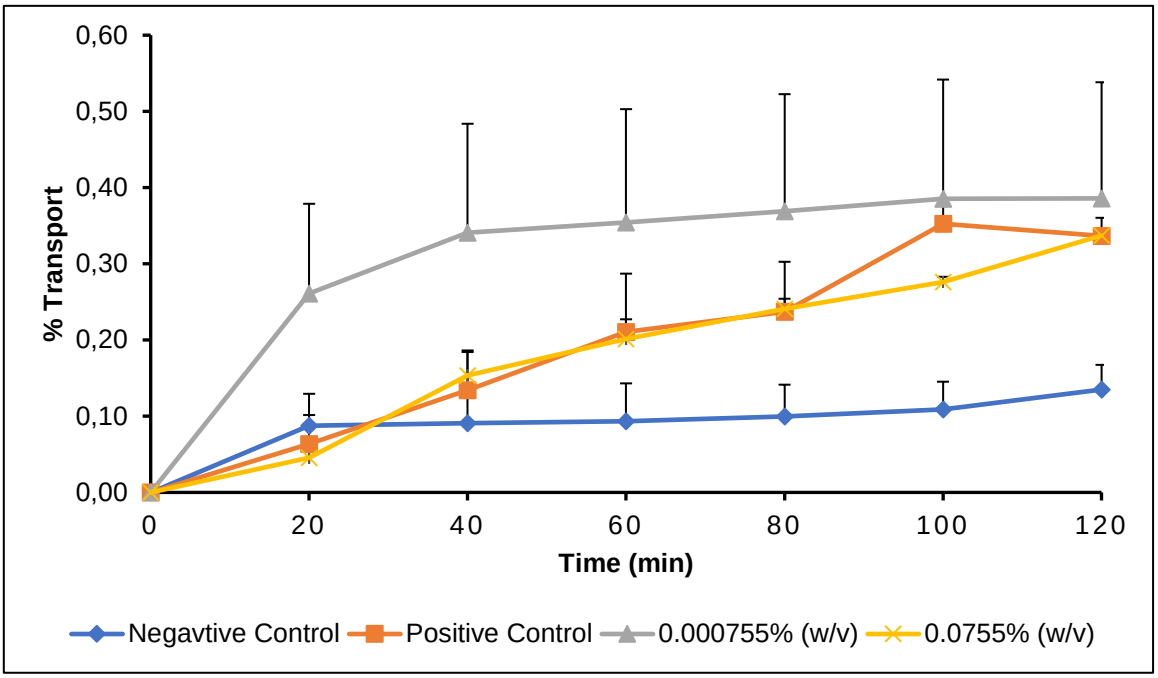

Figure 4.9: Apical-basolateral transport of Rhodamine-123 in the presence of a low and high concentration of chondroitin sulfate across excised pig intestinal tissue plotted as a function of time

CS showed an increase in the transport of RH-123 in the AP-BL direction when compared to the negative control in an inversely proportional manner with respect to CS concentration (seen from Figure 4.9). The low concentration CS (0.000755% w/v) had the most pronounced effect on RH-123 transport, increasing the transport by approximately 3-fold. For the high concentration CS (0.0755% w/v) the transport of RH-123 was increased by 2.5-fold when compared to the negative control. The % TEER reduction was calculated at 6.41% (0.000755% w/v) and 6.43% (0.0755% (w/v). The decrease in TEER values could possibly be due to tight junctions opening and this can also be a contributing factor to the increased transport of RH-123 mediated by the presence of CS.

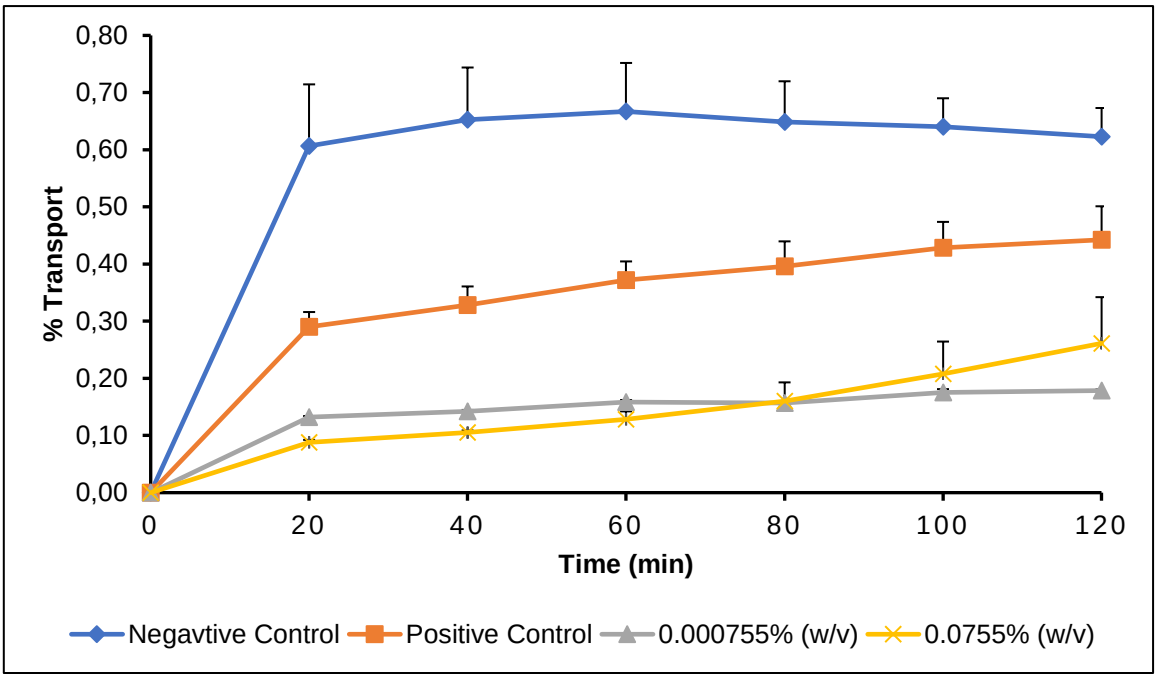

Figure 4.10: Basolateral-apical transport of Rhodamine-123 in the presence of two concentrations of chondroitin sulfate across excised pig intestinal tissue plotted as a function of time

CS inhibited the transport of RH-123 in the BL-AP direction by 2.4-fold (0.0755% w/v) and by 3.5-fold (0.000755% w/v) when compared to the negative control group as seen in Figure 4.10. The negative and positive controls are higher than that of the CS. This shows a decrease in the transport of RH-123 at the high (0.0755% w/v) and low (0.000755% w/v) concentrations of CS in the secretory (BL-AP) direction, which indicated an inhibition effect on the efflux of RH-123. According to a study conducted by Derrick-Roberts *et al.* (2012) the reduction in transport across the membrane could possibly be due to passive diffusion. The reduction in percentage TEER at the low CS concentration (0.000755% w/v) was 1.85% and at the high concentration (0.0755% w/v) it was reduced by 2.09% and this slight change could indicate that the tight junctions did not open successfully and why there was a decrease in RH-123 transport.

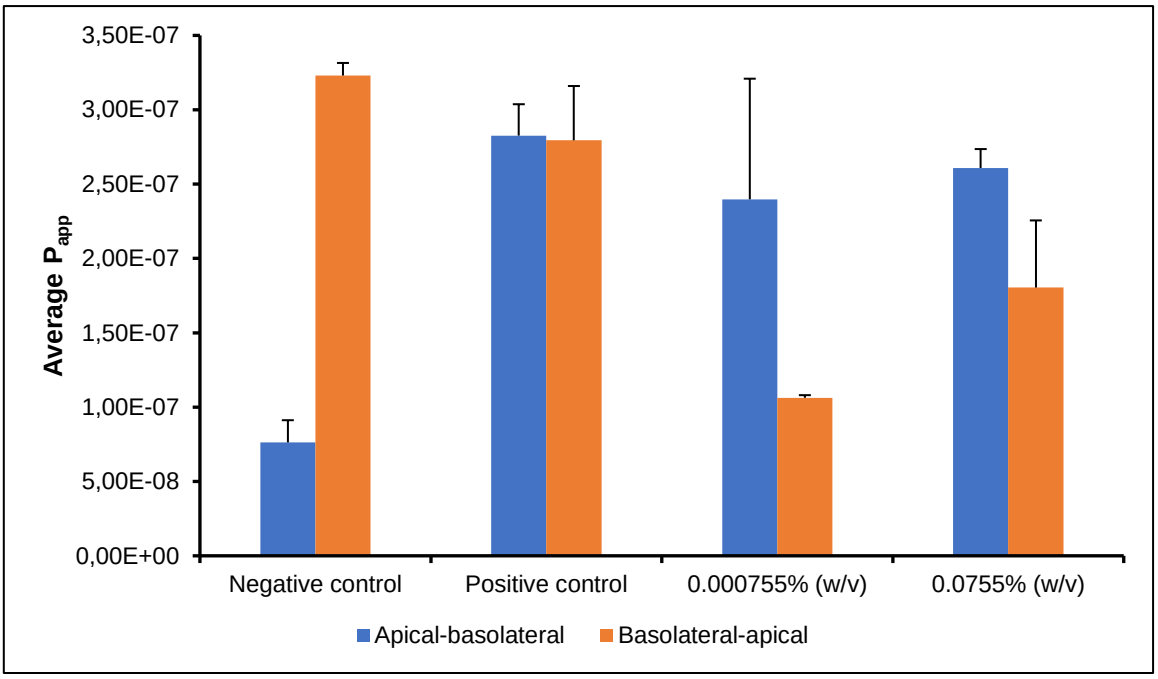

Figure 4.11: Average P_{app} values for bi-directional transport of Rhodamine-123 across excised pig intestinal tissue in the presence of chondroitin sulfate

Figure 4.11 depicts the P_{app} values for CS. For the uptake of RH-123 (transport in the AP-BL direction) an increase can be seen in the presence of CS when compared to the values of the negative control, but this effect was inversely proportional to the concentration of CS. For the secretory transport of RH-123 (BL-AP direction), a decrease is observed in a directly proportional manner with respect to CS concentration. The ER values for CS was calculated to be 0.44 (0.000755% w/v) and 0.69 (0.0755% w/v), respectively and if an ER value is << 1 it could be indicative that the transport was subjected to absorptive uptake (Bock *et al.,* 2003). The calculated change in percentage TEER can be seen in Table 4.14 and it showed that for BL-AP transport of the low concentration CS there was only a slight decrease in the TEER and this is a possible reason for the low transport of RH-123.

4.4.4 D-glucosamine

The AP-BL transport of RH-123 in the presence of different concentrations of D-glucosamine can be seen and in Figure 4.12, while the BL-AP transport of RH-123 in the presence of different concentrations of D-glucosamine can be seen in Figure 4.13.

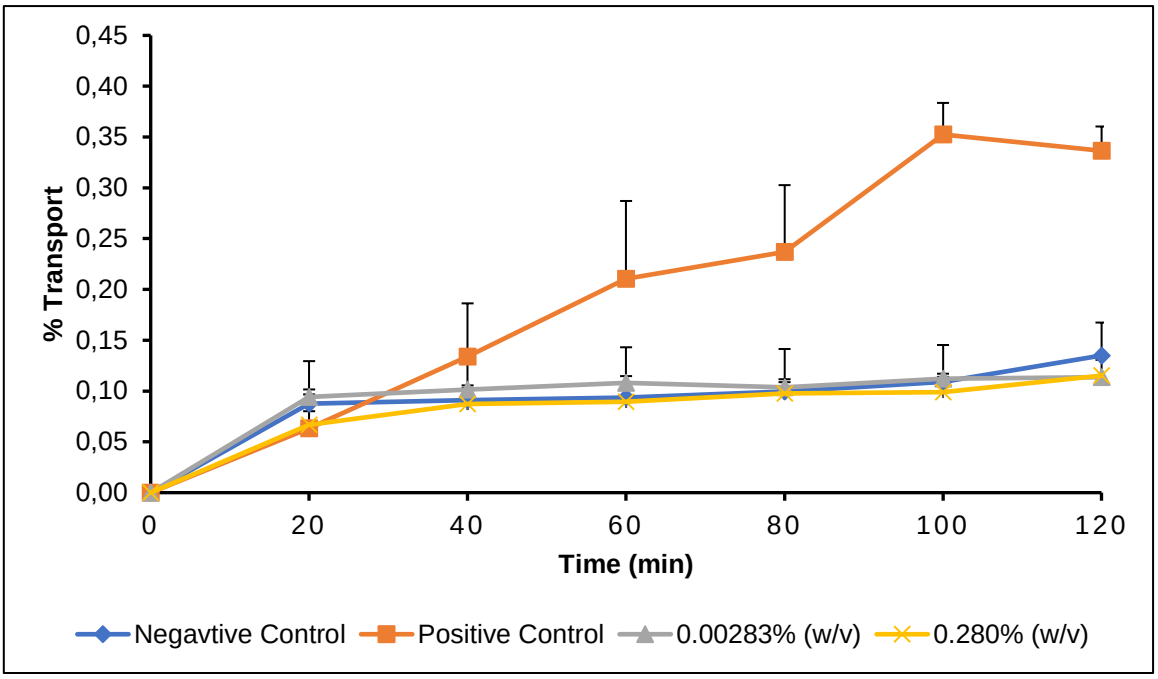

Figure 4.12: Apical-basolateral transport of Rhodamine-123 in the presence of two concentrations of D-glucosamine across excised pig intestinal tissue plotted as a function of time

In Figure 4.12, it can be observed that with the addition of verapamil, a known P-gp inhibitor (positive control) there was an increase in the uptake of RH-123 in the AP-BL direction. It is clear that the RH-123 transport is very similar in the presence of D-glucosamine to that of the negative control group. The high (0.283% w/v) and low (0.00283% w/v) concentrations of D-glucosamine had a similar negligible effect on RH-123 transport in the AP-BL direction. The calculated percentage TEER values were decreased by 3.73% (0.00283% w/v D-glucosamine) and by 3.51% (0.283% w/v D-glucosamine). The relatively low decrease in TEER values can be because of a slight opening of tight junctions, which had a negligible effect on the transport of RH-123 via the paracellular pathway. For this study a daily dose of 3000 mg D-glucosamine was chosen and according to the study by Ibrahim *et al.* (2012) when D-glucosamine was given at that dose there was reduced absorption which could possibly be because of the saturation of the transport proses (a capacity limited process).

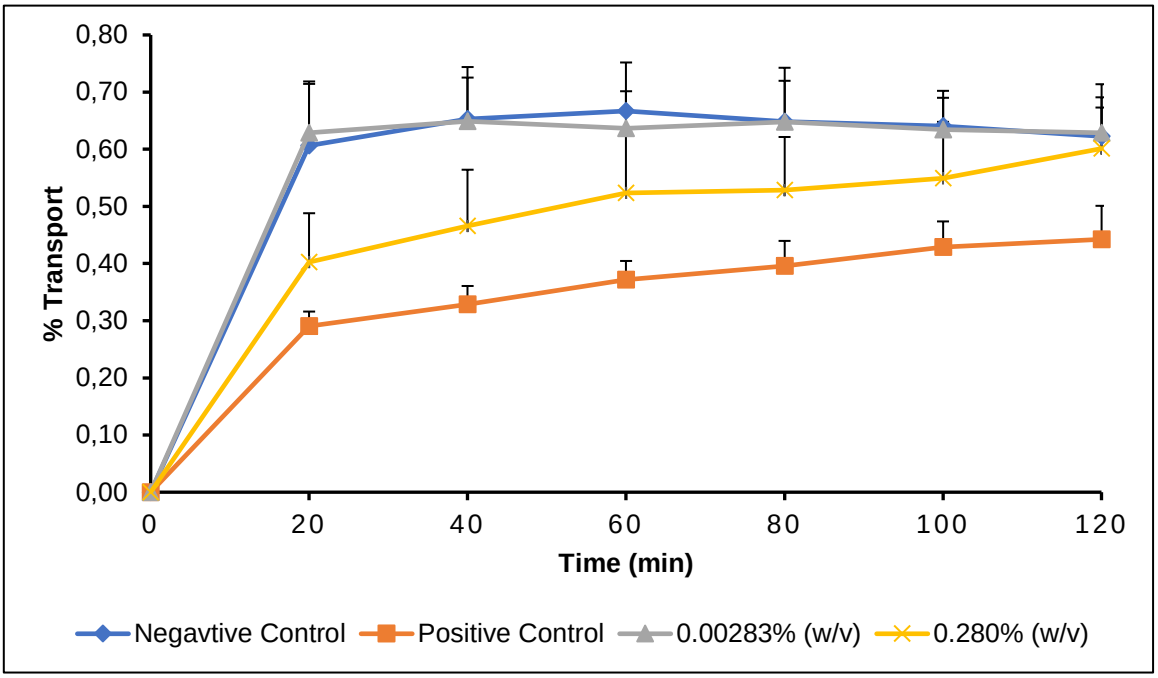

Figure 4.13: Basolateral-apical transport of Rhodamine-123 in the presence of two concentrations of D-glucosamine across excised pig intestinal tissue plotted as a function of time

In Figure 4.13, it can be seen that there was not a decrease in RH-123 transport in the presence of the low concentration (0.00283% w/v) of D-glucosamine when compared to the negative control group but the transport was relatively the same. The high concentration (0.283% w/v) of D-glucosamine, on the other hand, caused a decrease in RH-123 transport in the BL-AP direction. The change in TEER values as noted in Table 4.14 it can be seen that the slight decrease in TEER values, 5.21% for 0.00283% (w/v) and 5.27% for 0.283% (w/v), which did not have a noticeable effect on RH-123 transport.

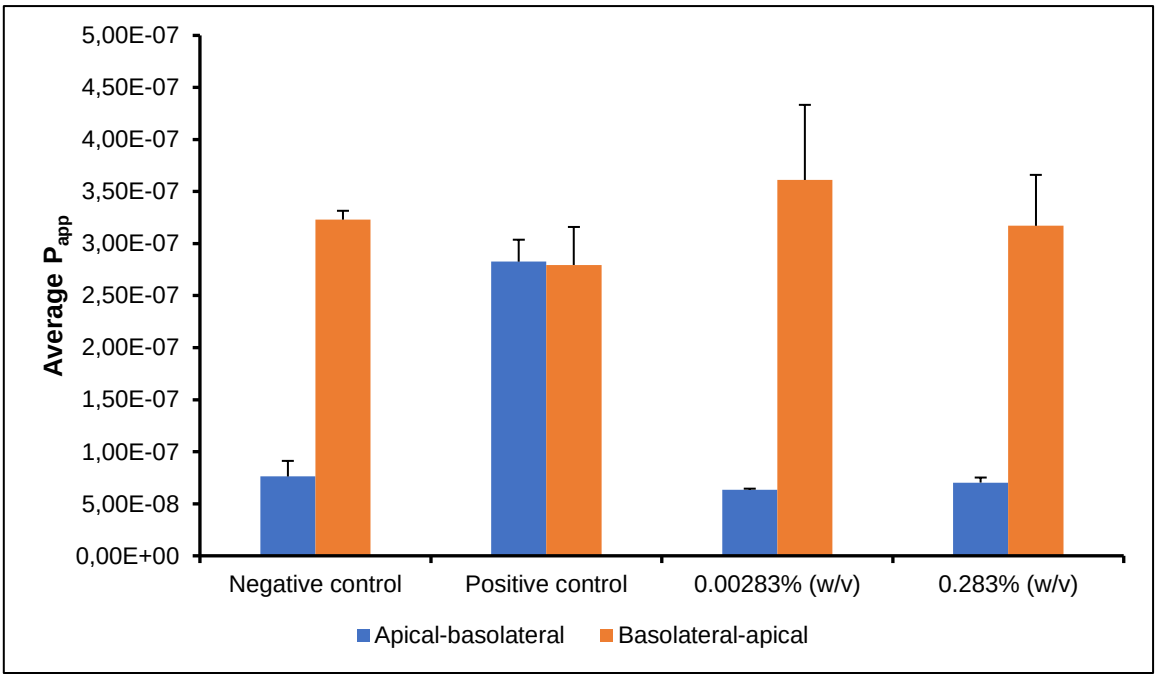

Figure 4.14: Average P_{app} values for bi-directional transport of Rhodamine-123 across excised pig intestinal tissue in the presence of D-glucosamine

From Figure 4.12 it is clear that the AP-BL transport of RH-123 in the presence of D-glucosamine was very similar to the negative control group and from Figure 4.14 this can also be seen because the P_{app} values for RH-123 in the presence of D-glucosamine when compared to the control group are also similar. While for the BL-AP P_{app} values of the low concentration (0.00283% w/v) D-glucosamine and RH-123 are also similar to the negative control groups P_{app} values. The TEER values (Table 4.14) showed a decrease and possibly tight junctions opening but it did not show significantly increased transport of RH-123. For the secretory direction a slight increase in the P_{app} value of RH-123 in the presence of low concentration (0.00283% w/v) D-glucosamine suggests that an apparent induction of P-gp related efflux occurred and for the high concentration (0.283% w/v) D-glucosamine possibly inhibited efflux based on the lower calculated P_{app} value when compared to the negative control. The ER values for the low concentration (0.00283% w/v) D-glucosamine was calculated at 5.71 and the ER values for the high concentration (0.283% w/v) of D-glucosamine was calculated at 4.51 which could indicate that the transport in the secretory direction could be due to induction or stimulation of P-gp related efflux transport.

4.4.5 Silymarin

Figure 4.15 represents the average percentage transport of RH-123 in the AP-BL direction in the presence of different concentrations of silymarin, while Figure 4.16 shows the average percentage transport of RH-123 in the BL-AP direction in the presence of different concentrations of silymarin.

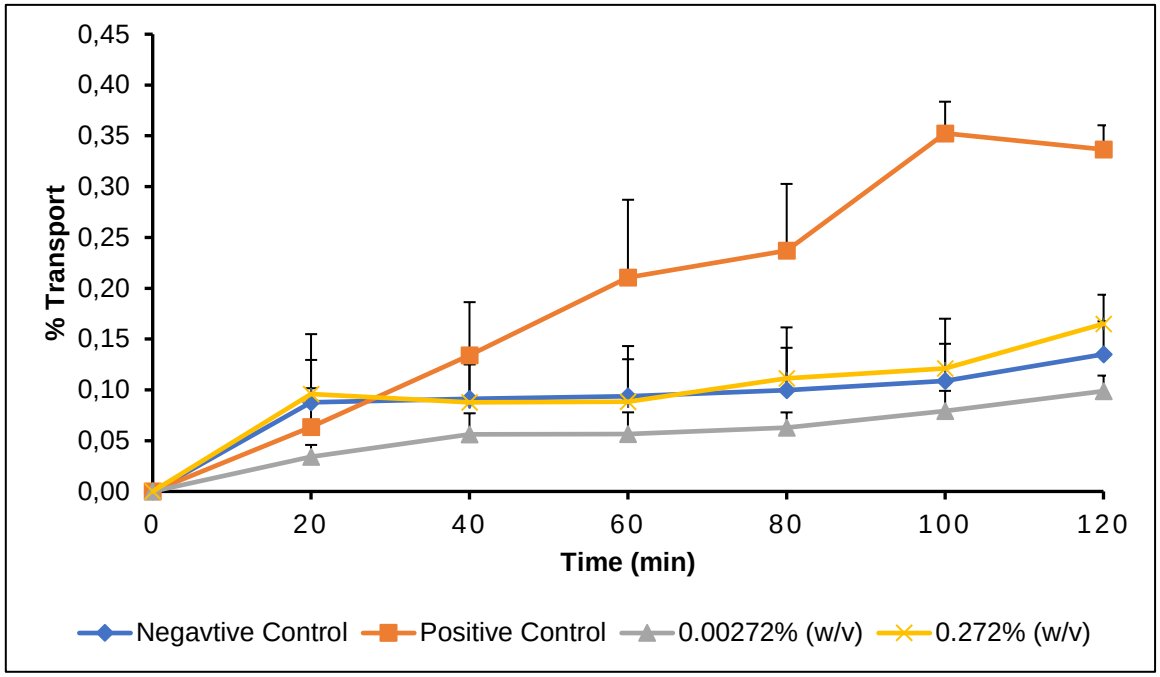

Figure 4.15: Apical-basolateral transport of Rhodamine-123 in the presence of two concentrations of silymarin across excised pig intestinal tissue plotted as a function of time

In Figure 4.15, it can be seen that the positive control (the addition of verapamil, a known P-gp inhibitor) increased the uptake of RH-123 in the AP-BL direction. It can also be observed that the high concentration (0.272% w/v) silymarin caused a slight increase in RH-123 transport when compared to the negative control. The low concentration (0.00272% w/v) of silymarin had a RH-123 transport of 0.099%, but when compared with the negative control, with a transport of 0.135%, it is clear that this concentration had a decreasing effect on RH-123 transport. There was a statistically significant difference ($p \leq 0.05$) noted between the positive control and RH-123 in the presence of the low concentration (0.00272% w/v) of silymarin. When considering that the TEER values, for the low concentration (0.00272% w/v) silymarin, was reduced by 1.01% and for the high concentration (0.272% w/v) silymarin was reduced by 3.74%, tight junction integrity might have been reduced and this could lead to higher transport of RH-123 as was evident at the high silymarin concentration (0.272% w/v).

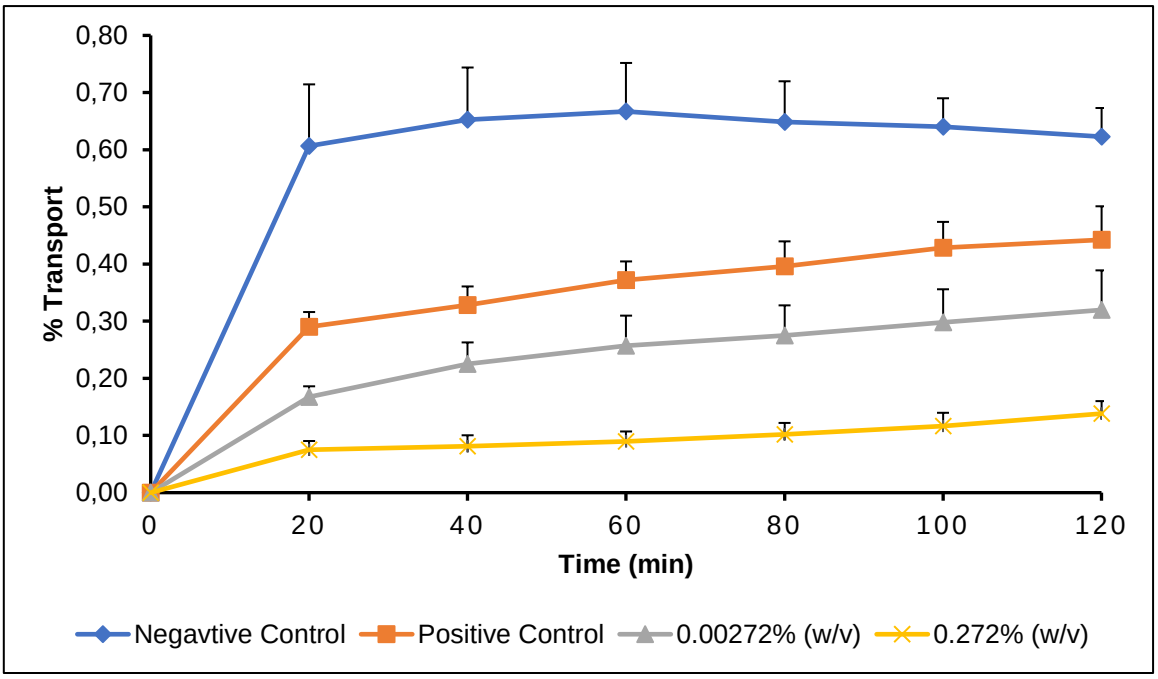

Figure 4.16: Basolateral-apical transport of Rhodamine-123 in the presence of two concentrations of silymarin across excised pig intestinal tissue plotted as a function of time

In Figure 4.16, a decrease in RH-123 transport is noted and the decrease shows it is concentration dependant in the presence of silymarin. The low concentration silymarin yield a percentage transport of 0.320% and the high concentration silymarin yield a percentage transport of 0.138% as calculated from the original 5µM RH-123 concentration. The high concentration (0.272% w/v) silymarin had the most significant reduction in RH-123 transport and the uptake of RH-123 was reduced by 4.5-fold when compared to the negative control. There was a statistically significant difference ($p \leq 0.05$) between the negative control and the high concentration (0.272% w/v) of silymarin. The reduction in % TEER values for low concentration (0.00272% w/v) silymarin was 4.55% and for the high concentration (0.272% w/v) silymarin it was 1.5%. This slight reduction however did not increase the RH-123 transport and thus did not open tight junctions. According to Ferreira *et al.* (2018) silymarin was identified as a P-gp inhibitor and the effect was concentration dependent, which increased with a higher dose of silymarin and this can be observed with the data obtained. Before silymarin has a positive effect on efflux inhibiting and thus absorptive transport it needs to attain a threshold concentration as seen from the high concentration (0.272% w/v) silymarin.

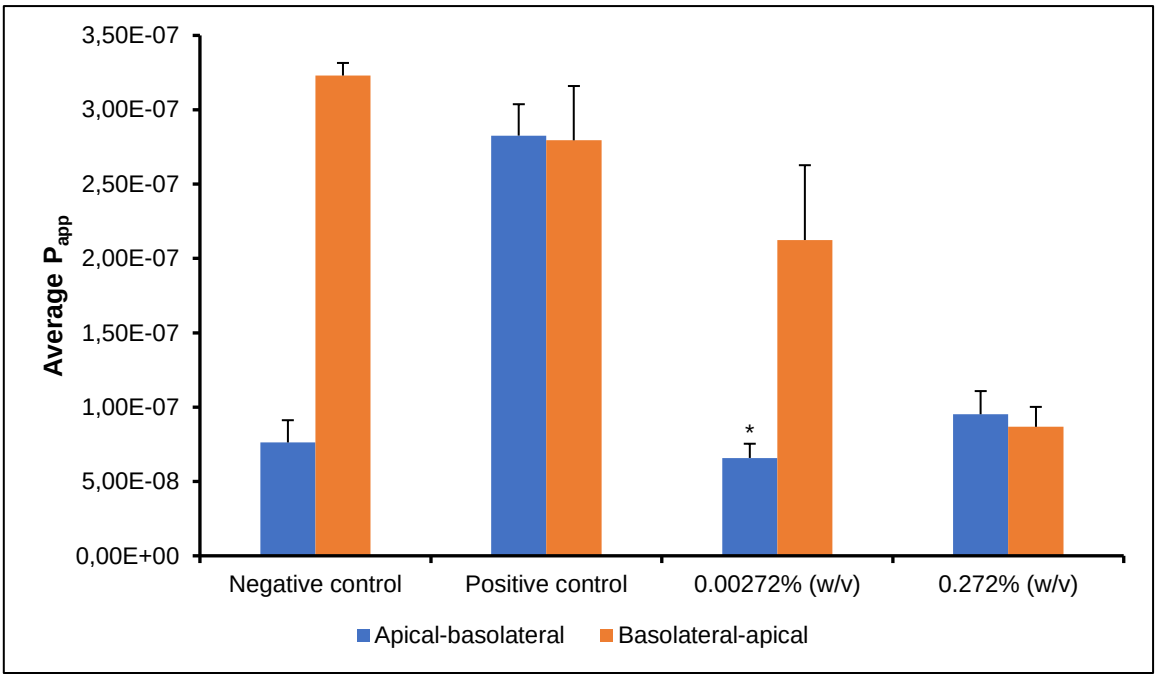

Figure 4.17: Average P_{app} values for bi-directional transport of Rhodamine-123 across excised pig intestinal tissue in the presence of silymarin (* shows statistically significant differences where $p \leq 0.05$)

In figure 4.17, the P_{app} values confirm a decrease of RH-123 transport in the BL-AP direction in the presence of silymarin. The change in percentage TEER for the high concentration (0.272% w/v) AP-BL could indicate why there was an increase in transport when compared to the low concentration (0.00272% w/v). The BL-AP percentage TEER reduction values for the high concentration (0.272% w/v) silymarin was less than the low concentration and this could indicate the significant decrease in transport of RH-123 in the BL-AP direction. There was a statistically significant difference (reduction) noted between the negative control and the high concentration (0.272% w/v) silymarin. ER values for the high concentration (0.272% w/v) was 0.91 which means there is possible inhibition of the P-gp function.

4.5 Efflux ratio evaluation

Table 4.13 contains all the ER values calculated from the experimental results of RH-123 in the presence of the selected health supplements. Calculated ER values indicate the degree of RH-123 transport in both AP-BL and BL-AP direction and aids as an indication of the likely foremost mechanisms of transport.

Table 4.13: Summary of the average P_{app} values and efflux ratio values for Rhodamine 123 in the presence of the selected commercially available health supplements at different concentrations

	Acetyl-L-carnitine	
	0.00566% (w/v)	**0.566% (w/v)**
Mean P_{app} (BL-AP)	5.99218E-07	1.1894E-07
Mean P_{app} (AP-BL)	1.3836E-07	3.63737E-07
Efflux ratio (ER)	4.33	0.33
	Berberine	
	0.000566% (w/v)	**0.0566% (w/v)**
Mean P_{app} (BL-AP)	5.38491E-08	1.48675E-07
Mean P_{app} (AP-BL)	1.01317E-07	1.62109E-07
Efflux ratio (ER)	0.53	0.92
	Chondroitin sulfate	
	0.000755% (w/v)	**0.0755% (w/v)**
Mean P_{app} (BL-AP)	1.06277E-07	1.80413E-07
Mean P_{app} (AP-BL)	2.39737E-07	2.60822E-07
Efflux ratio (ER)	0.44	0.69
	D-Glucosamine	
	0.00283% (w/v)	**0.283% (w/v)**
Mean P_{app} (BL-AP)	3.6111E-07	3.17072E-07
Mean P_{app} (AP-BL)	7.03495E-08	6.33401E-08
Efflux ratio (ER)	5.71	4.51
	Silymarin	
	0.00272% (w/v)	**0.272% (w/v)**
Mean P_{app} (BL-AP)	2.12376E-07	8.67444E-08
Mean P_{app} (AP-BL)	6.58217E-08	9.51968E-08
Efflux ratio (ER)	3.23	0.91

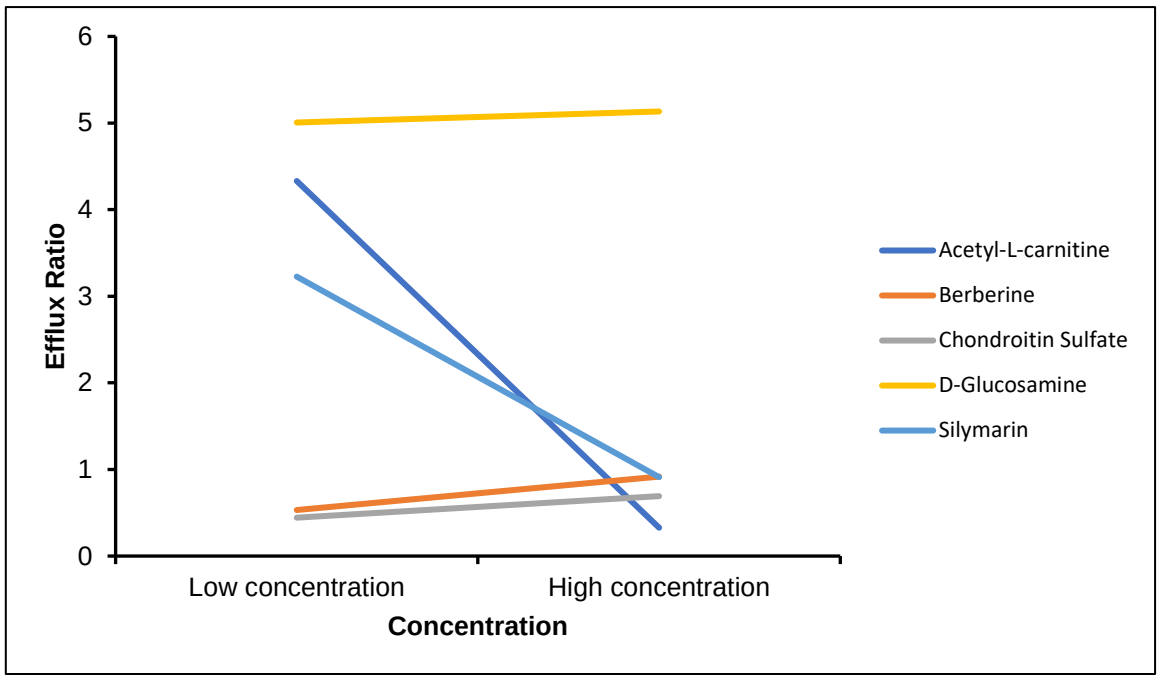

Figure 4.18: Graphic representation of the ER values of the selected commercially available health supplement at two different concentrations

In figure 4.18, the ER values of RH-123 in the presence of each health supplement are shown and the change in bi-directional transport can be seen for RH-123 in combination with these selected health supplements. Efflux occurs when RH-123 is pumped back into the apical side of intestines due to the active pumping of molecules from the basolateral to apical side and this leads to a lower concentration of the model compound in the blood and lower transport of RH-123. This phenomenon of efflux can be seen for RH-123 in the presence of berberine, CS and D-Glucosamine. ALC and silymarin showed a concentration dependant inhibition of RH-123 transport.

4.6 TEER evaluation and comparison

Trans-epithelial resistance (TEER) is used to determine if membrane integrity was maintained for the duration of the transport experiment, but also gives an indication of the modulation of tight junctions. TEER measurements were recorded at specific time points (at the beginning and end) of the experimental period (Irvine *et al.* 1999). Since TEER readings can be influenced by various factors such as the presence of health supplements which can modulate the tight junction integrity or affect paracellular transport it is important to know of any possible effects the selected health supplement can have that may affect the membrane integrity. At the beginning and end of each transport study the TEER was measured to determine the possible effect of commercially available health supplements on the tight junctions. The average percentage change between the T_0 and T_{120} TEER was calculated

and reported in Table 4.14 (all the values expressed in this table are expressed as an average percentage reduction from the initial T_0 value to T_{120}).

Table 4.14: Average % reduction in the TEER values across excised pig intestinal tissue exposed to the control formulation and selected commercially available health supplement formulations over a two-hour period (values are expressed as the average percentage TEER reduction between T_0 and T_{120})

	Positive control (RH-123 and verapamil)	
Apical to Basolateral	0.03	
Basolateral to Apical	2.05	
	Negative control (RH-123 alone)	
Apical to Basolateral	0.02	
Basolateral to Apical	0.10	
	Acetyl-L-Carnitine	
	0.00566% (w/v)	**0.566% (w/v)**
Apical to Basolateral	1.02	5.60
Basolateral to Apical	7.09	3.04
	Berberine	
	0.000566% (w/v)	**0.0566% (w/v)**
Apical to Basolateral	2.86	4.20
Basolateral to Apical	3.51	5.00
	Chondroitin Sulfate	
	0.000755% (w/v)	**0.0755% (w/v)**
Apical to Basolateral	6.41	6.43
Basolateral to Apical	1.85	2.09
	D-Glucosamine	
	0.00283% (w/v)	**0.283% (w/v)**
Apical to Basolateral	3.73	3.51
Basolateral to Apical	5.21	5.27
	Silymarin	
	0.00272% (w/v)	**0.272% (w/v)**
Apical to Basolateral	1.01	3.71
Basolateral to Apical	4.55	1.50

Since there were only small changes in the recorded TEER values for RH-123 in the presence of selected health supplements when compared to the TEER values of the control groups it may be concluded that this was an appropriate model to use for this study.

From the data obtained for ALC the TEER values and transport data for AP-BL transport of RH-123 shows that the integrity of the tight junctions had decreased and that there was an increase in RH-123 transport. For the BL-AP transport of RH-123 in the presence of ALC low concentration (0.00566% w/v) there was an increase in RH-123 transport and the reduction in TEER values indicate that the tight junctions had opened.

For berberine the AP-BL transport of RH-123 in the presence of the high concentration (0.0566% w/v) showed an increase in transport and a reduction in TEER values that could indicate tight junction modulation. For the BL-AP direction both concentrations decreased RH-123 transport and there was only a slight reduction in TEER values.

CS low concentration (0.000755% w/v) and high concentration (0.0755% w/v) both increased RH-123 transport in the AP-BL direction and the reduction in TEER indicates that an increase in RH-123 transport may have been mediated. BL-AP RH-123 transport was reduced, and this can be due to the higher TEER values and tight junctions that did not open successfully.

AP-BL transport of RH-123 in the presence of D-glucosamine high and low concentration had the same transport of RH-123 than that of the negative control and the slight reduction in TEER did not have a significant effect on RH-123 transport in the presence of D-glucosamine. BL-AP transport of RH-123 in the presence of both concentrations of D-glucosamine had the same effect as the negative control and the reduction in TEER did not have a significant effect on the transport of RH-123.

For AP-BL transport of RH-123 in the presence of 0.272% (w/v) silymarin increased RH-123 transport and the reduction in TEER values did not indicate that the tight junctions had opened and increased RH-123 transport. BL-AP RH-123 transport in the presence of silymarin decreased RH-123 transport and the minor reduction in TEER values was not significant enough to reduce tight junction integrity.

4.7 Membrane integrity study with Lucifer yellow

According to Irvine *et al.* (1999) the P_{app} values that indicate membrane integrity should be approximately 1 to 7 nm/sec (1 nm/sec = 1 x 10^{-7} cm/sec). In this study the average P_{app} value was 7.064 x10^{-7} and this shows that the method of mounting had no effect on the membrane integrity.

Table 4.15: The permeability coefficient values for Lucifer yellow across excised pig intestinal tissue

Chamber	P_{app} (x 10^{-7})
Chamber 1	8.544
Chamber 2	5.696
Chamber 3	6.952
Average	**7.064**

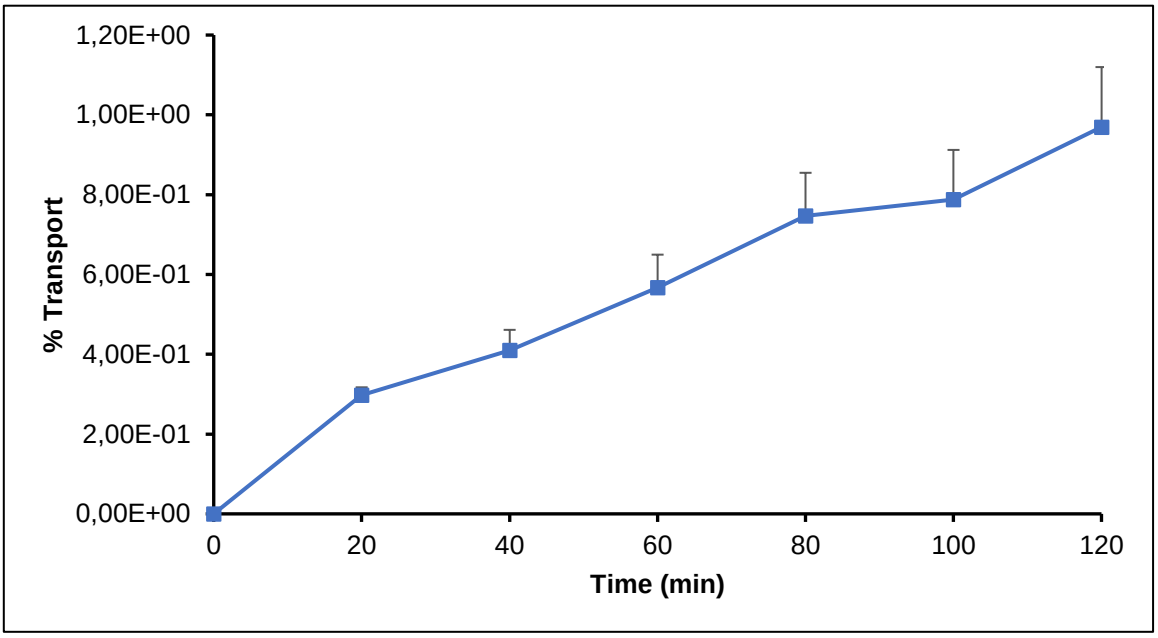

Figure 4.19: Apical to basolateral transport of Lucifer yellow across excised pig intestinal tissue plotted as a function of time

4.8 Conclusion

The analytical methods that were used in this study to quantify and measure RH-123 and LY content in the test samples from the experiments complied with all the validation criteria and specifications with regards to linearity, accuracy, precision and specificity.

The study conducted with RH-123 in the presence of ALC showed a statistically significant increase in transport of RH-123 (AP-BL) and this could possibly be due to the inhibition of P-gp related efflux. A statistically significant difference between the negative control and RH-123 in the presence of the low concentration (0.000566% w/v) berberine in the BL-AP direction was evident. While the slight decrease in % TEER values for D-glucosamine could indicate tight junctions opening but it did not have any significant effect on the transport of RH-123. The BL-AP transport of RH-123 in the presence of silymarin showed a statistically significant reduction in RH-123 transport when compared to the negative control. The ER values for the transport of RH-123 in the presence of a high concentration of silymarin showed a possible inhibitory effect of P-gp function.

CHAPTER 5: FINAL CONCLUSIONS AND FUTURE RECOMMENDATIONS

5.1 Final conclusions

The main goal of this study was to investigate potential pharmacokinetic interactions between selected commercially available health supplements, namely acetyl-L-carnitine, berberine, chondroitin sulfate, D-glucosamine and silymarin, and a model compound Rhodamine 123. Rhodamine 123 was included in this study because it is a well-known P-gp substrate which is susceptible to P-gp related efflux. Bi-directional transport studies were performed in an *ex vivo* permeation model to evaluate the effects of the selected commercially available health supplements on the intestinal epithelial permeation of RH-123 across excised pig intestinal tissue mounted between the half-cells of a Sweetana-Grass diffusion chamber apparatus.

Initially four objectives were identified for this study. The first objective was to conduct a comprehensive literature study to identify suitable health supplements and a model compound for inclusion in the study. The second objective was to identify and validate a fluorometric method for the analysis of RH-123 in the study samples in terms of linearity, specificity, precision and accuracy. Thirdly, it was decided that bi-directional transport studies should be conducted across excised pig intestinal tissue mounted between the half cells of a Sweetana-Grass diffusion apparatus and samples should be collected at pre-determined time intervals while measuring and recording the TEER values for the duration of each experiment. The fourth objective entailed the unbiased interpretation of the experimental data and statistical analysis of the processed data. The analytical method was validated with regards to linearity, accuracy, precision, limit of detection, limit of quantification and specificity and it complied with the criteria and specifications stated in the literature and because of this the data for the transport studies that were acquired could be deemed reliable.

The transport studies were conducted bi-directionally across excised pig intestinal tissue with RH-123 as a model compound in the presence and absence of the selected commercially available health supplements. The two concentrations at which the experiments were conducted was determined based on the article by Hellum *et al.* (2007). In chapter 3 of this dissertation all methods and procedures that were followed during this study are explained in detail. Chapter 4 entails the procedures pertaining to the calculation of the apparent permeability coefficient (P_{app}) values, efflux ratio (ER) values and the percentage change in trans-epithelial electrical resistance (% TEER).

The results from this study showed that a high concentration of acetyl-L-carnitine (ALC) mediated a statistically significant increase in RH-123 transport in the apical to basolateral (AP-BL) direction when compared to the negative control. TEER values for AP-BL transport of ALC at the high concentration indicated that the tight junction integrity might have decreased which mediated an increase in RH-123 transport. In the basolateral to apical (BL-AP) direction the ALC high concentration had no significant effect on RH-123 transport when compared to the control group and there was only a slight change in the percentage TEER which indicates that tight junction integrity was not compromised.

The high concentration of berberine mediated a 1.8-fold increase in RH-123 transport in the absorptive (AP-BL) direction when compared to the negative control. This was also the effect noted by Lin *et al.* (2017) that RH-123 efflux decreased when the concentration of berberine increased. The TEER values showed a decrease in percentage TEER (by 4.2% for the high concentration and by 2.86% for the low concentration), which indicated that the tight junction integrity was compromised that contributed to an increase in RH-123 transport when compared to the negative control group. The ER value for both concentrations was less than 1 and according to Bock *et al.* (2003) if an ER << 1 it could be indicative of absorptive uptake possibly due to decreased efflux. Berberine had a decreasing effect on the transport of RH-123 in the secretory (BL-AP) direction when compared to the control groups. When comparing the RH-123 transport in the experimental groups to the negative control group, the low concentration (0.000566% w/v) of berberine decreased RH-123 transport the most by 6.8-fold and there was a statistically significant ($p \leq 0.05$) difference between the low concentration and the negative control group. There was only a slight decrease in percentage TEER and this can indicate that the tight junctions did not open sufficiently to allow for RH-123 transport.

Chondroitin sulfate (CS) mediated a concentration dependant increase in the transport of RH-123 in the absorptive (AP-BL) direction when compared to the negative control but the increase in concentration was not statistically significant. The decrease in TEER values could possibly be due to tight junction openings and this can also be contributing factor to the increased transport of RH-123 caused by CS. Secretory (BL-AP) transport of RH-123 in the presence of the low and high concentration CS showed only a slight decrease in the TEER and this is a possible indication of the low transport of RH-123 that was noted when compared to the negative control for both concentrations of CS.

The RH-123 transport was very similar in the presence of D-glucosamine to that of the negative control group. The high (0.283% w/v) and low (0.00283% w/v) concentrations of D-glucosamine had a similar negligible effect on RH-123 transport in the absorptive (AP-BL)

direction. There was only a slight decrease in the calculated percentage TEER values and the relatively slight decrease in TEER values can be because of a slight opening of tight junctions, which had a negligible effect on the transport of RH-123 via the paracellular pathway. In the secretory (BL-AP) direction the transport of RH-123 in the presence of the low concentration (0.00283% w/v) D-glucosamine did not decrease but the transport was relatively the same as the negative control group. The high concentration (0.283% w/v) of D-glucosamine, on the other hand, caused a decrease in RH-123 transport when compared to the negative control. The slight decrease in TEER values noted for D-glucosamine can be because of tight junctions opening but it did not have a significant effect on the noted transport of RH-123 in both directions.

There was a statistically significant difference ($p \leq 0.05$) noted between the positive control and transport of RH-123 in the presence of the low concentration (0.00272% w/v) of silymarin. A high concentration of Silymarin mediated an increase in RH-123 transport in the absorptive (AP-BL) direction when compared to the negative control but the increase was not statistically significant. This result is in accordance with results that were reported by Ferreira *et al.* (2018) whom stated that silymarin was a promising P-gp inhibitor and the effect was concentration dependent. For secretory (BL-AP) transport of RH-123 in the presence of the low concentration silymarin the percentage transport yield was 0.320% and the high concentration silymarin yield a percentage transport of 0.138% as calculated from the original 5µM RH-123 concentration and the high concentration reduced the uptake of RH-123 by 4.5-fold when compared to the negative control. There was a statistically significant difference ($p \leq 0.05$) between the negative control and the high concentration (0.272% w/v) of silymarin in the secretory direction.

The results obtained from this study confirmed that commercially available health supplements which are taken in conjunction with other drugs can interfere with drug pharmacokinetics and may lead to possible pharmacokinetic interactions. This study can serve as a screening or reference for follow-up studies.

5.2 Future recommendations

Further studies should be conducted on the concomitant use of health supplements and drugs to identify potential pharmacokinetic interactions and to let health supplement users know about the possibility of interactions with other drugs.

It is important to consider possible inter-individual variations between the animals when using excised pig intestinal tissue as an *ex vivo* transport model. These variations may be minimised by including an additional control group during each experimental procedure

instead of using a single control data set as a standard reference against which the other transport values are compared.

Future studies can also be conducted on different parts of the pig intestine instead of only the proximal jejunum because each region differs in surface area, pH, thickness of the mucosa, possible enzyme activity and transporter expression. These mentioned factors need to be investigated because they can affect the degree of drug absorption.

To verify the results that are obtained with *in vitro* studies it is also recommended that *in vitro* studies should be conducted in conjunction with *in vivo* bioavailability studies. To see if there are any influences on the metabolic enzyme activity from the administration of commercially available health supplements in the presence of administered drugs a study should be conducted on the CYP450 enzymes to study the effect on bioavailability. This study will indicate what the bioavailability is of different drugs administered together by the modulation of enzymatic degradation.

REFERENCES

Al-Mohizea, A.M., Al-Jenoobi, F.I. & Alam, M.A. 2015. Rhodamine-123: A P-glycoprotein marker complex with sodium lauryl sulfate. *Pakistan Journal of Pharmaceutical Sciences,* 28:617-622.

Alolga, R.N., Fan, Y., Chen, Z., Liu, L.W., Zhao, Y.L., Li, J., Chen, Y., Lai, M.D., Li, P. & Qi, L.W. 2016. Significant pharmacokinetic differences of berberine are attributable to variations in gut microbiota between Africans and Chinese. *Scientific Reports,* 6:1-8.

Alqahtani, S., Mohamed, L.A. & Kaddoumi, A. 2013. Experimental models for predicting drug absorption and metabolism. *Expert opinion drug metabolism,* 9:1-14.

Annalora, A.J., Marcus, C.B. & Iversen, P.L. 2017. Alternative Splicing in the Cytochrome P450 Superfamily Expands Protein Diversity to Augment Gene Function and Redirect Human Drug Metabolism. *Drug Metabolism and Disposition,* 45:375-389.

Ashford, M. 2013. Introduction to biopharmaceutics. (*In* Aulton, M.E., *ed.* Aulton's Pharmaceutics: The Design and Manufacture of Medicines. 4th ed. Edinburg Churchill Livingstone. P. 292-295).

Ashford, M. 2013. Gastrointestinal tract – physiology and drug absorption. (*In* Aulton, M.E., *ed.* Aulton's Pharmaceutics: The Design and Manufacture of Medicines. 4th ed. Elsevier Churchill Livingstone. P. 314-333).

Ashford, M. 2013. Assessment of biopharmaceutical properties. (*In* Aulton, M.E., *ed.* Aulton's Pharmaceutics: The Design and Manufacture of Medicines. 4th ed. Elsevier Churchill Livingstone. P. 296-313).

Bahadur, S., Mukherjee, P.K., Pandit, S., Ahmmed, S.K.M. & Kar, A. 2017. Herb-drug interaction potential of *Berberis aristata* through cytochrome P450 inhibition assay. *Synergy,* 4:1-7.

Bock, U., Kottke, T., Gindorf, C. & Haltner, E. 2003. Validation of caco-2 cell monolayer system for determining the permeability of drug substances according to the Biopharmaceutics Classification System (BCS). (Unpublished)

Bourgeois, P., Chales, G., Dehais, J., Delcambre, B., Kuntz, J.L. & Rozenberg, S. 1998. Efficacy and tolerability of chondroitin sulfate 1200 mg/day vs chondroitin sulfate 3x400 mg/day vs placebo. *Osteoarthritis and Cartilage*, 6:25-30.

Bruyère, O., Altman, R.D. & Reginster, J.Y. 2016. Efficacy and safety of glucosamine sulfate in the management of osteoarthritis: Evidence from real-life setting trails and surveys. *Seminars in Arthritis and Rheumatism*, 45: 12-17.

Chang, L.W., Hou, M.L., Lin, L.C. & Tsai, T.H. 2015. Healthy supplements of silymarin and aqueous extract of *Salvia miltiorrhiza* on the pharmacokinetic interactions of lamivudine in rats. *Journal of Functional Foods*, 17:163-171.

Dahan, A. & Hoffman, A. 2007. The effects of different lipid based formulations on the oral absorption of lipophilic drugs: The ability of in vitro lipolysis and consecutive ex vivo intestinal permeability data to predict *in vivo* bioavailability in rats. *European Journal of Pharmaceutics and Biopharmaceutics,* 67:96-105.

Deferme, S., Annaert, P. & Augustijns, P. 2008. Drug absorption studies. (*In*: Ehrhardt, C. & Kim, K.-W., *eds*. *In vitro* screening models to assess intestinal drug absorption and metabolism, New York: Springer. p. 182-215.

de Oliveira, J.S., Abdalla, F.H., Dornelles, G.L., Adefegha, S.A., Palma, T.V., Signor, C., da Silva Bernardi, J., Baldissarelli, J., Lenz, L.S., Magni, L.P., Rubin, M.A., Pillat, M.M. & de Andrade, C.M. 2016. Berberine protects against memory impairment and anxiogenic-like behavior in rats submitted to sporadic Azheimer's-like dementia: Involvement of acetylcholinesterase and cell death. *Neuro Toxicology*, 57:241-250.

Derrick-Roberts, A.L.K., Marais, W. & Byers, S. 2012. Rhodamine B and 2-acetamido-1,3,6-tri-O-acetyl-4-deoxy-4-fluoro-D-glycopyranose (F-GlcNAc) inhibit chondroitin/dermatan and keratan sulphate synthesis by different mechanisms in bovine chondrocytes. *Molecular Genetics and Metabolism*, 106:214-220.

Doege, K., Chen, X., Cornuet, P.K. & Hassell, J. 1997. Non-Glycosaminoglycan Bearing Domains of Perlecan and Aggrecan Influence the Utilization of Sites for Heparan and Chondroitin Sulfate Synthesis. *Matrix Biology,* 16:211-221.

Evans, A.M. & Fornasini, G. 2003. Pharmacokinetics of L-Carnitine. *Clinical Pharmacokinetics*, 11:941-967.

Ferreira, A., Rodrigeus, M., Fortuna, A., Falcão, A. & Alves G. 2018. Flavonoid compounds as reversing agents of the P-glycoprotein-mediated multidrug resistance: An *in vitro* evaluation with focus on antiepileptic drugs. *Food Research International,* 103:110-120

Flaten, G.E, Dhanikula, A.B., Luthman, K. & Brandl, M. 2006. Drug permeability across a phospholipid vesicle based barrier: A novel approach for studying passive diffusion. *European Journal of Pharmaceutical Sciences,* 27:80-90.

Forster, S., Thumser, A.E., Hood, S.R. & Plant, N. 2012. Characterization of rhodamine-123 as a tracer dye for use in in vitro transport assays. *PLoS ONE*, 7:e33253. Doi:10.1371/journal.pone.0033253.

Gahche, J.J., Bailey, R.L., Potischman, N. & Dwyer J.T. 2017. Dietary supplements use was very high among older adults in the United States in 2011-2014. *The Journal of Nutrition*, 147:1968-1976.

Gardiner, P., Stargrove, M.B. & Dog, T.L. 2011. Concomitant use of prescription medications and dietary supplements in menopausal women: An approach to provider preparedness. *Maturitas*, 68:251-255.

Go, R., Hwang, K. & Choi, K. 2015. Cytochrome P450 1 family and cancers. *Journal of Steroid Biochemistry & Molecular Biology,* 147:24-30

Grime, K.H., Barton, P. & McGinnity, D.F. 2013. Application of In Silico, In Vitro and Preclinical Pharmaco kinetics Data for the Effective and Efficient Prediction of Human Pharmacokinetics. *Molecular Pharmaceutics*, 10:1191-1206.

Hellum, B.H., Hu, Z. & Nilsen, O.G. 2007. The induction of CYP1A2, CYP2D6 and CYP3A4 by six trade herbal products in cultured primary human hepatocytes. *Basic & clinical pharmacology and toxicology,* 100:23-30.

Hidalgo, I.J. 2001. Assessing the absorption of new pharmaceuticals. *Current Topics in Medicinal Chemistry*, 1:385-401.

Holmstock, N., Annaert, P. & Augustijns, P. 2012. Boosting of HIV protease inhibitors by ritonavir in the intestine: the relative role of cytochrome P450 and P-glycoprotein inhibition based on Caco-2 monolayers versus in situ intestinal perfusion in mice. *Drug Metabolism and Disposition*, 40:1473-1477.

Ibrahim, A., Gilzad-Kohan, M.H., Aghazadeh-Habashi, A. & Jamali, F. 2012. Absorption and Bioavailability of Glucosamine in the Rat. *Journal of Pharmaceutical Sciences*, 101:2574-2583

Irvine, J.D., Takahashi, L., Lockhart, K., Cheong., Tolan, J.W., Selick, H.E. & Grove, J.R. 1999. MDCK (Madin-Darby Canine Kidney) Cells: A Tool for Membrane Permeability Screening. *Journal of Pharmaceutical Sciences,* 88:28-33.

Jackson, C.G., Plaas, A.H., Sandy, J.D., Hua, C., Kim-Rolands, S., Barnhill, J.G., Harris, C.L. & Clegg, D.O. 2010. The human pharmacokinetics of oral ingestion of glucosamine and chondroitin sulfate taken separately or in combination. *Osteoarthritis and Cartilage,* 18:297-302.

Kang, D., Schwartz, J.B. & Verotta, D. 2004. A sample size computation for non-linear mixed effects models with applications to pharmacokinetics models. *Statistics in Medicine*, 23:2551-2566.

Kaprelyants, A.S. & Kell, D.B. 1992. Rapid assessment of bacterial viability and vitality by rhodamine 123 and flow cytometry. *Journal of Applied Bacteriology,* 72:410-422.

Kararli, T.T. 1995. Comparison of the Gastrointestinal Anatomy, Physiology, and Biochemistry of Humans and Commonly Used Laboratory Animals. *Biopharmaceutics and Drug Disposition*, 16:351-380.

Kobayashi, E., Hisikawa, S., Teratani, T. & Lefor, A.T. 2012. The pig as a model for translational research: overview of porcine animal models at Jichi Medical University. *Transplantation Research*, 1:1-9.

Komoroski, B.J. 2000. The direct and indirect effects of herbal products on common drug metabolizing enzymes and drug transporters. Pittsburgh: University of Pittsburgh. (Dissertation-PhD).

Legen, I., Salobir, M. & Kerč, J. 2005. Comparison of different intestinal epithelia as models for absorption enhancements studies. *Interantional Journal of Pharmaceutics*, 291:183-188.

Lennernäs, H. 2007. Animal data: The contributions of the Ussing Chamber and perfusion systems to predicting human oral drug delivery *in vivo*. Advanced Drug Delivery Reviews, 59:1103-1120.

Lin, J.H. & Lu, A.Y.H. 1998. Inhibition and Induction of Cytochrome P450 and the Clinical Implications. *Clinical Pharmacokinetics,* 35:361-390.

Lin, Y., Sheng, M., Weng, Y., Xu, R., Lu, N. & Du, H. 2017. Berberine protects against ischemia/reperfusion injury after orthotopic liver transplantation via activating Sirt1/FoxO3α induced autophagy. *Biochemical and Biophysical Research Communications*, 482:885-891.

Luo, Z., Liu, Y., Zhao, B., Tang, M., Dong, M., Zhang, L., Lv, B. & Wei, L. 2013. Ex vivo and in situ approaches used to study intestinal absorption. *Journal of Pharmacological and Toxicological Methodes*, 68:208-216.

Mak, S., Luk, W.W.K., Cui, W., Hu, S., Tsim, K.W.K. & Han, Y. 2014. Synergistic inhibition on acetylcholinesterase by the combination of berberine and palmatine originally isolated from Chinese medicinal herbs. *Journal of Molecular Neuroscience,* 53:511-516.

Malaguarnera, M., Gargante, M.P., Cristaldi, E., Colonna, V., Messano, M., Koverech, A., Neri, S., Vacante, M., Cammalleri, L. & Motta, M. 2008. Acetyl-L-carnitine (ALC) treatment in elderly patients with fatigue. *Archives of Gerontology and Geriatrics,* 46:181-190.

Martini, F.H., Nath, J.L. & Bartholomew, E.F. 2012. Fundamentals of Anatomy & Physiology. 9th ed. International Edition: Benjamin Cummings, P.862-915.

Mistry, B., Patel, R.V., Keum, Y.C. & Kim, D.H. 2017. Synthesis of *N*-Mannich bases of berberine linking piperazine moieties revealing anticancer and antioxidant effects. *Saudi Journal of Biological Sciences*, 24:36-44.

Onishi, H., Isoda, Y. & Matsuyama, M. 2013. *In vivo* evaluation of chondroitin sulfate-glycyl-prednisolone for anti-arthritic effectiveness and pharmacokinetic characteristics. *International Journal of Pharmaceutics,* 456:113-120.

Pavek, P. & Dvorak, Z. 2008. Xenobiotic-Induced Transcriptional Regulation of Xenobiotic Metabolizing Enzymes of the Cytochrome P450 Superfamily in Human Extrahepatic Tissues. *Current Drug Metabolism,* 9:129-143.

Pelkonen, O., Turpeinen, M., Hakkola, J., Honkakoski, P., Hukkaken, J. & Raunio, H. 2008. *Archives of Toxicology,* 82:667-715.

Pettegrew, J.W., Klunk, W.E., Panchalingam, K., Kanfer, J.N. & McClure, R.J. 1995. Clinical and Neurochemical Effects of Acetyl-L-carnitine in Alzheimer's Disease. *Neurobiology of Aging,* 16:1-4.

Pietzonka, P., Walter, E., Duda-Johner, S., Langguth, P. & Merkle, H.P. 2002. Compromised integrity of excised porcine intestinal epithelium obtained from the abattoir

affects the outcome of *in vitro* particle uptake studies. *European journal of pharmaceutical sciences,* 15:39-47.

Qiu, W., Jiang, X.H., Liu, C.X., Ju, Y. & Jin J.X. 2009. Effects of berberine on the pharmacokinetics of substrates of CYP3A and P-gp. *Phytotherapy Research,* 23:1553-1558.

Rani, A., Baruah, R. & Goyal, A. 2017. Physicochemical, antioxidant and biocompatible properties of chondroitin sulphate isolated from chicken keel bone for potential biomedical applications. *Carbohydrate Polymers*, 159:11-19.

Roman-Blas, J.A., Mediero, A., Tardío, L., Portal-Nuñez, S., Gratal, P., Herrero-Beaumont, G. & Largo, R. 2017. The combined therapy with chondroitin sulfate plus glucosamine sulfate or chondroitin sulfate plus glucosamine hydrochloride does not improve joint damage in an experimental model of knee osteoarthritis in rabbits. *European Journal of Pharmacology,* 794:8-14.

Rozehnal, V., Nakai, D., Hoepner, U., Fischer, T., Kamiyama, E., Takahashi, M., Yasuda, S. & Mueller, J. 2012. Human small intestinal and colonic tissue mounted in the Ussing chamber as a tool for characterizing the intestinal absorption of drugs. *European Journal of Pharmaceutical Sciences,* 46:367-373.

Sarmento, B., Andrade, F., da Silva, S.B., Rodrigues, F., das Neves, J. & Ferreira, D. 2012. Cell-based in vitro models for predicting drug permeability. *Expert opinion on Drug Metabolism and Toxicology*, 8: 607-621.

Shabir, G.A. 2003. Validation of high-performance liquid chromatography methods for pharmaceutical analysis understanding the differences and similarities between validation requirements of the US Food and Drug Administration, the US Pharmacopeia and the International Conference on Harmonization. *Journal of chromatography A,* 987:57-66.

Shang, Q., Shi, J., song, G., Zhang, M., Cai, C., Hao, J., Li, G. & Yu, G. 2016. Structural modulation of gut microbiota by chondroitin sulphate and its oligosaccharide. *International Journal of Biological Macromolecules*, 86:489-498.

Shargel, L., Wu-Pong, S. & Yu, A.B.C. 2012. Pharmacogenetics. (In: Shargel, L., Wu-Pong, S. & Yu, A.B.C. ed. Applied biopharmaceutics & pharmacokinetics. 6th ed. New York: McGraw Hill, P. 301-320.)

Shargel, L., Wu-Pong, S. & Yu. A.B.C. 2012. Physiologic factors related to drug absorption. (In: Shargel, L., Wu-Pong, S. & Yu, A.B.C. ed. Applied biopharmaceutics & pharmacokinetics. 6th ed. Boston: McGraw-Hill, P.321-360.)

Shargel, L., Wu-Pong, S. & Yu. A.B.C. 2012. Biopharmaceutic considerations in drug product design and *in vitro* drug product performance. (In: Shargel, L., Wu-Pong, S. & Yu, A.B.C. ed. Applied biopharmaceutics & pharmacokinetics. 6th ed. Boston: McGraw-Hill, P.361-402.)

Singh, R. 2013. HPLC method development and validation: an overview. *Indian journal of pharmaceutical education and research,* 4:26-33.

Smeland, O.B., Meisingset, T.W., Borges, K. & Sonnewald, U. 2012. Chronic acetyl-L-carnitine alters brain energy metabolism and increases noradrenaline and serotonin content in healthy mice. *Neurochemistry International*, 61:100-107.

Tarirai, C. 2011. Effect of commonly consumed botanicals on drug efflux across intestinal epithelial cells and excised tissues. Pretoria:TUT (Thesis-DTech).

Tsang,C.M., Lau, E.P.W., Di, K., Cheung, P.Y., Hau, P.M., Ching, Y.P., Wong, Y.C., Cheung, A.L.M., Wan, T.S.K., Tong, Y., Tsao, S.W. & Feng, Y. 2009. Berberine inhibits Rho GTPases and cell migration at low doses but induces G2 arrest and apoptosis at high doses in human cancer cells. International Journal of Molecular Medicine, 24:131-138.

United States Pharmacopeial Convention. 2018. Validations of compendial methods. http://www.pharmacopeia.cn/v29240/usp29nf24s0_c1225.html. Date of access: 20 Aug 2018.

Wempe, M.F., Wright, C., Little, J.L., Lightner, J.W., Large, S.E., Caflisch, G.B., Buchanan, C.M., Rice, P.J., Wacher, V.J., Ruble, K.M. & Edgar, K.J. 2009. Inhibiting efflux with novel non-ionic surfactants: Rational design based on vitamin E TPGS. *International Journal of Pharmaceutics*, 370:93-102.

Wu, C.H., Wang, C.C., Tsai, M.T., Huang, W.T. & Kennedy, J. 2014. Trend and Pattern of Herb and Supplement Use in the United States: Results from the 2002, 2007, and 2012 National Health Interview Surveys. *Evidence-Based Complementary and Alternative Medicine*, 2014:1-7

Wu, J.W., Lin, L.C. & Tsai, T.H. 2009. Drug-drug interactions of silymarin on the perspective of pharmacokinetics. *Journal of Ethnopharmacology*, 121:185-193.

Wu, X., Ma, J., Ye, Y. & Lin, G. 2016. Transporter modulation by Chinese herbal medicines and its mediated pharmacokinetic herb-drug interactions. *Journal of Chromatography B*, 1026:236-253.

Xiao, Y., Li, P., Cheng, Y., Zhang, Q. & Wang, F. 2016. Effect of α-linolenic acid-modified low molecular weight chondroitin sulfate on atherosclerosis in apoE-deficient mice. *Biochimica et Biophysica Acta*, 1860:2589-2597.

Xie, F., Ding, X. & Zhang, Q.Y. 2016. An update on the role of intestinal cytochrome P450 enzymes in drug disposition. *Acta Pharmaceutica Sinica B*, 6:374-383.

Xu, Q., Liu, K., Lin, X., Qin, Y., Chen, L., Cheng, J., Zhong, M., He, Q., Li, Y., Wang, T., Pan, J., Peng, M., Yao, L. & Ji, Z. 2017. ADMETNet: The knowledge base of pharmacokinetics and toxicology network. *Journal of Genetics and Genomes*, 44:273-276.

Yamada, S., Misaka, S., Tanabe, K., Osano, A., Takeuchi, K., Werba, H. & Watanabe, H. 2014. Effect of consumption of catechin-rich green tea on pharmacokinetics of simvastatin in health volunteers. *PharmaNutrition*, 2:75-119.

Yang, L. 2009. Study of herb-drug interactions. Melbourne: RMIT University (Thesis-PhD).

Ye, L., Liang, S., Gua, C., Yu, X., Zhao, J., Zhang, H. & Shang, W. 2016. Inhibition of M1 macrophage activation in adipose tissue by berberine improves insulin resistance. *Life Sciences*, 116:82-91.

Yin, J., Xing, H. & Ye, Jainping. 2008. Effects of Berberine in patients with type 2 diabetes mellitus. *Metabolism Clinical and Experimental*, 57:712-717.

Yong, P.W., Tan, L.B. & Loh, Y.H. 2014. Consumption of dietary health supplements among hospitalized patients at an acute tertiary Hospital. *PharmaNutrition*, 2:135-140.

Young, L.A., Faurot, K.R. & Gaylord, S.A. 2008. Use of and Communications about Dietry Supplements Among Hospitalized Patients. *Journal of General Internal Medicine*, 24:366-369.

Zaitone, S.A., Abo-Elmatty, D.M. & Shaalan, A.A. 2012. Acetyl-L-carnitine and α-lipoic acid affect rotenone-induced damage in nigral dopaminergic neurons of rat brain, implication for Parkinson's disease therapy. *Pharmacology, Biochemistry and Behavior*, 100:347-360.

Zhang, Y., Cui, Y., Gao, L. & Jiang, H. 2013. Effects of β-cyclodextrin on the intestinal absorption of berberine hydrochloride, a P-glycoprotein substrate. *International Journal of Biological Macromolecules*, 59:363-371.

Zhao, W., Uehera, S., Tanaka, K., Tadokoro, S., Kusamori, K., Katsumi, H., Sakane, T. & Yamamoto, A. 2016. Effects of Polyoxyethylene Alkyl Ethers on the Intestinal Transport and Absorption of Rhodamine 123: A P-glycoprotein Substrate by *In Vitro* and *In Vivo* Studies. *Journal of Pharmaceutical Sciences*, 105:1526-1534.

ADDENDUM A

ETHICAL APPROVAL

NORTH-WEST UNIVERSITY
YUNIBESITI YA BOKONE-BOPHIRIMA
NOORDWES-UNIVERSITEIT

Private Bag X6001, Potchefstroom
South Africa 2520

Tel: (018) 299-4900
Faks: (018) 299-4910
Web: http://www.nwu.ac.za

Ethics Committee
Tel +27 18 299 4849
Email Ethics@nwu.ac.za

ETHICS APPROVAL OF PROJECT

The North-West University Research Ethics Regulatory Committee (NWU-RERC) hereby approves your project as indicated below. This implies that the NWU-RERC grants its permission that provided the special conditions specified below are met and pending any other authorisation that may be necessary, the project may be initiated, using the ethics number below.

Project title: Excised pig buccal and intestinal tissues as in vitro models for pharmacokinetic studies

Project Leader: Prof Sias Hamman

Ethics number:

N	W	U	-	0	0	0	2	5	-	1	5	-	A	5
Institution				Project Number						Year			Status	

Status: S = Submission; R = Re-Submission; P = Provisional Authorisation; A = Authorisation

Approval date: 2015-04-16 **Expiry date**: 2020-04-15

Special conditions of the approval (if any): None

General conditions:

While this ethics approval is subject to all declarations, undertakings and agreements incorporated and signed in the application form, please note the following:

- x *The project leader (principle investigator) must report in the prescribed format to the NWU-RERC:*
  - *annually (or as otherwise requested) on the progress of the project,*
  - *without any delay in case of any adverse event (or any matter that interrupts sound ethical principles) during the course of the project.*
- x *The approval applies strictly to the protocol as stipulated in the application form. Would any changes to the protocol be deemed necessary during the course of the project, the project leader must apply for approval of these changes at the NWU-RERC. Would there be deviated from the project protocol without the necessary approval of such changes, the ethics approval is immediately and automatically forfeited.*
- x *The date of approval indicates the first date that the project may be started. Would the project have to continue after the expiry date, a new application must be made to the NWU-RERC and new approval received before or on the expiry date.*
- x *In the interest of ethical responsibility the NWU-RERC retains the right to:*
  - *request access to any information or data at any time during the course or after completion of the project;*
  - *withdraw or postpone approval if:*
    - *any unethical principles or practices of the project are revealed or suspected,*
    - *it becomes apparent that any relevant information was withheld from the NWU-RERC or that information has been false or misrepresented,*
    - *the required annual report and reporting of adverse events was not done timely and accurately,*
    - *new institutional rules, national legislation or international conventions deem it necessary.*

The Ethics Committee would like to remain at your service as scientist and researcher, and wishes you well with your project. Please do not hesitate to contact the Ethics Committee for any further enquiries or requests for assistance.

Yours sincerely

Linda du Plessis

Digitally signed by Linda du Plessis
DN: cn=Linda du Plessis, o=NWU, Vaal Triangle Campus, ou=Vice-Rector: Academic, email=linda.duplessis@nwu.ac.za, c=US
Date: 2015.04.20 20:35:13 +02'00'

Prof Linda du Plessis
Chair NWU Research Ethics Regulatory Committee (RERC)

ADDENDUM B

EX VIVO TRANSPORT DATA OF RHODAMINE 123 ACROSS EXCISED PIG INTESTINAL TISSUE AND APPARENT PERMEABILITY

Table B.1: Apical to basolateral cumulative percentage transport of Lucifer yellow alone across excised pig intestinal tissue for determining membrane integrity

Time (min)	Percentage transport: chamber 1	Percentage transport: chamber 2	Percentage transport: chamber 3	Standard deviation	Mean percentage transport
0	0.000	0.000	0.000	0.000	0.000
20	0.323	0.295	0.275	0.019	0.298
40	0.482	0.369	0.379	0.051	0.410
60	0.677	0.479	0.546	0.082	0.567
80	0.867	0.604	0.769	0.108	0.747
100	0.915	0.619	0.829	0.124	0.788
120	1.180	0.841	0.887	0.150	0.969
P_{app} ($x10^{-7}$)	8.544	5.696	6.952	1.166	

Table B.2: Apical to basolateral cumulative percentage transport of Rhodamine 123 in the presence of Verapamil across excised pig intestinal tissue

Time (min)	Percentage transport: chamber 1	Percentage transport: chamber 2	Percentage transport: chamber 3	Standard deviation	Mean percentage transport
0	0.000	0.000	0.000	0.000	0.000
20	0.075	0.103	0.012	0.038	0.063
40	0.106	0.207	0.089	0.052	0.134
60	0.200	0.309	0.122	0.077	0.210
80	0.251	0.309	0.150	0.066	0.237
100	0.313	0.355	0.389	0.031	0.352
120	0.304	0.362	0.343	0.024	0.336
P_{app} ($x10^{-7}$)	2.567	2.828	3.084	0.211	

Table B.3: Basolateral to apical cumulative percentage transport of Rhodamine 123 in the presence of Verapamil across excised pig intestinal tissue

Time (min)	Percentage transport: chamber 1	Percentage transport: chamber 2	Percentage transport: chamber 3	Standard deviation	Mean percentage transport
0	0.000	0.000	0.000	0.000	0.000
20	0.306	0.311	0.254	0.026	0.290
40	0.350	0.353	0.566	0.032	0.328
60	0.390	0.399	0.326	0.033	0.372
80	0.444	0.405	0.338	0.044	0.396
100	0.432	0.482	0.372	0.045	0.429
120	0.438	0.516	0.373	0.059	0.442
P_{app} ($x10^{-7}$)	2.778	3.250	2.356	0.365	

Table B.4: Apical to basolateral cumulative percentage transport of Rhodamine 123 alone across excised pig intestinal tissue

Time (min)	Percentage transport: chamber 1	Percentage transport: chamber 2	Percentage transport: chamber 3	Standard deviation	Mean percentage transport
0	0.000	0.000	0.000	0.000	0.000
20	0.147	0.061	0.055	0.042	0.088
40	0.153	0.064	0.056	0.044	0.091
60	0.164	0.060	0.057	0.050	0.094
80	0.158	0.065	0.075	0.042	0.100
100	0.160	0.076	0.090	0.036	0.109
120	0.181	0.108	0.116	0.032	0.135
P_{app} ($x10^{-7}$)	0.959	0.597	0.731	0.150	

Table B.5: Basolateral to apical cumulative percentage transport of Rhodamine 123 alone across excised pig intestinal tissue

Time (min)	Percentage transport: chamber 1	Percentage transport: chamber 2	Percentage transport: chamber 3	Standard deviation	Mean percentage transport
0	0.000	0.000	0.000	0.000	0.000
20	0.471	0.735	0.614	0.108	0.607
40	0.540	0.763	0.655	0.091	0.653
60	0.559	0.766	0.676	0.085	0.667
80	0.571	0.743	0.633	0.071	0.649
100	0.576	0.697	0.648	0.050	0.640
120	0.572	0.691	0.605	0.050	0.623
P_{app} ($x10^{-7}$)	3.272	3.306	3.112	0.085	

Table B.6: Apical to basolateral cumulative percentage transport of Rhodamine 123 in the presence of 0.00566% (w/v) acetyl-L-carnitine across excised pig intestinal tissue

Time (min)	Percentage transport: chamber 1	Percentage transport: chamber 2	Percentage transport: chamber 3	Standard deviation	Mean percentage transport
0	0.000	0.000	0.000	0.000	0.000
20	0.051	0.101	0.075	0.020	0.076
40	0.072	0.119	0.116	0.021	0.102
60	0.084	0.139	0.138	0.026	0.120
80	0.102	0.161	0.180	0.033	0.147
100	0.118	0.176	0.205	0.036	0.166
120	0.168	0.198	0.235	0.027	0.201
P_{app} ($x10^{-7}$)	1.115	1.314	1.721	0.252	

Table B.7: Basolateral to apical cumulative percentage transport of Rhodamine 123 in the presence of 0.00566% (w/v) acetyl-L-carnitine across excised pig intestinal tissue

Time (min)	Percentage transport: chamber 1	Percentage transport: chamber 2	Percentage transport: chamber 3	Standard deviation	Mean percentage transport
0	0.000	0.000	0.000	0.000	0.000
20	0.599	0.544	0.753	0.088	0.632
40	0.773	0.678	0.919	0.099	0.790
60	0.917	0.811	1.015	0.084	0.914
80	0.955	0.816	1.019	0.085	0.930
100	1.026	0.839	1.005	0.083	0.957
120	0.999	0.792	1.003	0.098	0.931
P_{app} ($x10^{-7}$)	6.742	5.194	6.041	0.633	

Table B.8: Apical to basolateral cumulative percentage transport of Rhodamine 123 in the presence of 0.566% (w/v) acetyl-L-carnitine across excised pig intestinal tissue

Time (min)	Percentage transport: chamber 1	Percentage transport: chamber 2	Percentage transport: chamber 3	Standard deviation	Mean percentage transport
0	0.000	0.000	0.000	0.000	0.000
20	0.717	0.572	0.577	0.067	0.622
40	0.728	0.609	0.604	0.057	0.647
60	0.763	0.630	0.649	0.059	0.681
80	0.766	0.626	0.632	0.065	0.674
100	0.743	0.627	0.631	0.054	0.667
120	0.747	0.673	0.638	0.045	0.686
P_{app} ($x10^{-7}$)	3.897	3.588	3.427	0.195	

Table B.9: Basolateral to apical cumulative percentage transport of Rhodamine 123 in the presence of 0.566% (w/v) acetyl-L-carnitine across excised pig intestinal tissue

Time (min)	Percentage transport: chamber 1	Percentage transport: chamber 2	Percentage transport: chamber 3	Standard deviation	Mean percentage transport
0	0.000	0.000	0.000	0.000	0.000
20	0.137	0.174	0.144	0.016	0.152
40	0.150	0.197	0.160	0.020	0.169
60	0.153	0.216	0.161	0.028	0.177
80	0.158	0.226	0.175	0.029	0.186
100	0.158	0.226	0.184	0.028	0.189
120	0.171	0.237	0.211	0.027	0.206
P_{app} ($x10^{-7}$)	0.944	1.409	1.215	0.191	

Table B.10: Apical to basolateral cumulative percentage transport of Rhodamine 123 in the presence of 0.000566% (w/v) berberine across excised pig intestinal tissue

Time (min)	Percentage transport: chamber 1	Percentage transport: chamber 2	Percentage transport: chamber 3	Standard deviation	Mean percentage transport
0	0.000	0.000	0.000	0.000	0.000
20	0.064	0.070	0.079	0.006	0.071
40	0.076	0.089	0.095	0.008	0.087
60	0.096	0.112	0.120	0.010	0.109
80	0.101	0.116	0.120	0.008	0.113
100	0.133	0.134	0.146	0.006	0.138
120	0.150	0.283	0.154	0.005	0.149
P_{app} ($x10^{-7}$)	1.026	0.973	1.041	0.029	

Table B.11: Basolateral to apical cumulative percentage transport of Rhodamine 123 in the presence of 0.000566% (w/v) berberine across excised pig intestinal tissue

Time (min)	Percentage transport: chamber 1	Percentage transport: chamber 2	Percentage transport: chamber 3	Standard deviation	Mean percentage transport
0	0.000	0.000	0.000	0.000	0.000
20	0.080	0.063	0.073	0.007	0.072
40	0.091	0.070	0.084	0.009	0.082
60	0.097	0.075	0.092	0.009	0.088
80	0.097	0.073	0.093	0.010	0.088
100	0.099	0.077	0.098	0.010	0.092
120	0.097	0.079	0.101	0.0106	0.092
P_{app} ($x10^{-7}$)	0.560	0.451	0.604	0.064	

Table B.12: Apical to basolateral cumulative percentage transport of Rhodamine 123 in the presence of 0.0566% (w/v) berberine across excised pig intestinal tissue

Time (min)	Percentage transport: chamber 1	Percentage transport: chamber 2	Percentage transport: chamber 3	Standard deviation	Mean percentage transport
0	0.000	0.000	0.000	0.000	0.000
20	0.107	0.117	0.120	0.006	0.114
40	0.121	0.148	0.155	0.015	0.141
60	0.163	0.188	0.188	0.012	0.180
80	0.190	0.208	0.188	0.009	0.195
100	0.215	0.253	0.220	0.017	0.229
120	0.210	0.245	0.232	0.014	0.229
P_{app} ($x10^{-7}$)	1.530	1.783	1.551	0.115	

Table B.13: Basolateral to apical cumulative percentage transport of Rhodamine 123 in the presence of 0.0566% (w/v) berberine across excised pig intestinal tissue

Time (min)	Percentage transport: chamber 1	Percentage transport: chamber 2	Percentage transport: chamber 3	Standard deviation	Mean percentage transport
0	0.000	0.000	0.000	0.000	0.000
20	0.187	0.132	0.223	0.037	0.180
40	0.219	0.145	0.257	0.047	0.207
60	0.242	0.162	0.280	0.049	0.228
80	0.245	0.165	0.286	0.050	0.232
100	0.257	0.175	0.305	0.054	0.246
120	0.252	0.175	0.306	0.054	0.244
P_{app} ($x10^{-7}$)	1.540	1.057	1.863	0.331	

Table B.14: Apical to basolateral cumulative percentage transport of Rhodamine 123 in the presence of 0.000755% (w/v) chondroitin sulfate across excised pig intestinal tissue

Time (min)	Percentage transport: chamber 1	Percentage transport: chamber 2	Percentage transport: chamber 3	Standard deviation	Mean percentage transport
0	0.000	0.000	0.000	0.000	0.000
20	0.423	0.212	0.148	0.118	0.261
40	0.528	0.312	0.182	0.143	0.341
60	0.556	0.305	0.202	0.149	0.354
80	0.579	0.310	0.217	0.154	0.369
100	0.599	0.327	0.229	0.156	0.385
120	0.594	0.329	0.234	0.152	0.386
P_{app} ($x10^{-7}$)	3.655	2.032	1.506	0.915	

Table B.15: Basolateral to apical cumulative percentage transport of Rhodamine 123 in the presence of 0.000755% (w/v) chondroitin sulfate across excised pig intestinal tissue

Time (min)	Percentage transport: chamber 1	Percentage transport: chamber 2	Percentage transport: chamber 3	Standard deviation	Mean percentage transport
0	0.000	0.000	0.000	0.000	0.000
20	0.131	0.135	0.131	0.002	0.132
40	0.140	0.146	0.141	0.002	0.283
60	0.157	0.163	0.154	0.004	0.158
80	0.157	0.161	0.152	0.004	0.157
100	0.173	0.183	0.169	0.006	0.175
120	0.178	0.182	0.176	0.002	0.179
P_{app} ($x10^{-7}$)	1.062	1.098	1.029	0.028	

Table B.16: Apical to basolateral cumulative percentage transport of Rhodamine 123 in the presence of 0.0755% (w/v) chondroitin sulfate across excised pig intestinal tissue

Time (min)	Percentage transport: chamber 1	Percentage transport: chamber 2	Percentage transport: chamber 3	Standard deviation	Mean percentage transport
0	0.000	0.000	0.000	0.000	0.000
20	0.027	0.050	0.060	0.014	0.046
40	0.131	0.197	0.132	0.031	0.153
60	0.209	0.229	0.166	0.026	0.201
80	0.248	0.252	0.222	0.013	0.241
100	0.566	0.279	0.267	0.007	0.276
120	0.346	0.333	0.333	0.006	0.337
P_{app} ($x10^{-7}$)	2.784	2.529	2.511	0.125	

Table B.17: Basolateral to apical cumulative percentage transport of Rhodamine 123 in the presence of 0.0755% (w/v) chondroitin sulfate across excised pig intestinal tissue

Time (min)	Percentage transport: chamber 1	Percentage transport: chamber 2	Percentage transport: chamber 3	Standard deviation	Mean percentage transport
0	0.000	0.000	0.000	0.000	0.000
20	0.083	0.094	0.087	0.004	0.088
40	0.100	0.109	0.106	0.004	0.105
60	0.109	0.133	0.143	0.014	0.128
80	0.115	0.174	0.192	0.033	0.160
100	0.133	0.221	0.269	0.056	0.208
120	0.158	0.270	0.355	0.081	0.261
P_{app} ($x10^{-7}$)	0.986	1.889	2.537	0.636	

Table B.18: Apical to basolateral cumulative percentage transport of Rhodamine 123 in the presence of 0.00283% (w/v) D-glucosamine across excised pig intestinal tissue

Time (min)	Percentage transport: chamber 1	Percentage transport: chamber 2	Percentage transport: chamber 3	Standard deviation	Mean percentage transport
0	0.000	0.000	0.000	0.000	0.000
20	0.095	0.091	0.097	0.003	0.094
40	0.104	0.096	0.105	0.004	0.102
60	0.104	0.102	0.117	0.007	0.108
80	0.103	0.098	0.110	0.005	0.104
100	0.109	0.108	0.119	0.005	0.112
120	0.112	0.113	0.116	0.002	0.114
P_{app} ($x10^{-7}$)	0.606	0.630	0.664	0.024	

Table B.19: Basolateral to apical cumulative percentage transport of Rhodamine 123 in the presence of 0.00283% (w/v) D-glucosamine across excised pig intestinal tissue

Time (min)	Percentage transport: chamber 1	Percentage transport: chamber 2	Percentage transport: chamber 3	Standard deviation	Mean percentage transport
0	0.000	0.000	0.000	0.000	0.000
20	0.345	0.339	0.523	0.086	0.403
40	0.427	0.369	0.601	0.099	0.466
60	0.571	0.374	0.626	0.108	0.524
80	0.557	0.402	0.625	0.093	0.528
100	0.617	0.410	0.621	0.099	0.549
120	0.658	0.475	0.671	0.090	0.601
P_{app} ($x10^{-7}$)	4.428	2.673	3.732	0.722	

Table B.20: Apical to basolateral cumulative percentage transport of Rhodamine 123 in the presence of 0.283% (w/v) D-glucosamine across excised pig intestinal tissue

Time (min)	Percentage transport: chamber 1	Percentage transport: chamber 2	Percentage transport: chamber 3	Standard deviation	Mean percentage transport
0	0.000	0.000	0.000	0.000	0.000
20	0.058	0.086	0.056	0.013	0.067
40	0.076	0.110	0.076	0.016	0.087
60	0.077	0.111	0.080	0.016	0.089
80	0.083	0.117	0.093	0.014	0.098
100	0.085	0.120	0.092	0.015	0.099
120	0.118	0.133	0.095	0.016	0.115
P_{app} ($x10^{-7}$)	0.694	0.791	0.625	0.068	

Table B.21: Basolateral to apical cumulative percentage transport of Rhodamine 123 in the presence of 0.283% (w/v) D-glucosamine across excised pig intestinal tissue

Time (min)	Percentage transport: chamber 1	Percentage transport: chamber 2	Percentage transport: chamber 3	Standard deviation	Mean percentage transport
0	0.000	0.000	0.000	0.000	0.000
20	0.748	0.607	0.531	0.090	0.629
40	0.733	0.665	0.548	0.076	0.649
60	0.688	0.677	0.545	0.065	0.637
80	0.731	0.697	0.515	0.095	0.648
100	0.705	0.655	0.542	0.068	0.634
120	0.676	0.701	0.509	0.085	0.629
P_{app} ($x10^{-7}$)	3.243	3.731	2.539	0.489	

Table B.22: Apical to basolateral cumulative percentage transport of Rhodamine 123 in the presence of 0.00272% (w/v) silymarin across excised pig intestinal tissue

Time (min)	Percentage transport: chamber 1	Percentage transport: chamber 2	Percentage transport: chamber 3	Standard deviation	Mean percentage transport
0	0.000	0.000	0.000	0.000	0.000
20	0.025	0.051	0.026	0.012	0.034
40	0.043	0.086	0.039	0.021	0.056
60	0.045	0.086	0.038	0.021	0.057
80	0.050	0.084	0.055	0.015	0.063
100	0.062	0.107	0.069	0.020	0.079
120	0.085	0.120	0.092	0.015	0.099
P_{app} ($x10^{-7}$)	0.559	0.787	0.629	0.096	

Table B.23: Basolateral to apical cumulative percentage transport of Rhodamine 123 in the presence of 0.00272% (w/v) silymarin across excised pig intestinal tissue

Time (min)	Percentage transport: chamber 1	Percentage transport: chamber 2	Percentage transport: chamber 3	Standard deviation	Mean percentage transport
0	0.000	0.000	0.000	0.000	0.000
20	0.153	0.194	0.156	0.019	0.167
40	0.195	0.278	0.203	0.038	0.225
60	0.221	0.332	0.219	0.053	0.257
80	0.235	0.350	0.240	0.053	0.275
100	0.254	0.380	0.262	0.058	0.298
120	0.266	0.418	0.275	0.069	0.320
P_{app} ($x10^{-7}$)	1.739	2.835	1.798	0.503	

Table B.24: Apical to basolateral cumulative percentage transport of Rhodamine 123 in the presence of 0.272% (w/v) silymarin across excised pig intestinal tissue

Time (min)	Percentage transport: chamber 1	Percentage transport: chamber 2	Percentage transport: chamber 3	Standard deviation	Mean percentage transport
0	0.000	0.000	0.000	0.000	0.000
20	0.081	0.174	0.032	0.059	0.096
40	0.065	0.140	0.058	0.037	0.088
60	0.046	0.145	0.074	0.042	0.088
80	0.081	0.182	0.071	0.050	0.111
100	0.091	0.190	0.083	0.049	0.121
120	0.155	0.204	0.272	0.029	0.165
P_{app} ($x10^{-7}$)	0.834	1.146	0.876	0.138	

Table B.25: Basolateral to apical cumulative percentage transport of Rhodamine 123 in the presence of 0.272% (w/v) silymarin across excised pig intestinal tissue

Time (min)	Percentage transport: chamber 1	Percentage transport: chamber 2	Percentage transport: chamber 3	Standard deviation	Mean percentage transport
0	0.000	0.000	0.000	0.000	0.000
20	0.091	0.054	0.080	0.015	0.075
40	0.104	0.056	0.083	0.019	0.081
60	0.108	0.066	0.096	0.017	0.090
80	0.122	0.074	0.110	0.020	0.102
100	0.141	0.085	0.123	0.023	0.117
120	0.168	0.115	0.132	0.022	0.138
P_{app} ($x10^{-7}$)	1.039	0.711	0.853	0.134	

ADDENDUM C

APPARENT PERMEABILITY AND EFFLUX RATIOS

Table C.1: Apparent permeability (P_{app}) values and efflux ratio (ER) values for acetyl-L-carnitine at selected concentrations

Concentration (% w/v)	Transport direction	P_{app} (x 10^{-7})	Average P_{app} (x 10^{-7})	Efflux ratio
0.00566	**Apical to basolateral**	1.115	1.384	4.331
		1.314		
		1.721		
	Basolateral to apical	6.742	5.992	
		5.194		
		6.041		
0.566	**Apical to basolateral**	3.897	3.637	0.327
		3.588		
		3.427		
	Basolateral to apical	0.944	1.189	
		1.409		
		1.215		

Table C.2: Apparent permeability (P_{app}) values and efflux ratio (ER) values for berberine at selected concentrations

Concentration (% w/v)	Transport direction	P_{app} (x 10^{-7})	Average P_{app} (x 10^{-7})	Efflux ratio
0.000566	**Apical to basolateral**	1.026	1.013	0.531
		0.973		
		1.041		
	Basolateral to apical	0.560	0.538	
		0.451		
		0.604		
0.0566	**Apical to basolateral**	1.530	1.621	0.917
		1.783		
		1.551		
	Basolateral to apical	1.540	1.487	
		1.057		
		1.863		

Table C.3: Apparent permeability (P_{app}) values and efflux ratio (ER) values for chondroitin sulfate at selected concentrations

Concentration (% w/v)	Transport direction	P_{app} (x 10^{-7})	Average P_{app} (x 10^{-7})	Efflux ratio
0.000755	**Apical to basolateral**	3.655	2.397	0.443
		2.032		
		1.506		
	Basolateral to apical	1.062	1.063	
		1.098		
		1.029		
0.0755	**Apical to basolateral**	2.784	2.608	0.692
		2.529		
		2.511		
	Basolateral to apical	0.986	1.804	
		1.889		
		2.537		

Table C.4: Apparent permeability (P_{app}) values and efflux ratio (ER) values for D-glucosamine at selected concentrations

Concentration (% w/v)	Transport direction	P_{app} (x 10^{-7})	Average P_{app} (x 10^{-7})	Efflux ratio
0.00283	**Apical to basolateral**	0.606	0.633	5.705
		0.630		
		0.664		
	Basolateral to apical	4.428	3.611	
		2.673		
		3.732		
0.283	**Apical to basolateral**	0.694	0.703	4.511
		0.791		
		0.625		
	Basolateral to apical	3.243	3.171	
		3.731		
		2.539		

Table C.5: Apparent permeability (P_{app}) values and efflux ratio (ER) values for silymarin at selected concentrations

Concentration (% w/v)	Transport direction	P_{app} (x 10^{-7})	Average P_{app} (x 10^{-7})	Efflux ratio
0.00272	**Apical to basolateral**	0.559	0.658	3.227
		0.787		
		0.629		
	Basolateral to apical	1.739	2.124	
		2.835		
		1.798		
0.272	**Apical to basolateral**	0.834	0.952	0.911
		1.146		
		0.876		
	Basolateral to apical	1.039	0.867	
		0.711		
		0.853		

ADDENDUM D

TRANS-EPITHELIAL ELECTRICAL RESISTANCE (TEER) MEASUREMENTS

Table D.1: Apical to basolateral trans-epithelial electrical resistance (TEER) measurements across excised pig intestinal tissue of the positive control (Rhodamine 123 and Verapamil)

	TEER			
Time (min)	**Chamber 1**	**Chamber 2**	**Chamber 3**	**Average**
0	36.00	35.00	36.00	35.67
120	37.00	34.00	36.00	35.67
Percentage change	102.78	97.14	100.00	99.97
Average % TEER reduction				**0.03**

Table D.2: Basolateral to apical trans-epithelial electrical resistance (TEER) measurements across excised pig intestinal tissue in the presence of the positive control (Rhodamine 123 and Verapamil)

	TEER			
Time (min)	**Chamber 1**	**Chamber 2**	**Chamber 3**	**Average**
0	34.00	33.00	35.00	34.00
120	33.00	31.00	36.00	33.33
Percentage change	97.06	93.94	102.86	97.95
Average % TEER reduction				**2.05**

Table D.3: Apical to basolateral trans-epithelial electrical resistance (TEER) measurements across excised pig intestinal tissue in the presence of the negative control (Rhodamine 123 alone)

	TEER			
Time (min)	**Chamber 1**	**Chamber 2**	**Chamber 3**	**Average**
0	45.00	47.00	46.00	46.00
120	44.00	47.00	47.00	46.00
Percentage change	97.78	100.00	102.17	99.98
Average % TEER reduction				**0.02**

Table D.4: Basolateral to apical trans-epithelial electrical resistance (TEER) measurements across excised pig intestinal tissue in the negative control (Rhodamine 123 alone)

	TEER			
Time (min)	**Chamber 1**	**Chamber 2**	**Chamber 3**	**Average**
0	47.00	42.00	41.00	43.33
120	48.00	42.00	40.00	43.33
Percentage change	102.13	100.00	97.56	99.90
Average % TEER reduction				**0.10**

Table D.5: Apical to basolateral trans-epithelial electrical resistance (TEER) measurements across excised pig intestinal tissue in the presence of 0.00566% (w/v) acetyl-L-carnitine

	TEER			
Time (min)	**Chamber 1**	**Chamber 2**	**Chamber 3**	**Average**
0	39.00	38.00	42.00	39.67
120	38.00	36.00	44.00	39.33
Percentage change	97.44	94.74	104.76	98.98
Average % TEER reduction				**1.02**

Table D.6: Basolateral to apical trans-epithelial electrical resistance (TEER) measurements across excised pig intestinal tissue in the presence of 0.00566% (w/v) acetyl-L-carnitine

	TEER			
Time (min)	**Chamber 1**	**Chamber 2**	**Chamber 3**	**Average**
0	34.00	41.00	39.00	38.00
120	31.00	38.00	37.00	35.33
Percentage change	91.17	92.68	94.87	92.91
Average % TEER reduction				**7.09**

Table D.7: Apical to basolateral trans-epithelial electrical resistance (TEER) measurements across excised pig intestinal tissue in the presence of 0.566% (w/v) acetyl-L-carnitine

	TEER			
Time (min)	**Chamber 1**	**Chamber 2**	**Chamber 3**	**Average**
0	40.00	42.00	43.00	41.67
120	38.00	39.00	41.00	39.33
Percentage change	95.00	92.86	95.35	94.40
Average % TEER reduction				**5.60**

Table D.8: Basolateral to apical trans-epithelial electrical resistance (TEER) measurements across excised pig intestinal tissue in the presence of 0.566% (w/v) acetyl-L-carnitine

	TEER			
Time (min)	**Chamber 1**	**Chamber 2**	**Chamber 3**	**Average**
0	33.00	31.00	35.00	33.00
120	32.00	30.00	34.00	32.00
Percentage change	96.97	96.77	97.14	96.96
Average % TEER reduction				**3.04**

Table D.9: Apical to basolateral trans-epithelial electrical resistance (TEER) measurements across excised pig intestinal tissue in the presence of 0.000566% (w/v) berberine

	TEER			
Time (min)	**Chamber 1**	**Chamber 2**	**Chamber 3**	**Average**
0	38.00	37.00	34.00	36.33
120	38.00	36.00	32.00	35.33
Percentage change	100.00	97.30	94.12	97.14
Average % TEER reduction				**2.86**

Table D.10: Basolateral to apical trans-epithelial electrical resistance (TEER) measurements across excised pig intestinal tissue in the presence of 0.000566% (w/v) berberine

	TEER			
Time (min)	**Chamber 1**	**Chamber 2**	**Chamber 3**	**Average**
0	33.00	40.00	40.00	37.67
120	32.00	38.00	39.00	36.33
Percentage change	96.97	95.00	97.50	96.49
Average % TEER reduction				**3.51**

Table D.11: Apical to basolateral trans-epithelial electrical resistance (TEER) measurements across excised pig intestinal tissue in the presence of 0.0566% (w/v) berberine

	TEER			
Time (min)	**Chamber 1**	**Chamber 2**	**Chamber 3**	**Average**
0	37.00	42.00	39.00	39.33
120	36.00	40.00	37.00	37.67
Percentage change	97.30	95.24	94.87	95.80
Average % TEER reduction				**4.20**

Table D.12: Basolateral to apical trans-epithelial electrical resistance (TEER) measurements across excised pig intestinal tissue in the presence of 0.0566% (w/v) berberine

	TEER			
Time (min)	**Chamber 1**	**Chamber 2**	**Chamber 3**	**Average**
0	35.00	31.00	33.00	33.00
120	33.00	30.00	31.00	31.33
Percentage change	94.29	96.77	93.94	95.00
Average % TEER reduction				**5.00**

Table D.13: Apical to basolateral trans-epithelial electrical resistance (TEER) measurements across excised pig intestinal tissue in the presence of 0.000755% (w/v) chondroitin sulfate

	TEER			
Time (min)	**Chamber 1**	**Chamber 2**	**Chamber 3**	**Average**
0	39.00	43.00	42.00	41.33
120	37.00	40.00	39.00	38.67
Percentage change	94.87	93.02	92.86	93.59
Average % TEER reduction				**6.41**

Table D.14: Basolateral to apical trans-epithelial electrical resistance (TEER) measurements across excised pig intestinal tissue in the presence of 0.000755% (w/v) chondroitin sulfate

	TEER			
Time (min)	**Chamber 1**	**Chamber 2**	**Chamber 3**	**Average**
0	37.00	35.00	37.00	36.33
120	36.00	34.00	37.00	35.67
Percentage change	97.30	97.14	100.00	98.15
Average % TEER reduction				**1.85**

Table D.15: Apical to basolateral trans-epithelial electrical resistance (TEER) measurements across excised pig intestinal tissue in the presence of 0.0755% (w/v) chondroitin sulfate

	TEER			
Time (min)	**Chamber 1**	**Chamber 2**	**Chamber 3**	**Average**
0	44.00	45.00	47.00	41.33
120	42.00	44.00	45.00	38.67
Percentage change	94.87	93.02	92.86	93.57
Average % TEER reduction				**6.43**

Table D.16: Basolateral to apical trans-epithelial electrical resistance (TEER) measurements across excised pig intestinal tissue in the presence of 0.0755% (w/v) chondroitin sulfate

	TEER			
Time (min)	**Chamber 1**	**Chamber 2**	**Chamber 3**	**Average**
0	33.00	34.00	31.00	32.37
120	32.00	34.00	30.00	32.00
Percentage change	96.97	100.00	96.77	97.91
Average % TEER reduction				**2.09**

Table D.17: Apical to basolateral trans-epithelial electrical resistance (TEER) measurements across excised pig intestinal tissue in the presence of 0.00283% (w/v) D-glucosamine

	TEER			
Time (min)	**Chamber 1**	**Chamber 2**	**Chamber 3**	**Average**
0	36.00	34.00	37.00	35.67
120	34.00	33.00	36.00	34.33
Percentage change	94.44	97.06	97.30	96.27
Average % TEER reduction				**3.73**

Table D.18: Basolateral to apical trans-epithelial electrical resistance (TEER) measurements across excised pig intestinal tissue in the presence of 0.00283% (w/v) D-glucosamine

	TEER			
Time (min)	**Chamber 1**	**Chamber 2**	**Chamber 3**	**Average**
0	46.00	42.00	46.00	44.67
120	43.00	40.00	44.00	42.33
Percentage change	93.48	95.24	95.65	94.79
Average % TEER reduction				**5.21**

Table D.19: Apical to basolateral trans-epithelial electrical resistance (TEER) measurements across excised pig intestinal tissue in the presence of 0.283% (w/v) D-glucosamine

	TEER			
Time (min)	**Chamber 1**	**Chamber 2**	**Chamber 3**	**Average**
0	38.00	37.00	39.00	38.00
120	38.00	35.00	37.00	36.67
Percentage change	100.00	94.59	94.87	96.49
Average % TEER reduction				**3.51**

Table D.20: Basolateral to apical trans-epithelial electrical resistance (TEER) measurements across excised pig intestinal tissue in the presence of 0.283% (w/v) D-glucosamine

	TEER			
Time (min)	**Chamber 1**	**Chamber 2**	**Chamber 3**	**Average**
0	37.00	39.00	38.00	38.00
120	35.00	37.00	36.00	36.00
Percentage change	94.59	94.87	94.74	94.73
Average % TEER reduction				**5.27**

Table D.21: Apical to basolateral trans-epithelial electrical resistance (TEER) measurements across excised pig intestinal tissue in the presence of 0.00272% (w/v) silymarin

	TEER			
Time (min)	**Chamber 1**	**Chamber 2**	**Chamber 3**	**Average**
0	37.00	33.00	30.00	38.00
120	37.00	32.00	30.00	36.67
Percentage change	100.00	96.97	100.00	98.99
Average % TEER reduction				**1.01**

Table D.22: Basolateral to apical trans-epithelial electrical resistance (TEER) measurements across excised pig intestinal tissue in the presence of 0.00272% (w/v) silymarin

	TEER			
Time (min)	**Chamber 1**	**Chamber 2**	**Chamber 3**	**Average**
0	37.00	37.00	36.00	36.67
120	35.00	36.00	34.00	35.00
Percentage change	94.59	97.30	94.44	95.45
Average % TEER reduction				**4.55**

Table D.23: Apical to basolateral trans-epithelial electrical resistance (TEER) measurements across excised pig intestinal tissue in the presence of 0.272% (w/v) silymarin

	TEER			
Time (min)	**Chamber 1**	**Chamber 2**	**Chamber 3**	**Average**
0	43.00	46.00	45.00	44.67
120	42.00	44.00	43.00	43.00
Percentage change	97.67	95.65	95.56	96.29
Average % TEER reduction				**3.71**

Table D.24: Basolateral to apical trans-epithelial electrical resistance (TEER) measurements across excised pig intestinal tissue in the presence of 0.272% (w/v) silymarin

	TEER			
Time (min)	**Chamber 1**	**Chamber 2**	**Chamber 3**	**Average**
0	44.00	45.00	45.00	44.67
120	43.00	45.00	44.00	44.00
Percentage change	97.73	100.00	97.78	98.50
Average % TEER reduction				**1.50**

ADDENDUM E

STATISTICAL ANALYSIS

Table E.1: Kruskal-Wallis test for non-parametric comparison of apical to basolateral transport of Rhodamine 123 in the prescence of acetyl-L-carnatine (*statisticallly significant differences $p \leq 0.05$)

Depend.: A-B	Multiple Comparisons p values (2-tailed); A-B (DuPlessisS) Independent (grouping) variable: Var1 Kruskal-Wallis test: H (3, N= 12) =10.38462 p =.0156 Positive Control R:8.0000	Negative Control R:2.0000	ALC (Low Concentration) R:5.0000	ALC (High Concentration) R:11.000
Positive Control		0.249240	1.000000	1.000000
Negative Control	0.249240		1.000000	* 0.013407
ALC (Low Concentration)	1.000000	1.000000		0.249240
ALC (High Concentration)	1.000000	* 0.013407	0.249240	

Table E.2: Kruskal-Wallis test for non-parametric comparison of basolateral to apical transport of Rhodamine 123 in the prescence of acetyl-L-carnatine (*statisticallly significant differences $p \leq 0.05$)

Depend.: B-A	Multiple Comparisons p values (2-tailed); B-A (DuPlessisS) Independent (grouping) variable: Var3 Kruskal-Wallis test: H (3, N= 12) =9.974359 p =.0188 Positive Control R:5.3333	Negative Control R:7.6667	ALC (Low Concentration) R:11.000	ALC (High Concentration) R:2.0000
Positive Control		1.00000(	0.32547(	1.00000
Negative Control	1.00000(		1.00000(	0.32547
ALC (Low Concentration)	0.32547(	1.00000(		* 0.01340
ALC (High Concentration)	1.00000(	0.32547(	* 0.013407	

Table E.3: Kruskal-Wallis test for non-parametric comparison of apical to basolateral transport of Rhodamine 123 in the prescence of berberine (*statisticallly significant differences $p \leq 0.05$)

Depend.: A-B	Multiple Comparisons p values (2-tailed); A-B (DuPlessisS) Independent (grouping) variable: Var5 Kruskal-Wallis test: H (3, N= 12) =10.38462 p =.0156 Positive Control R:11.000	Negative Control R:2.0000	BRB (Low Concentration) R:5.0000	BRB (High Concentration) R:8.0000
Positive Control		* 0.013407	0.24924(	1.00000
Negative Control	* 0.013407		1.00000(	0.2492
BRB (Low Concentration)	0.24924(	1.00000(		1.00000
BRB (High Concentration)	1.00000(	0.24924(	1.00000(	

Table E.4: Kruskal-Wallis test for non-parametric comparison of basolateral to apical transport of Rhodamine 123 in the prescence of berberine (*statisticallly significant differences p ≤ 0.05)

Depend.: B-A	Multiple Comparisons p values (2-tailed); B-A (DuPlessisS) Independent (grouping) variable: Var7 Kruskal-Wallis test: H (3, N= 12) =9.974359 p =.0188 Positive Control R:8.3333	Negative Control R:10.667	BRB (Low Concentration) R:2.0000	BRB (High Concentration) R:5.0000
Positive Control		1.00000(	0.18870(	1.00000(
Negative Control	1.00000(		* 0.01944(	0.3254(
BRB (Low Concentration)	0.18870(	* 0.01944(		1.00000(
BRB (High Concentration)	1.00000(	0.32547(	1.00000(	

Table E.5: Kruskal-Wallis test for non-parametric comparison of apical to basolateral transport of Rhodamine 123 in the prescence of chondroitin sulfate

Depend.: A-B	Multiple Comparisons p values (2-tailed); A-B (DuPlessisS) Independent (grouping) variable: Var9 Kruskal-Wallis test: H (3, N= 12) =7.205128 p =.0656 Positive Control R:9.6667	Negative Control R:2.0000	CS (Low Concentration) R:7.0000	CS (High Concentration) R:7.3333
Positive Control		0.05524(	1.00000(	1.00000(
Negative Control	0.05524(		0.53657(	0.42024(
CS (Low Concentration)	1.00000(	0.53657(		1.00000(
CS (High Concentration)	1.00000(	0.42024(	1.00000(	

Table E.6: Kruskal-Wallis test for non-parametric comparison of basolateral to apical transport of Rhodamine 123 in the prescence of chondroitin sulfate

Depend.: B-A	Multiple Comparisons p values (2-tailed); B-A (DuPlessisS) Independent (grouping) variable: Var11 Kruskal-Wallis test: H (3, N= 12) =8.435897 p =.0378 Positive Control R:8.0000	Negative Control R:10.667	CS (Low Concentration) R:3.0000	CS (High Concentration) R:4.3333
Positive Control		1.00000(	0.53657(	1.00000(
Negative Control	1.00000(		0.05524(	0.18870(
CS (Low Concentration)	0.53657(	0.05524(		1.00000(
CS (High Concentration)	1.00000(	0.18870(	1.00000(	

Table E.7: Kruskal-Wallis test for non-parametric comparison of apical to basolateral transport of Rhodamine 123 in the prescence of D-glucosamine

Depend.: A-B	Multiple Comparisons p values (2-tailed); A-B (DuPlessisS) Independent (grouping) variable: Var13 Kruskal-Wallis test: H (3, N= 12) =6.846154 p =.0770 Positive Control R:11.000	Negative Control R:5.6667	DGA (Low Concentration) R:3.6667	DGA (High Concentration R:5.6667
Positive Control		0.42024(	0.07642(	0.4202
Negative Control	0.42024(		1.00000(	1.0000
DGA (Low Concentration)	0.07642(	1.00000(		1.0000
DGA (High Concentration)	0.42024(	1.00000(	1.00000(	

Table E.8: Kruskal-Wallis test for non-parametric comparison of basolateral to apical transport of Rhodamine 123 in the prescence of D-glucosamine

Depend.: B-A	Multiple Comparisons p values (2-tailed); B-A (DuPlessisS) Independent (grouping) variable: Var15 Kruskal-Wallis test: H (3, N= 12) =2.743590 p =.4329 Positive Control R:4.0000	Negative Control R:7.3333	DGA (Low Concentration) R:6.0000	DGA (High Concentration R:8.6667
Positive Control		1.00000(	1.00000(	0.6775
Negative Control	1.00000(		1.00000(	1.0000
DGA (Low Concentration)	1.00000(	1.00000(		1.0000
DGA (High Concentration)	0.67754:	1.00000(	1.00000(	

Table E.9: Kruskal-Wallis test for non-parametric comparison of apical to basolateral transport of Rhodamine 123 in the prescence of silymarin (*statisticallly significant differences p ≤ 0.05)

Depend.: A-B	Multiple Comparisons p values (2-tailed); A-B (DuPlessisS) Independent (grouping) variable: Var17 Kruskal-Wallis test: H (3, N= 12) =8.435897 p =.0378 Positive Control R:11.000	Negative Control R:4.6667	SILY (Low Concentration) R:3.0000	SILY (High Concentration R:7.3333
Positive Control		0.18870:	0.03947(	1.0000
Negative Control	0.18870:		* 1.00000(	1.0000
SILY (Low Concentration)	0.03947(	1.00000(		0.8461
SILY (High Concentration)	* 1.00000(	1.00000(	0.84619(	

Table E.10: Kruskal-Wallis test for non-parametric comparison of basolateral to apical transport of Rhodamine 123 in the prescence of silymarin (*statisticallly significant differences p ≤ 0.05)

Depend.: B-A	Multiple Comparisons p values (2-tailed); B-A (DuPlessisS) Independent (grouping) variable: Var19 Kruskal-Wallis test: H (3, N= 12) =9.153846 p =.0273 Positive Control R:7.6667	Negative Control R:10.667	SILY (Low Concentration) R:5.6667	SILY (High Concentration R:2.0000
Positive Control		1.00000(	1.00000(	0.3254
Negative Control	1.00000(		0.53657(	* 0.0194
SILY (Low Concentration)	1.00000(	0.53657(		1.0000
SILY (High Concentration)	0.32547:	* 0.01944:	1.00000(	